

Evolution of a low convergence collisional orogen: a review of Pyrenean orogenesis

Mary Ford^{1,*}, Emmanuel Masini^{2,3}, Jaume Vergés⁴, Raphael Pik¹, Sébastien Ternois^{1,5}, Julien Léger¹, Armin Dielforder^{1,6}, Gianluca Frasca^{1,7}, Arjan Grool¹, Constance Vinciguerra⁸, Thomas Bernard⁹, Paul Angrand¹⁰, Antoine Crémades¹, Gianreto Manatschal¹¹, Sébastien Chevrot¹⁰, Laurent Jolivet¹², Frédéric Mouthereau¹¹, Isabelle Thinon¹³ and Sylvain Calassou¹⁴

¹ Université de Lorraine, CNRS, CRPG, UMR 7358, Nancy, France

² M&U SAS, Saint-Égrève, France

³ ISTERRE, Université Grenoble Alpes, CNRS, Grenoble, France

⁴ Group of Dynamics of the Lithosphere, GDL, Geosciences Barcelona (Geo3Bcn), CSIC, Lluís Solé i Sabarís, s/n, 08028 Barcelona, Spain

⁵ Institut des Sciences de la Terre d'Orléans, Université d'Orléans, 1A rue de la Férollerie, 45071 Orléans Cedex 2, France

⁶ Institute of Geology, Leibniz University Hannover, Hannover, Germany

⁷ National Research Council of Italy, Institute of Geosciences and Earth Resources (IGG-CNR), Torino, Italy

⁸ EA 4592 Géoresources et Environnement, Université Bordeaux Montaigne, Pessac, France

⁹ School of Geosciences, University of Edinburgh, Drummond Street, Edinburgh EH8 9XP, Scotland, UK

¹⁰ GET-OMP, UMR 5563, Université Paul Sabatier, Toulouse, France

¹¹ ITES_EOST, UMR 7063, Université de Strasbourg, CNRS, Strasbourg, France

¹² Sorbonne Université, UMR 7193 CNRS-UPMC, Institut des Sciences de la Terre de Paris, Paris, France

¹³ French Geological Survey (BRGM), Orléans, France

¹⁴ Centre de recherches de TotalEnergie, Pau, France

Published online: 14 December 2022

Abstract – The Pyrenees is a collisional orogen built by inversion of an immature rift system during convergence of the Iberian and European plates from Late Cretaceous to late Cenozoic. The full mountain belt consists of the pro-foreland southern Pyrenees and the retro-foreland northern Pyrenees, where the inverted lower Cretaceous rift system is mainly preserved. Due to low overall convergence and absence of oceanic subduction, this orogen preserves one of the best geological records of early orogenesis, the transition from early convergence to main collision and the transition from collision to post-convergence. During these transitional periods major changes in orogen behavior reflect evolving lithospheric processes and tectonic drivers. Contributions by the OROGEN project have shed new light on these critical periods, on the evolution of the orogen as a whole, and in particular on the early convergence stage. By integrating results of OROGEN with those of other recent collaborative projects in the Pyrenean domain (*e.g.*, PYRAMID, PYROPE, RGF-Pyrénées), this paper offers a synthesis of current knowledge and debate on the evolution of this immature orogen as recorded in the synorogenic basins and fold and thrust belts of both the upper European and lower Iberian plates. Expanding insight on the role of salt tectonics at local to regional scales is summarised and discussed. Uncertainties involved in data compilation across a whole orogen using different datasets are discussed, for example for deriving shortening values and distribution.

Keywords: Pyrenees / foreland systems / collisional orogen / foreland basins / rift inheritance

Résumé – **Évolution d'un orogène collisionnel à faible convergence: une revue de l'orogénèse pyrénéenne.** Les Pyrénées sont un petit orogène de collision à faible convergence construit par inversion d'un système de rift immature au cours de la convergence des plaques ibérique et européenne du Crétacé supérieur au Cénozoïque. La ceinture montagneuse comprend les Pyrénées méridionales (pro-avant-pays) et

*Corresponding author: mary.ford@univ-lorraine.fr

les Pyrénées septentrionales (rétro-avant-pays), où le système de rift hérité du Crétacé inférieur est principalement préservé. En raison de la faible convergence globale et de l'absence de subduction océanique, l'orogène pyrénéen conserve l'un des meilleurs enregistrements géologiques de l'orogène précoce, de la transition de la convergence précoce à la collision principale et de la transition de la collision à la post-convergence. Ces périodes de transition enregistrent des changements majeurs dans le comportement de l'orogène, reflétant l'évolution des processus lithosphériques et des moteurs tectoniques. Les contributions du projet OROGEN ont apporté un nouvel éclairage sur ces périodes critiques, sur l'évolution de l'orogène dans son ensemble, et en particulier sur la phase de convergence précoce. En intégrant les résultats d'OROGEN aux résultats d'autres projets de recherche collaboratifs récents sur le domaine pyrénéen (PYRAMID, PYROPE, RGF-Pyrénées), cet article propose une synthèse des connaissances actuelles et des débats sur l'évolution de cet orogène immature tel qu'enregistré en particulier dans les bassins synorogéniques et les chaînes plissées des plaques européennes et ibériques. L'élargissement des connaissances sur le rôle de la tectonique salifère aux échelles locales et régionales est résumé et discuté. Les incertitudes impliquées dans la compilation des données sur l'ensemble d'un orogène à l'aide de différents ensembles de données sont discutées, par exemple pour estimer les valeurs de raccourcissement et sa distribution.

Mots clés : Pyrénées / systèmes d'avant-pays / orogène collisionnel / Bassin d'avant pays / héritage de rift

1 Introduction

Fold and thrust belts, their flexural basins and forelands develop as integrated systems during plate convergence (DeCelles and Giles, 1996; Ford, 2004; Sinclair, 2012; DeCelles, 2012; Horton and Plate, 2018), thus preserving valuable records of interacting orogenic and surface processes in their stratigraphy and structure. The application of rapidly evolving technologies, analytical and numerical techniques to external orogenic systems over the last 20 years has led to many new insights and innovative research, nowhere more-so than in the Pyrenean orogen. The Pyrenees is one of several relatively small alpine orogens created across southern Europe during convergence of the African and European plates from Late Cretaceous to present day (Fig. 1; Platt *et al.*, 1989; Rosenbaum *et al.*, 2002a; Schettino and Turco, 2009, 2011; Handy *et al.*, 2010). This small orogen has become one of the best-studied natural laboratories for collisional orogenic processes. Over the last 10 years, four major projects funded by French research agencies and industry have focused on various aspects of the Pyrenean Orogen: PYROPE (deep seismic tomography, funded by the French National Funding Agency, the ANR), PYRAMID (North Pyrenean foreland systems, funded by the ANR), the RGF-Pyrenees project (funded by the BRGM), and OROGEN (Orogenic Systems, funded by Total, CNRS and BRGM). These large collaborative projects, combined with other research programs in Spanish, French and international research institutions are driving an exceptional outpouring of new research on the Pyrenean orogen. As well as contributing to the ever-improving standard geological databases, these research efforts are building outstanding new datasets such as for passive seismic tomographic imagery of the orogen's deep structure and physical properties (*e.g.*, Chevrot *et al.*, 2022) and thermochronology datasets using a variety of isotopic systems (*e.g.*, Bosch *et al.*, 2016; Labaume *et al.*, 2016, Labaume *et al.*, 2016; Vacherat *et al.*, 2016, 2017; Bernard *et al.*, 2019; Odlum *et al.*, 2019; Ternois *et al.*, 2019a, b; Fillon *et al.*, 2020; Milesi *et al.*, 2020; Waldner *et al.*, 2021), that provide insight into crustal thermal evolution and deformation during orogenesis. Thermomechanical modelling also offers an increasingly powerful and effective tool to investigate complex geodynamic systems and processes

and their controlling parameters (*e.g.*, Beaumont *et al.*, 2000; Sinclair *et al.*, 2005; Mouthereau *et al.*, 2014; Erdős *et al.*, 2014a, b; Curry *et al.*, 2019; Grool *et al.*, 2019; Jourdon *et al.*, 2019, 2020). Finally, major advances in our conceptual understanding of the pre-orogenic magma-poor extensional systems, salt tectonics and mantle dynamics are impacting research in the Pyrenees as well as in other orogens (*e.g.*, Alps). New Pyrenean research is thus contributing to paradigm shifts in our global understanding of orogenesis and full Wilson cycle dynamics.

As with all orogens, the unique geodynamic characteristics of the Pyrenees can be seen as opportunities or limitations. Here, we emphasize the opportunities offered by the low convergence orogenic cycle (referred to as an immature Wilson cycle). The orogen's notable characteristics are the following:

- No oceanic crust was produced during the separation of the Iberian and European plates by magma-poor hyperextension (although an unknown amount of upper mantle was exhumed). Hence continental collision was not preceded by oceanic subduction. A critical change in stress distribution and lithospheric deformation occurred through the initiation of continental subduction.
- Convergence began less than 10 Myrs after the termination of rifting so that the hot, rifted lithosphere had not yet attained thermal equilibrium.
- Due to its overall low convergence, the orogen preserves not only the main collision stage but also the full record of orogenesis from onset of convergence to post-convergence stages.
- No record of syn-orogenic high-grade metamorphism and/or high temperature ductile deformation of basement nappes is observed at outcrop level. The pro and retro low-grade wedge systems therefore essentially form the full mountain belt.
- Upper Triassic evaporites play a key role in both the extensional and convergence histories of the orogen.

Due to these characteristics, the Pyrenean orogen notably preserves one of the best geological records of onset and early orogenesis, the early convergence-to-collision transition and the transition from collision to post-convergence. Much recent research has focused on the less well-known northern

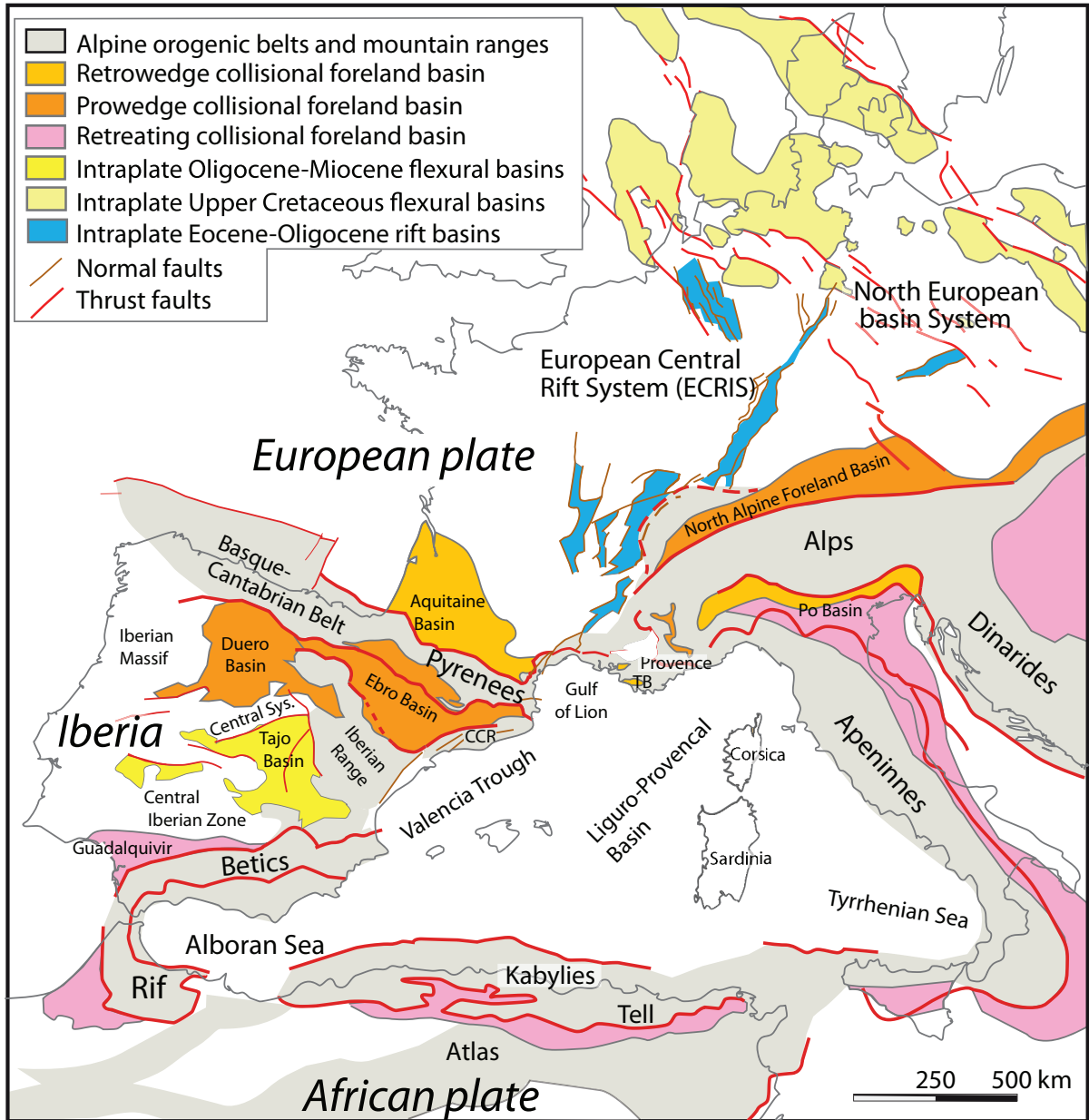


Fig. 1. West Mediterranean and western Europe alpine orogens, and onshore synorogenic basins (Late Cretaceous-Cenozoic). Abbreviations: TB: Toulon Belt, Provence; CCR: Catalan Coastal Ranges.

Pyrenees, where the inherited rift system is mainly preserved, and has thus shed new light on these critical periods and their role in progressively building the Pyrenean mountain belt. In larger orogens, these early and late records of orogenesis tend to be strongly overprinted or destroyed by collisional processes and strong post-convergence processes (*e.g.*, rebound, relief rejuvenation, erosion) respectively.

This paper presents a synthesis of the current state of knowledge on Pyrenean orogenesis recorded in its foreland systems, their progressive evolution and controlling factors, by integrating the results of the OROGEN project (2015–2020) with the rich and continuing flow of research emerging on the Pyrenees. It is one of a collection of overview papers of the

Orogen project. Readers are directed to sister papers on complimentary subjects related to the role of rift inheritance in Pyrenean orogenesis (Manatschal *et al.*, 2021), geophysical imaging of the deep orogenic structure (Chevrot *et al.*, 2022), Mesozoic to present-day plate tectonic processes in the western Mediterranean (Jolivet *et al.*, 2021a) and how rheological and structural inheritance at lithospheric and crustal scales impact mountain building processes in the alpine domain (Mouthereau *et al.*, 2021). Here, we first summarize the regional and plate tectonic setting of the Pyrenean orogen and briefly describe the pre-orogenic rift template. We then explore the evolution of retro and pro foreland basins and deformation wedges to clarify sediment supply, basin

dynamics and distribution of deformation during early convergence, the early convergence-to-collision transition, main collision and, finally, the transition from collision to post-convergence. We highlight the importance of emerging research on the role of evaporite layers in deformation distribution and style, the thermal signature of early convergence and modelling of crustal scale processes that initiated subduction of the Iberian plate. Finally, we summarize the principal outcomes and wider implications of these findings and identify future challenges for research in the Pyrenees and in orogens more globally.

2 Regional overview

2.1 European and west Mediterranean alpine orogens and syn-orogenic basins

Around the Western Mediterranean small orogens developed within the larger Alpine-Himalayan system (Fig. 1) from Late Cretaceous to present day (*e.g.*, Roure, 2008; Vergés *et al.*, 2002, 2019). These orogens can be described as either collisional orogens or retreating thrust belts, each type having distinctive foreland systems (Fig. 1; DeCelles, 2012). The collisional Alpine and Pyrenean orogens developed along the southern margin of the European plate, due to collision with the Apulian and Iberian plates respectively. The Basque-Cantabrian belt is the westward continuation of the Pyrenees. Each orogen has a retro and pro-foreland system. Proforeland basins (North Alpine basin, Ebro and Duero basins) develop on the downgoing plate (Europe and Iberia respectively). The North Alpine Basin shows the “classic” stratigraphic infill recording an initial marine transgression, an undersupplied, deepening marine basin (underfilled basin), evolving to a continental basin with high sediment supply from growing orogen relief (overfilled basin; *e.g.*, Sinclair, 2012). The proforeland basins of the Pyrenean system show a more complex history, due largely to inheritance, but also to a marked late endorheic stage, which will be described below. Developing on the upper plate, the retroforeland basins (Po, Aquitaine) record low flexural subsidence during the full convergence history. They are strongly influenced by inherited crustal structure and rheology (*e.g.*, Angrand *et al.*, 2018; Manatschal *et al.*, 2021).

Further south and east in southern Europe and Mediterranean regions, younger retreating thrust systems (Apennines, Betics, Rif, Tell, Carpathians, Fig. 1) developed above Tethyan rollback subduction systems. These retreating convergence zones are characterized by low relief thrust belts and broad, highly subsiding, mainly marine flexural basins on the subducting plate (DeCelles, 2012) with backarc extensional basins on the upper plate (Jolivet *et al.*, 2021b).

Syn-orogenic intraplate basins of variable character developed across the Iberian and European plates (Fig. 1). Across the Iberian plate Mesozoic rift systems were inverted during Oligocene-Miocene convergence to create a series of local intraplate thrust belts (Iberian Range, Central System) associated with largely endorheic flexural basins (Duero, Tajo basins; Fig. 1; Vergés and Fernández, 2006, and references therein). In contrast, the European plate preserves two distinct families of syn-orogenic basins. The North European Basin system (Fig. 1) consists of Late Cretaceous flexural basins that

developed in association with inversion of Mesozoic rift systems (Kley and Voigt, 2008; Voigt *et al.*, 2021) while during the Late Eocene to Oligocene the European Central Rift System (ECRIS) cut across the western European plate from the Mediterranean to the North Sea during alpine collision (Bourgeois *et al.*, 2007; Dèzes *et al.*, 2004; Mouthereau *et al.*, 2021). The southern branch of this rift system continued to evolve to form the Gulf of Lion and Liguro-Provençal backarc basin (*e.g.*, Séranne, 1999; Ethève *et al.*, 2018; Jolivet *et al.*, 2021a, 2021b; Séranne *et al.*, 2021 and references therein).

2.2 Santonian to Miocene Iberia-Europe Plate Kinematics

During the Mesozoic and Cenozoic, the relative motions of the African, European and North American plates were controlled by the northward propagation and opening of the Central and North Atlantic oceans (Dewey *et al.*, 1989; Srivastava *et al.*, 1990b; Rosenbaum *et al.*, 2002b; Schettino and Turco, 2011; Macchiavelli *et al.*, 2017; Hinsbergen *et al.*, 2020; Angrand and Mouthereau, 2021). Africa-Europe plate convergence was accommodated by orogenesis distributed along the boundaries of the African (Rif, Atlas), Iberian (Betics, Pyrenees, Pyrenean-Provençal domain, Fig. 2) and Apulian plates (Alpine and Apennine domains; Fig. 2) with some belts of intraplate shortening (*e.g.*, Iberian Range and Central System on the Iberian plate, North European Basin system; Figs. 1 and 2). From Late Cretaceous to Oligocene, deformation of the Iberian plate was principally partitioned between the Pyrenean and Betic-Rif orogenic domains. According to Macchiavelli *et al.* (2017), the N-S convergence rate between Africa and Europe was approx. 6.0 mm/yr from the Santonian-Campanian boundary to Late Maastrichtian and convergence was mainly accommodated along the Africa-Iberia boundary (Betics) with a minor component absorbed along the Iberia-Europe margin (~1 mm/yr; early convergence). This model contrasts markedly with the earlier model of Rosenbaum *et al.* (2002b), which predicts a high Africa-Europe convergence during this period accommodated mainly in the Pyrenees (Fig. 2a). We here mainly refer to the model of Macchiavelli *et al.* (2017) and its convergence rates between Iberia and Europe across the Pyrenees as it is based on a completely new and well documented recalculation of the magnetic anomalies of the southern North Atlantic for the 83.5 Ma to 0 Ma period and is coherent with geological observations. In this model, the Iberian plate is defined as a rigid block along its current coastlines to simplify calculations and to facilitate checks. Other recent models partition the Iberian plate into 2 or 3 crustal blocks to allow the inclusion of intraplate deformation in both the Iberian Range and the Central System (Fig. 1) as well as relative movements along the main Iberia-Africa boundary (Betics) and Iberia-Europe plate boundary (Pyrenees) (Angrand and Mouthereau, 2021; Asti *et al.*, 2022). Angrand and Mouthereau (2021) analyze the Ebro Block with motions independent of the South Iberian block, from earliest Jurassic to earliest Campanian. On a large scale, the two models are similar in recognizing three phases of N-S convergence starting in the earliest Campanian with a first period of convergence (83.5–69 Ma), a nearly quiescent tectonic period (69–56 Ma) and a main convergence period

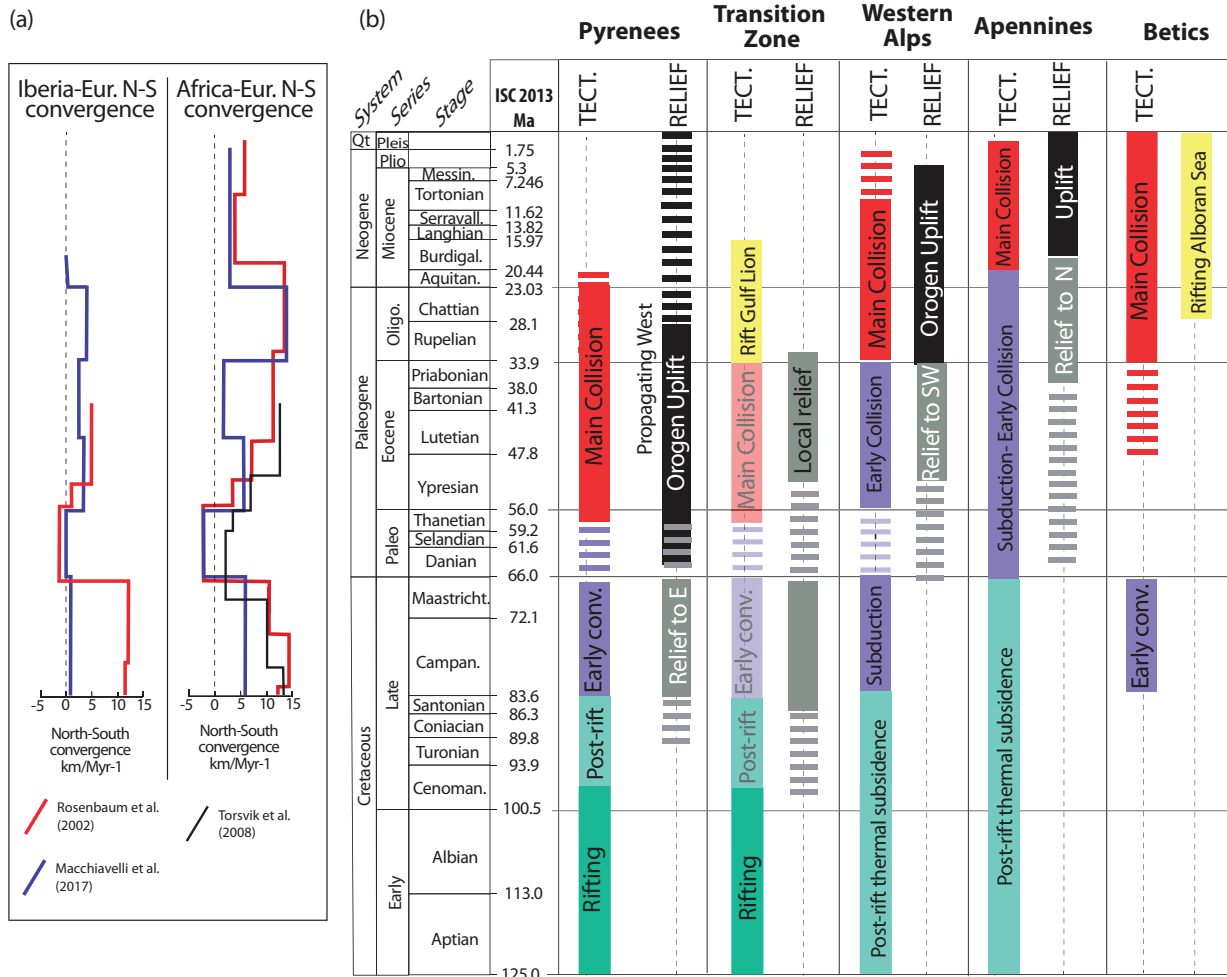


Fig. 2. Plate kinematics and distribution of deformation across the west Mediterranean. (a) North-south component of Iberia-Europe and Africa-Europe plate movement vectors from Rosenbaum *et al.* (2002a, b), Macchiavelli *et al.* (2017) and Torsvik *et al.* (2008). The vertical scale is the same time scale as in b. (b) Chronology of major tectonic events and evolution of orogenic relief around the western Mediterranean using the International Stratigraphic Chart (2013), IUGS. Data supporting the tectonic stages and relief of the Pyrenees and in the transition zone (Provence, Fig. 1) between the Pyrenees and Alps are presented in this paper. For the Alps see Le Breton *et al.* (2020) and references therein; for the Apennines see Marroni *et al.* (1992), Molli (2008) and Conti *et al.* (2020); for the Betics see Vergés and Fernández (2012).

during Eocene and Oligocene. The main difference between the models is the contrasting convergence rates for the first and last periods. In the Macchiavelli *et al.* (2017) model, convergence occurs at rates of ~0.8 mm/yr during the Late Cretaceous and ~2.4 to ~4.0 mm/yr during the Eocene-Oligocene. For about the same periods, Angrand and Mouthereau (2021) determine ~3.2 mm/yr and ~2.25 mm/yr respectively, based on the relative position of the independent Ebro block in their interpretation. Despite these differences, both approximations are quite reliable and, in any case, must be considered and integrated with quantified field observations. As will be shown later, shortening records across the orogen are more consistent with convergence estimates of Macchiavelli *et al.* (2017).

All plate kinematic models predict sinistral transpressional motion between Iberia and Europe during convergence, however the amount is difficult to constrain (Srivastava

et al., 1990a, b; Luis, 2001; Rosenbaum *et al.*, 2002b; Vissers and Meijer, 2012a, b; Macchiavelli *et al.*, 2017). Reconstructions from 84 Ma to 66 Ma of Macchiavelli *et al.* (2017) estimate some 60 km of sinistral motion combined with slow convergence, associated with high uncertainty. The N-S convergence rate decreases laterally from 1.1 mm/a in the eastern Pyrenees (total convergence, 20 km) to 0.5 mm/a in the west (Basque-Cantabrian area; 9 km). During the Selandian and Thanetian (66–56 Ma; Fig. 2) little or no convergence occurred between Iberia and Europe and between Africa and Europe (“Paleocene standstill phase” of Roest and Srivastava, 1991 Schettino and Turco, 2011; Fig. 2). Similar Paleocene quiescence is also recorded in the Alpine orogenic belt (Fig. 2; e.g., Trümpy, 1980). Africa-Europe and Iberia-Europe convergence resumed in the Thanetian (Fig. 2). In the Pyrenees, the overall motion of Iberia relative to Europe is characterized by NW-directed transpressional movement from

base Ypresian until the Lutetian and overall NNW directed convergence from Bartonian to Chattian (Macchiavelli *et al.*, 2017). During the Eocene and Oligocene N-S Iberia-Europe convergence reached a maximum of 4 mm/a (Ypresian-Lutetian 3.2 mm/a; Bartonian-Priabonian 2.4 mm/a; Oligocene 4 mm/a; Macchiavelli *et al.*, 2017). Plate convergence slowed down abruptly to 0.2 mm/yr in the Aquitanian in the central and eastern Pyrenees continuing into the Burdigalian in the west on the Galicia margin (Macchiavelli *et al.*, 2017). From Oligocene onward deformation became focused into the Betic-Rif domain (Vergés and Fernández, 2012; Fig. 2). The Macchiavelli *et al.* (2017) model estimates total N-S Iberia-Europe plate convergence accommodated within the Pyrenean domain as decreasing westward from 143 km (eastern Pyrenees) to 125 km (central Pyrenees) to 85 km in the Basque-Cantabrian belt. These convergence rates will be compared with NS shortening estimates derived from cross-section restorations across the orogen.

Although pure shear models for the Pyrenean orogenic cycle currently dominate the literature, plate reconstructions clearly indicate that strike-slip deformation played a significant role during both extensional and convergence stages with variable distributions in time and space proposed along the Pyrenean plate boundary and along the Iberian Chain (Fig. 3; Beltrando *et al.*, 2012; Angrand *et al.*, 2020; Hinsbergen *et al.*, 2020; Angrand and Mouthereau, 2021; Frasca *et al.*, 2021; Asti *et al.*, 2022), however field quantification of strike-slip deformation in both belts is an ongoing challenge.

2.3 The Pyrenean orogen

The complete Iberia-Europe convergent plate boundary is over 1200 km long, encompassing from west to east the Basque-Cantabrian Belt (500 km), the Pyrenees *sensu stricto* (400 km) and the Pyrenean-Provençal belt in SE France (300 km) that links the Pyrenees eastward with the SW Alps (Fig. 1). The eastern Pyrenean to Provençal plate boundary was later fragmented by Oligo-Miocene backarc extension that led to the opening of the Gulf of Lion and Ligurian Ocean (Jolivet *et al.*, 2021b and references therein). No Alpine high-grade metamorphism or high temperature ductile deformation of basement nappes are recorded in surface outcrops across the Pyrenees. Instead, the core of the eastern and central orogen (Axial Zone) consists of upper crustal Variscan basement and its Paleozoic to Lower Triassic sedimentary cover, thrust southward in a series of upper crustal imbricates. South Pyrenean thrust sheets of Cenozoic and Mesozoic strata detached on Upper Triassic evaporites restore above these basement units or may root further north (Muñoz, 1992; Vergés *et al.*, 1992; Teixell, 1996; Vergés and Burbank, 1996; Laumonier, 2015; Teixell *et al.*, 2018; Espurt *et al.*, 2019a). The Axial Zone can thus be understood as a structural equivalent of the external crystalline massifs of the Western Alps (*e.g.*, Bellahsen *et al.*, 2012, 2014). The North Pyrenean Fault defines the northern boundary of the Axial Zone in the central and eastern Pyrenees. This steep to vertical fault terminates at depth on the North Pyrenean frontal thrust (Fig. 4; Choukroune, 1976, 1989; Roure *et al.*, 1989). To the north, the retrowedge consists of the narrow North Pyrenean

Zone and the Aquitaine foreland basin, both of which preserve inverted remnants of the pre-orogenic Mesozoic rift system.

From the onset of plate convergence in earliest Campanian (84 Ma) to Late Maastrichtian, the Pyrenean orogen accommodated distributed gentle shortening by inversion of inherited rift structures and closure of exhumed mantle domains. This stage is here referred to as early convergence. During the late Maastrichtian, Danian and Selandian, Africa-Europe plate convergence was negligible (Fig. 2; Macchiavelli *et al.*, 2017), which correlates with a period of tectonic quiescence across the west Mediterranean region including the Pyrenees (quiescence/stasis) and the Alps. From Thanetian to Aquitanian, main Pyrenean collision was accommodated by crustal thickening. The presence of northward subducted of Iberian crust below the European plate was first imaged on deep seismic reflection profiles shot in the late 80's across the central and western Pyrenees (ECORS lines, Fig. 4 located in Fig. 3; Choukroune, 1989; Choukroune *et al.*, 1990; Roure *et al.*, 1989). Strong positive Bouguer gravity anomalies indicate the presence of dense bodies below the North Pyrenean Zone, identified as slices of mantle or lower crustal material thrust into the upper European crust (Muñoz, 1992; Casas *et al.*, 1997; Angrand *et al.*, 2018; Wehr *et al.*, 2018). Recent 2D passive seismic imaging along Pyrenean transects (PYROPE and OROGEN projects; Chevrot *et al.*, 2014, 2018, 2022) have permitted high resolution mapping of seismic discontinuities in the crust and mantle as well as providing new insight into the nature and geometry of the high-density bodies below the orogen (Casas *et al.*, 1997; Chevrot *et al.*, 2014; García-Senz *et al.*, 2020). They reveal along-strike variations in major lithospheric boundaries due, in part, to inherited rift segmentation but also to lateral variations in orogenic processes and amount of plate convergence. Prevalent models of crustal thickening by southward stacking of upper crustal imbricates with subduction of Iberian lower crust give relatively high estimates of total shortening along the ECORS-Central profile (120–165 km; Fig. 4a; Beaumont *et al.*, 2000; Muñoz, 1992, 2002, 2019). Alternative models for this section propose full crustal imbrication giving lower shortening estimates (92–100 km; Roure *et al.*, 1989; Mouthereau *et al.*, 2014; Cochelin *et al.*, 2018; Bellahsen *et al.*, 2019; Waldner *et al.*, 2021). This illustrates how uncertainties in structural interpretation and in the datasets used can strongly impact cross-sectional models (see Bond, 2015; Randle *et al.*, 2018 for discussion). Factors contributing to differences in crustal restorations in the Pyrenees are uncertainties in displacement on basement faults in the Axial Zone, their traces, lateral linkage and timing of activity. New tomographic data along the ECORS-Central line should allow better definition of deep geometries (Chevrot *et al.*, 2018). To the east of the ECORS-Central section, Grool *et al.* (2018) derive a shortening estimate of > 111 km on the Lavelanet-Pedraforca section (Fig. 4e) while further east again on the Agly-Ripoll section, Ternois *et al.* (2019a, b) propose very low shortening of 43 km (Fig. 4f). In this eastern sector, crust has undergone post-orogenic thinning. Evidence of underthrusting of Iberian crust is subdued due in part to overprinting by Oligocene-Miocene rifting (Diaz *et al.*, 2018; Wehr *et al.*, 2018; Chevrot *et al.*, 2018, 2022; Jolivet *et al.*, 2021a). This young rifting has also led to major uplift and deep erosion of the easternmost Pyrenees, that may contribute to very low

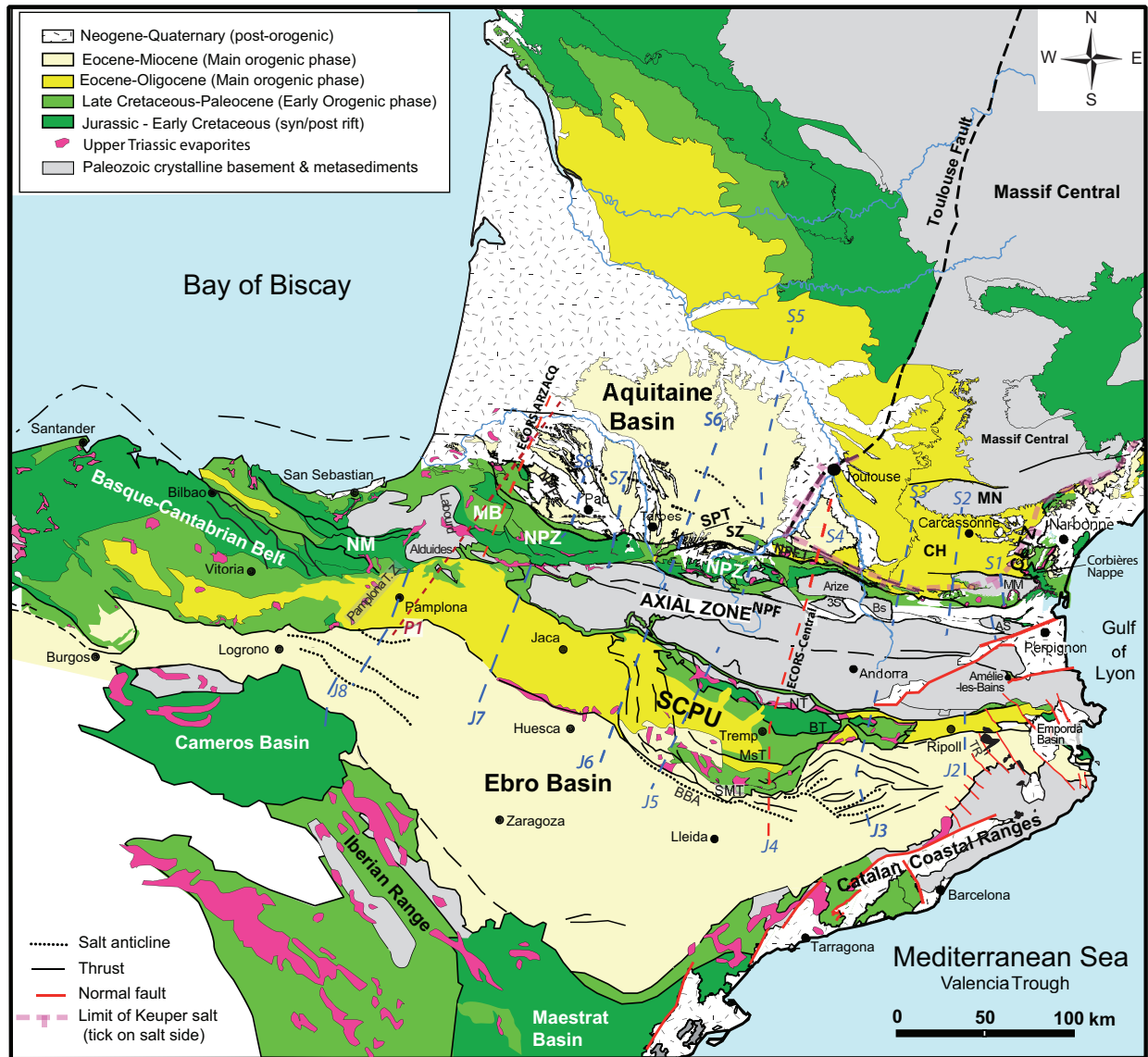


Fig. 3. Simplified geological map of Pyrenees. Abbreviations in northern Pyrenees: NPFT: North Pyrenean Frontal Thrust; NPZ: North Pyrenean Zone; NPF: North Pyrenean Fault; SZ: Subpyrenean Zone; MB: Mauléon Basin; CH: Carcassonne High; CLTZ: Corbières-Languedoc Transfer Zone. North Pyrenean basement massifs: AS: Agly-Salvezines; MM: Mouthoumet; MN: Montagne Noire Massif; BS: Saint Barthelemy; 3S: Trois Seigneurs. Abbreviations in southern Pyrenees: South Central Pyrenean Units; NT: Noguères Thrust; BT: Bóixols Thrust; MsT: Monsec Thrust; SMT: Serres Marginals Thrust; BBA: Barbastro-Balaguer Anticline; SA: Sanauja Anticline; TR: Transverse Ranges. Blue dashed lines locate cross-sections in [Figures 7](#) and [8](#) and some crustal scale cross-sections along the same lines in [Figure 4](#). Red dashed lines ECORS deep seismic crustal cross-sections ([Fig. 4](#)) and the deep seismic tomography profile P1 ([Chevrot et al., 2018](#)) in the NW Pyrenees.

shortening estimates based on surface geology. West of the ECORS-Central profile, a restored crustal section on the Vallée de Nestes-Huesca line ([Fig. 4c](#)) by [Espurt et al. \(2019a\)](#) provides a shortening estimate of 127 km, while on the ECORS Arzacq section ([Fig. 4b](#)), [Teixell et al. \(2016\)](#) derive a shortening of 114 km. New 2D and 3D tomographic data in the Mauléon basin ([Figs. 3](#) and [4a](#)) indicate the presence of a laterally restricted, dense body at shallow depth (11 km) below the Mauléon Basin ([Fig. 4a](#); [Wang et al., 2016](#); [Chevrot et al., 2018](#); [Lehujeur et al., 2021](#)) corresponding to the Labourd positive Bouguer anomaly ([Casas et al., 1997](#); [Jammes et al.,](#)

[2010](#); [Wehr et al., 2018](#)). Recent models propose that this is caused by mantle exhumed to shallow depths during Apt-Cenomanian hyper-extensional rifting and later passively integrated into the orogen above the northward subducting Iberian crust ([Fig. 4a](#); [Wang et al., 2016](#); [Lescoutre and Manatschal, 2020](#); [Saspiturry et al., 2020](#); [Lehujeur et al., 2021](#)). This model is strongly debated, for example, by [Teixell et al. \(2018\)](#) who instead argue that the tomographic and gravity data as well as the adjacent ECORS-Arzacq seismic reflection line ([Fig. 4b](#)) indicate the presence of an imbricate of mantle or lower crustal material thrust northward onto the

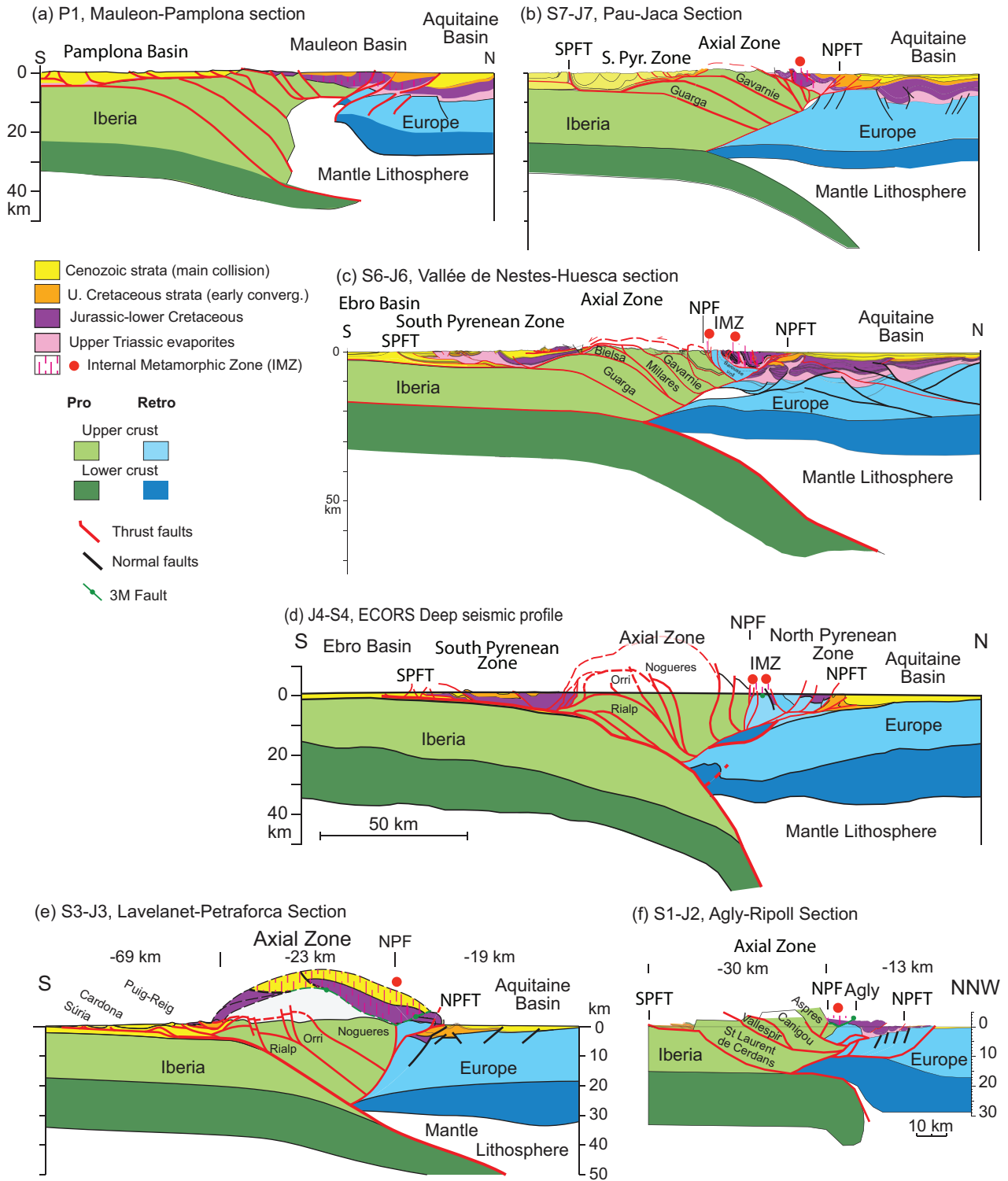


Fig. 4. Published crustal scale cross-sectional models across the Pyrenees from west to east, located in Figure 3. Authors estimated total shortening across the orogen is shown in brackets. (a) Interpretation of the deep seismic tomography model of Wang *et al.* (2016) along P1 adapted from Saspiturry *et al.* (2020) and Lehujeur *et al.* (2021). These authors do not provide a shortening estimate and do not distinguish upper and lower crust. (b) J7-S8 adapted from Teixell *et al.* (2016) (114 km). (c) J6-S6 adapted from Espurt *et al.* (2019a) (127 km). (d) J4-S4 (ECORS central deep seismic line) based on Muñoz (1992) and redrawn from Mencos *et al.* (2015) (147 km). (e) J3-S3 simplified from Grool *et al.* (2018) (> 111 km, distribution shown). (f) J2-S2 adapted from Ternois *et al.* (2019a, b) (43 km, distribution shown). Abbreviations: SPFT: South Pyrenean Frontal Thrust; NPFT: North Pyrenean Frontal Thrust; NPF: North Pyrenean Fault; IMZ: Internal Metamorphic Zone. The 3M Fault is identified on sections d, e and f.

European plate in the manner similar to that proposed on the ECORS-Central line (Fig. 4d; see also Lescoutre and Manatschal 2020).

2.4 Precursor rift architecture

From the Triassic to Late Cretaceous Iberian plate kinematics were mainly controlled by the opening of the Tethys Ocean to the east, and from late Jurassic onward, also by the northward propagation of the southern North Atlantic Ocean to the west (Dewey *et al.*, 1989; Srivastava *et al.*, 1990a; Rosenbaum *et al.*, 2002b; Schettino and Turco, 2011; Macchiavelli *et al.*, 2017; Nirrengarten *et al.*, 2018; Angrand *et al.*, 2020; Hinsbergen *et al.*, 2020; Frasca *et al.*, 2021). During the Triassic, distributed rifting affected the Iberian block on all four sides with facies varying regionally from continental, through evaporitic to marine from west to east (e.g., Critelli *et al.*, 2008; Martin-Rojas *et al.*, 2009; Leleu *et al.*, 2016). Broad shallow seaways of gentle subsidence developed across Iberia during Late Jurassic and into the mid early Cretaceous with some notable localized areas of strong subsidence, for example, locally along the Iberian Range (e.g., Cameros Basin, Fig. 3; Salas *et al.*, 2001; Rat *et al.*, 2019) and in the Cantabrian Ranges and margin where transtension is recorded (Cadenas *et al.*, 2021). Plate kinematics of Iberia from Jurassic to Cenomanian is a subject of considerable debate, in particular regarding the timing, distribution and amount of sinistral strike-slip between Iberia and Europe (see discussions in Angrand *et al.*, 2020; Manatschal *et al.*, 2021; Mouthereau *et al.*, 2021; Asti *et al.*, 2022). While it is generally agreed that Iberia moved some 400 km eastward with respect to Europe during the Jurassic-early Cretaceous, exactly where and when this movement took place differ between models. Many models trace this strike-slip along the Pyrenean corridor (e.g., Olivet, 1996a, b; Sibuet *et al.*, 2004; Vissers and Meijer, 2012a, b). Alternatively, other authors propose significant oblique movement along the NW-SE trending fault system of the Iberian Range (e.g., Angrand *et al.*, 2020; Frasca *et al.*, 2021), recorded by rapidly subsiding Jurassic depocentres (Tugend *et al.*, 2014b; Cadenas *et al.*, 2018, 2021; Nirrengarten *et al.*, 2018; Rat *et al.*, 2019; Manatschal *et al.*, 2021). Most recently, Asti *et al.* (2022) propose Jurassic to Cenomanian diffuse transtension along a broad plate margin between the Iberian Range and the Massif Central. These differences arise from the difficulties in precisely defining Lower Cretaceous and Jurassic magnetic anomalies within the southern North Atlantic (for review see Nirrengarten *et al.*, 2017) and in the Bay of Biscay (see Barnett-Moore *et al.*, 2016; Nirrengarten *et al.*, 2018; Angrand *et al.*, 2020; Frasca *et al.*, 2021; Le Maire *et al.*, 2021). An additional issue relates to the restoration of conjugate rifted margin domains that can hide hundreds of kilometers of divergence preceding the formation of first oceanic crust (Sutra *et al.*, 2013; Tugend *et al.*, 2015; Nirrengarten *et al.*, 2018).

From Aptian to early Cenomanian, magma-poor rifting between Europe and Iberia produced a complex network of marine depocentres, today preserved below the Aquitaine Basin (Angrand *et al.*, 2018), in the North Pyrenean Zone, the Iberian Range and Basque-Cantabrian belt. Mesozoic basins

below the Aquitaine Basin hold rich hydrocarbon resources exploited from the 1950s to 2012 (e.g., Biteau *et al.*, 2006; Serrano *et al.*, 2006). Reconstructions of the rift generally propose a narrow, rifted domain of some 10 s of km in width in the eastern Pyrenees, which broadens considerably to the west before branching into the Bay of Biscay oceanic domain to the NW and the Basque-Cantabrian rift system further south (see García-Senz *et al.*, 2020; Manatschal *et al.*, 2021). Upper Triassic evaporites also thicken westward (Curnelle *et al.*, 1982; Serrano *et al.*, 2006). In the NW Iberian plate a major inherited segment boundary (Pamplona Transfer Zone, Fig. 3; Saspiturry *et al.*, 2022) links the Pyrenean and Basque-Cantabrian rift segments. The nature of this transfer zone continues to be debated (e.g., Lescoutre *et al.*, 2021). Further east on the European plate margin a major transfer zone links the Pyrenean and Provençal rift systems (Corbières-Languedoc Transfer Zone, CLTZ, Fig. 3; Crémades *et al.*, 2021). Although some plate tectonic models integrate a wide early Cretaceous oceanic domain between Europe and Iberia (some 300 km wide; e.g., Sibuet *et al.*, 2004; Vissers and Meijer, 2012a, b), no evidence of oceanic crust (*i.e.*, ophiolites) or of oceanic subduction of appropriate age (e.g., calc-alkaline volcanism) has been found. However, remnants of subcontinental mantle peridotites occur as isolated blocks up to 3 km long, or as clasts within syn-rift sediments in the North Pyrenean Zone (e.g., Lagabrielle and Bodinier, 2008; Jammes *et al.*, 2009; Lagabrielle *et al.*, 2010) and are interpreted as having been exhumed during Aptian-Cenomanian rifting and later integrated into the orogen. The Internal Metamorphic Zone found along the North Pyrenean Zone is defined here as areas in which Mesozoic strata record syn-rift high temperature-low pressure metamorphism (Lagabrielle *et al.*, 2010; Clerc and Lagabrielle, 2014; de Saint Blanquat *et al.*, 2016; Lagabrielle *et al.*, 2020; Ducoux *et al.*, 2021b). Similar areas recording syn-rift HT-LP metamorphism occur within the Basque-Cantabrian belt (Ducoux *et al.*, 2019, 2021b; García-Senz *et al.*, 2020).

Constraining the original width, form and distribution of exhumed mantle domains represents one of the major challenges for Pyrenean reconstructions (e.g., Tugend *et al.*, 2014a, 2014b; García-Senz *et al.*, 2020). Some models envisage exhumed mantle as a laterally continuous domain between symmetric or asymmetric hyperextended rift margins in a pure shear extensional model (e.g., Tugend *et al.*, 2014a, 2014b; see Manatschal *et al.*, 2021 for discussion). Given the highly segmented nature of the rift system (e.g., Jammes *et al.*, 2009), mantle exhumation may alternatively have occurred in distinct rift segments (e.g., García-Senz *et al.*, 2020; Lescoutre and Manatschal, 2020; Lehujeur *et al.*, 2021) or in a patchwork of isolated transtensional or pull-apart basins if strike-slip played an important role along the Pyrenean domain (e.g., Lagabrielle and Bodinier, 2008; Canérot, 2017; Ford and Vergès, 2021; Asti *et al.*, 2022).

The role of inherited crustal structure and the physical properties of the lithosphere were major research themes in the Orogen project (e.g., Dielforder *et al.*, 2019; Jourdon *et al.*, 2019, 2020; Saspiturry *et al.*, 2019, 2022; Cadenas *et al.*, 2021; Lescoutre *et al.*, 2021; Miró *et al.*, 2021). While certain aspects of these subjects are considered here, results are principally presented and discussed in Manatschal *et al.* (2021).

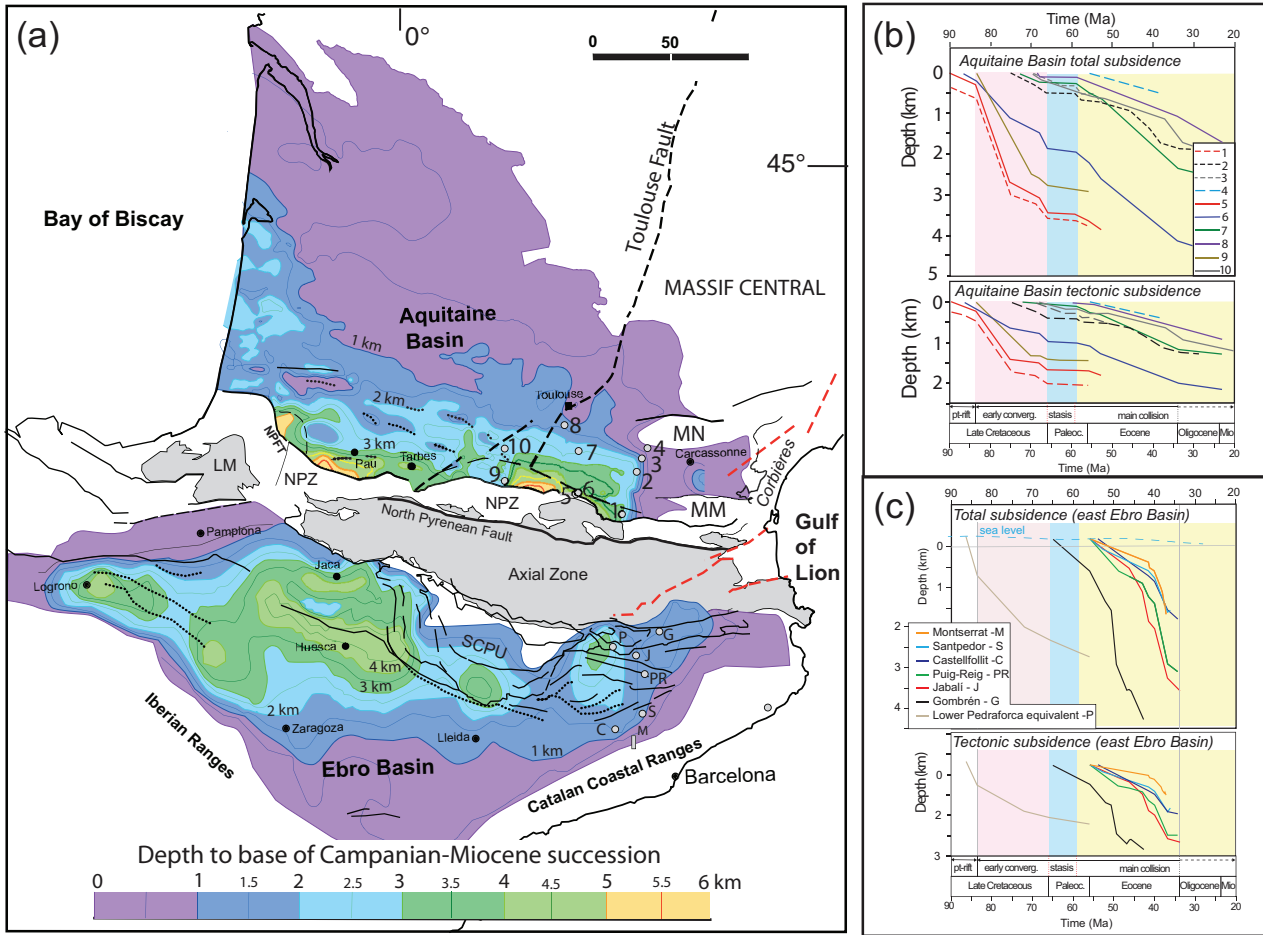


Fig. 5. (a) Present day isodepth map to base of syn-orogenic sediments in km in the onshore Ebro and Aquitaine basins compiled from [Angrand *et al.* \(2018\)](#) for the Aquitaine basin and [Garcia-Castellanos *et al.* \(2003\)](#) for the Ebro Basin. (b) Total and tectonic synorogenic subsidence curves for ten boreholes in the central and eastern Aquitaine basin. Boreholes are located in (a). Data compiled from [Groot *et al.* \(2018; 1–4\)](#), [Ford *et al.* \(2016; 5–8\)](#) and [Rougier *et al.* \(2016, 9–10\)](#) where details of data and calculations can be found. (c) Total and tectonic synorogenic subsidence curves for seven boreholes in the eastern Ebro basin (for details see [Groot *et al.*, 2018](#)). Boreholes and stratigraphic logs used in these calculations are located in (a). The orogenic stages of early convergence, quiescence (stasis) and main collision are indicated by colored bands on the graphs. For abbreviations see [Figure 3](#) caption.

3 Foreland basins and sediment routing systems

Although today, the Pyrenean orogen has distinct pro and retro foreland basins ([Figs. 3 and 5a](#)), during the Late Cretaceous and Paleocene a single large marine basin covered the whole Pyrenean realm, closing to the east (Pyrenean Trough; [Fig. 6a](#)). Several studies also demonstrate that orogenic relief developed first in the east and migrated westward, accelerating in the Eocene and in particular the late Eocene, progressively separating the pro and retroforeland basins ([Puigdefàbregas *et al.*, 1992; Sinclair *et al.*, 2005; Whitchurch *et al.*, 2011; Roigé *et al.*, 2016, 2019; Vacherat *et al.*, 2017](#)). The stratigraphy and sediment routing systems of the pro-foreland basin have been particularly well studied and linked to a southward and westward propagation of growing orogenic relief (*e.g.*, [Puigdefàbregas *et al.*, 1992; Sinclair *et al.*, 2005; Whitchurch *et al.*, 2011; Allen *et al.*, 2013](#)). The

palinspastically restored paleogeographic maps of [Figure 6](#) provide an overview of the distribution of major facies belts and evolution of relief during the main stages of orogenesis with a focus on creation of relief and sediment routing systems. Their construction is summarised in the [Figure 6](#) caption.

3.1 Pyrenean Trough and Aquitaine Basin

The Aquitaine Basin preserves a complete and relatively undeformed syn- to post-orogenic stratigraphy ([Barnolas and Courbouleix, 2001; Serrano *et al.*, 2006; Ford *et al.*, 2016; Rougier *et al.*, 2016; Ortiz *et al.*, 2020, 2022](#)). [Figure 5a](#) shows depth to base of the syn-orogenic succession, which, in the relatively undeformed Aquitaine basin provides a reasonable representation of sediment thickness that decreases northward from over 5 km near the orogen ([Angrand *et al.*, 2018](#)). In the west and central basin and offshore into the Bay of Biscay sedimentation continued into the Neogene ([Bernard *et al.*,](#)

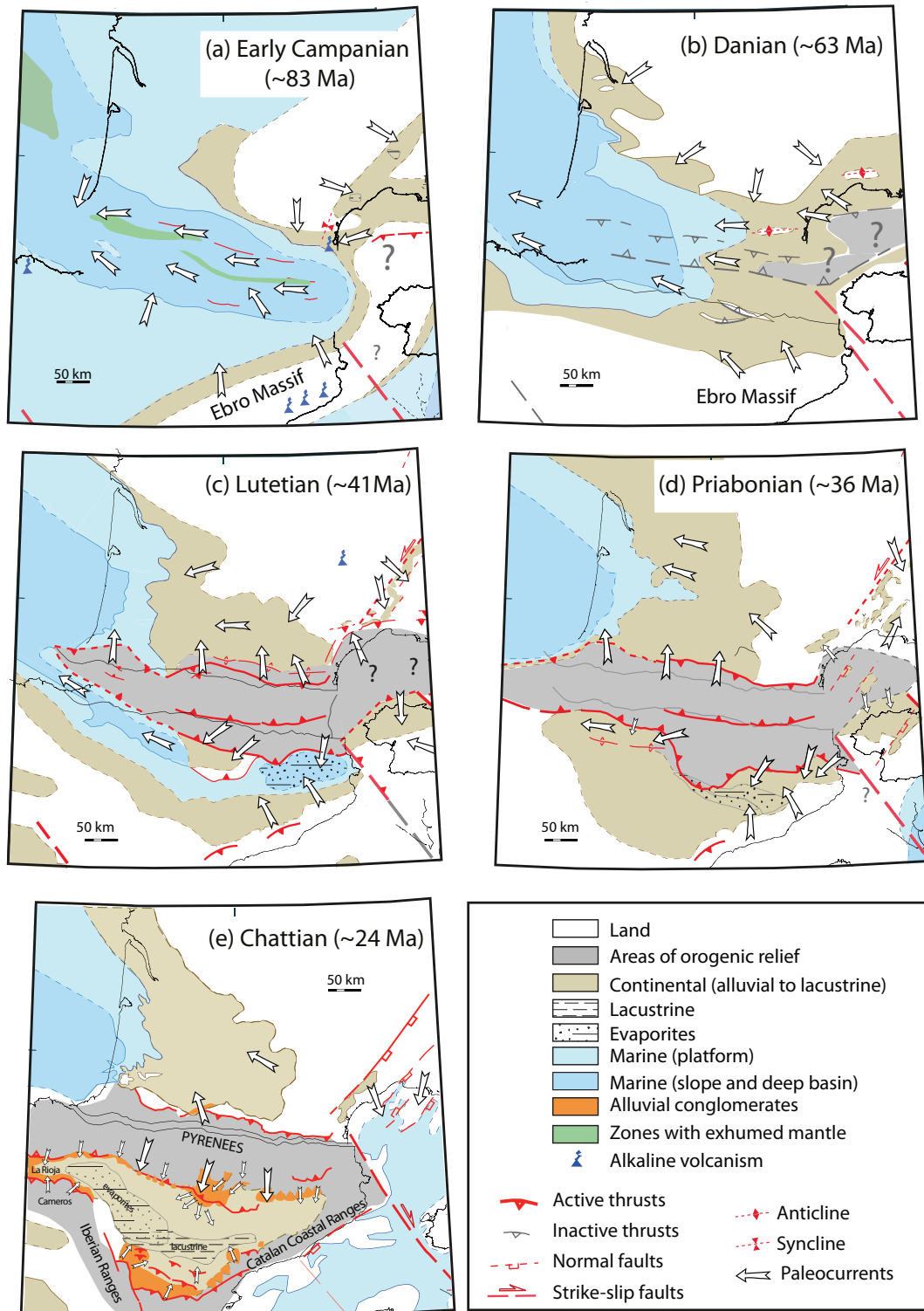


Fig. 6. Paleogeographic reconstructions of the evolution of Pyrenean synorogenic basins, orogenic relief and sediment supply from base Campanian to Oligocene. Using the free G-Plates 2.0 software (Müller *et al.*, 2018) present-day coastlines were restored back in time following the plate kinematic model of Macchiavelli *et al.* (2017) for the western Mediterranean. Paleoenvironments are based on Plaziat (1981), Debrand-Passard *et al.* (1984), Barnolas and Courbouleix (2001), Serrano *et al.* (2006) and Monod and Bourroullec (2014) with restorations by G. Frasca using balanced cross-section presented in Figures 7 and 8 and Vergés (1993). Deformation characteristics (timing, principal structures, amount of shortening) and basin evolution (basin limits, dynamics, major facies, paleocurrents) were integrated using published data. Uncertainties related to the plate kinematic model were reduced by assuring that each step honored data on vertical motion, structural and stratigraphic history.

2020: Ortiz *et al.*, 2020). The Aquitaine basin overlies a salt-rich Aptian-Cenomanian rift system that widens westward (Tugend *et al.*, 2014a; Angrand *et al.*, 2018; Gómez-Romeu *et al.*, 2019; García-Senz *et al.*, 2020; Issautier *et al.*, 2020; Andrieu *et al.*, 2021; Barré *et al.*, 2021; Ducoux *et al.*, 2022). Pre-orogenic Jurassic and Cretaceous diapiric growth sourced from Triassic evaporites has long been recognized across this region (James and Canérot, 1999; Canérot *et al.*, 2005; Biteau *et al.*, 2006; Serrano *et al.*, 2006; Ducoux *et al.*, 2022). Diapiric activity accelerated during Aptian-Cenomanian rifting and later impacted syn-orogenic stratigraphic architecture (Figs. 7a–7d). Top basement today remains in net extension below salt to the west of the Toulouse Fault (Figs. 7a–7d). East of this fault, basin fill onlaps directly onto Variscan basement of the Carcassonne High (Figs. 7e–7g), an area uplifted as part of the Durancian High along the northern shoulder of the eastern and Provençal Albian rift (Peyaud *et al.*, 2005; Séranne *et al.*, 2021). Youngest preserved strata young westward due in part to later uplift and erosion of eastern sectors. Lateral stratigraphic thinning and facies changes, however, show that the basin always closed eastward (Plaziat, 1981; Ford *et al.*, 2016; Figs. 3, 5, 6 and 7). The original width of the eastern Aquitaine Basin is poorly constrained due to late Cenozoic uplift of the southern Massif Central (Barbarand *et al.*, 2001; Peyaud *et al.*, 2005).

Throughout its syn-orogenic history, the Aquitaine Basin opened westward into the Bay of Biscay (Fig. 6). Throughout its history, sediment routing was dominated by longitudinal systems, flowing west. Transverse systems draining from the mountain belt were established only from early Eocene (Fig. 6c). From east to west, facies belts change from continental to marine with a progressive westward migration of continental facies (Fig. 6), interspersed with higher order marine transgressions that can reach to the eastern boundaries of the basin (Plaziat, 1981; Barnolas and Courbouleix, 2001; Serrano *et al.*, 2006; Calvet *et al.*, 2020). Two main phases of subsidence (lasting ~16 myr and ~36 myr respectively) correspond to two regressive cycles associated with early convergence and main collision (Fig. 5b) separated by a period of 7–9 Myrs of little or no subsidence that corresponds to the Paleocene quiescence or stasis (Fig. 5b). These stages correlate well with plate convergence history (Fig. 2: Rougier *et al.*, 2016; Ford *et al.*, 2016; Grool *et al.*, 2018).

The Aquitaine Basin is not a typical retro-foreland basin but has a composite history of subsidence driven initially by post-rift thermal cooling and later by orogenesis (Fig. 5b: *e.g.*, (Desegaulx and Brunet, 1990; Desegaulx *et al.*, 1990; Angrand *et al.*, 2018; Sinclair *et al.*, 2005; Curry *et al.*, 2019). Early convergence did not create significant subaerial relief in the Pyrenees. Instead, structures principally developed below the subsiding Late Cretaceous marine Pyrenean Trough (Fig. 6a: Mouthereau *et al.*, 2014; Vacherat *et al.*, 2014; Ford *et al.*, 2016; Angrand *et al.*, 2018). There is evidence of small local highs within the basin sourcing local sedimentary systems (*e.g.*, Van Hoorn, 1970; Puigdefàbregas and Souquet, 1986). The onset of convergence at 84 Ma correlates with a marked acceleration in subsidence rate and basin deepening in the basin (Fig. 5b: Ford *et al.*, 2016; Rougier *et al.*, 2016; Grool *et al.*, 2018). Substantial volumes of marine clastics sourced principally from the east were deposited during the first regressive cycle in a deep central basin surrounded by shallow

marine carbonate platforms (Fig. 6a: Barnolas and Courbouleix, 2001; Dubois and Seguin, 1978; Serrano *et al.*, 2006; Vacherat *et al.*, 2017). Over 3 km of Upper Cretaceous strata record moderate tectonic subsidence in central and eastern sectors (max. 0.05 to 0.09 mm/yr, Fig. 5b), while in the western basin, subsidence was considerably lower (0.008–0.01 mm/yr; Desegaulx and Brunet, 1990). Equivalent allochthonous basin remnants in the South Central Pyrenees preserve some 6 km of Upper Cretaceous stratigraphy thinning south to 2 km (*e.g.*, Puigdefàbregas *et al.*, 1986, 1992; Thomson *et al.*, 2019; Figs. 8c, 8d and 8f).

During tectonic quiescence from Late Maastrichtian to end Selandian, a low energy fluvial succession (Garumnian facies) sourced from the east (and from local highs) and interspersed with lacustrine and palustrine units, was deposited in the eastern sector passing westward into marine facies (Fig. 6b: Plaziat, 1981; Calvet *et al.*, 2020; Vinciguerra, 2020). This succession marks the top of the first regressive cycle. High resolution dating and correlation of such key non-marine, fossil-poor successions is a major challenge. In the Orogen project, high resolution chemostratigraphy ($\delta^{13}\text{C}_{\text{org}}$) using terrestrial organic matter was combined with magnetostratigraphic and sparse biostratigraphic data to achieve a high resolution chronostratigraphy in this continental succession both in the NE Pyrenees (Maufrangeas *et al.*, 2020) and in the Tremp Basin, SE Pyrenees (Vinciguerra, 2020; Vinciguerra *et al.*, 2022). Thermal or climatic events in the global isotopic record are identified by correlation with the $\delta^{13}\text{C}$ record of marine reference successions. As well as being a powerful correlation tool, such high-resolution chemostratigraphy allows us to better constrain how much time is missing in the stratigraphic record and to understand why such gaps are created. In the fluvial Garumnian facies, for example, Maufrangeas *et al.* (2020) and Vinciguerra *et al.* (2022) propose that gaps can be created by autogenic processes such as river channel avulsion or by external factors such as tectonic or climatic forcing.

At the onset of main collision at the Paleocene-Eocene boundary, acceleration of Aquitaine subsidence correlates with a basin-wide marine transgression (Fig. 5b: Plaziat, 1981; Barnolas and Courbouleix, 2001; Ford *et al.*, 2016; Grool *et al.*, 2018; Calvet *et al.*, 2020). In the east this was followed by a rapid return to continental conditions, while marine facies endured in the west, with a gradual westward migration of the shoreline (Figs. 6c–6e: Ortiz *et al.*, 2020, 2022). Tectonic subsidence in central and eastern areas remained moderate and constant, not exceeding rates achieved during early convergence (0.05 mm/yr, Ford *et al.*, 2016; Rougier *et al.*, 2016; Grool *et al.*, 2018), while to the west it decreased to 0.008 to 0.024 mm/yr at the coast (Desegaulx and Brunet 1990). Transverse sediment routing systems from the growing Pyrenean edifice were established in the Eocene-Oligocene (Figs. 6c–6e: Sinclair *et al.*, 2005; Ternois *et al.*, 2019a, b; Al Reda *et al.*, 2021). A secondary influx from the Massif Central increased toward the end of collision and into the post-convergence phase (Ortiz *et al.*, 2020).

The Aquitaine Basin shows some characteristics of a retro-foreland basin in a collisional orogen, such as a full stratigraphic record of orogenic history and low deformation relative to the proforeland system (Naylor and Sinclair, 2008; Sinclair, 2012; Sinclair and Naylor, 2012; Ortiz *et al.*, 2020,

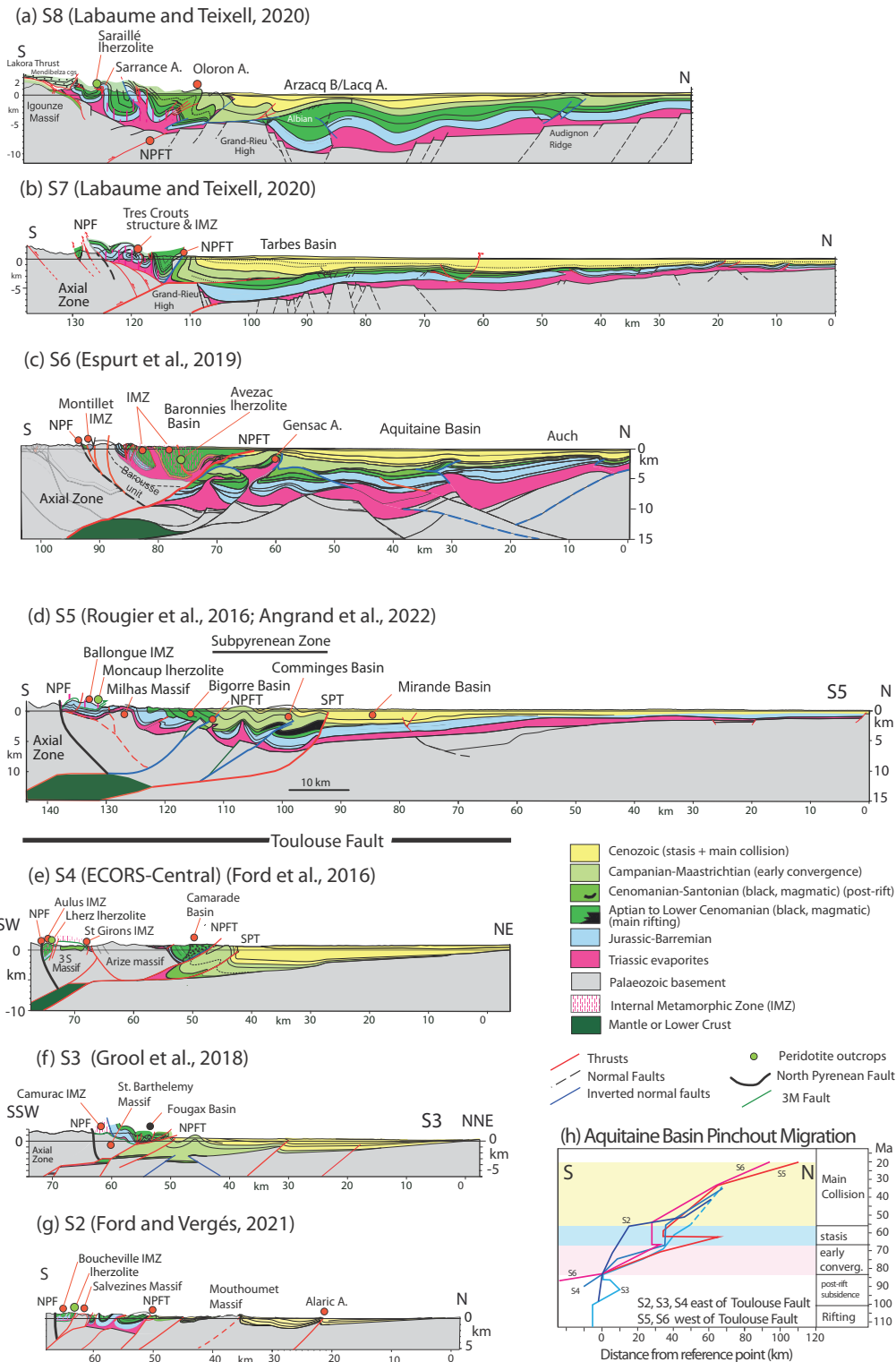


Fig. 7. Compilation of seven cross-sections across the Pyrenean retroforeland system from west to east and located on [Figure 3](#). Authors' estimates of retrowedge shortening are shown in brackets. Estimates derived from cross-section restoration are indicated with an R. Sections are simplified and adapted from (a) and (b) [Labaume and Teixell \(2020\)](#) and [Jourdan *et al.* \(1998\)](#) for northern basins (10–15 km), (c) [Espurt *et al.* \(2019a, b\)](#) (R ~ 42 km), (d) [Rougier *et al.* \(2016\)](#) and [Angrand *et al.* \(2022\)](#) (R ~ 12.5 km), (e) [Ford *et al.* \(2016\)](#) (R ~ 30 km), (f) [Grool *et al.* \(2018\)](#) (R ~ 19 km) and (g) [Ford and Vergés \(2021\)](#) (R ~ 10–12 km). Estimates of shortening exclude emplacement of the Internal Metamorphic Zone (IMZ) and closure of exhumed mantle domains. (h) Graph of pinchout migration of the northern margin of the Aquitaine basin on sections S2 to S6. Colored bars represent orogenic stages as in [Figures 5b](#) and [5c](#).

2022). However, its flexural behavior, subsidence history and pinchout migration pattern, do not correspond to model predictions due mainly to the impact of post-rift thermal cooling (Desegaulx and Brunet, 1990). Using a broken plate flexural model and elastic thickness values for the European plate that correspond to the degree of early Cretaceous rifting, Angrand *et al.* (2018) show flexure of the eastern Aquitaine Basin can be fully accounted for by orogenic loading alone. Immediately west of the Toulouse fault, basin flexure requires contributions from orogenic load, a hidden load (a mantle or lower crustal imbricate(s) in the European upper crust, see Figs. 4c, 4d, 7c and 7d) and a component of post-rift thermal subsidence. In the western Aquitaine Basin, post-rift cooling alone can simulate observed basin subsidence. Tectonic subsidence remained relatively low throughout orogenesis, with a hiatus during late Maastrichtian and Paleocene. There is no indication of a marked decrease in subsidence during late collision as predicted in some models (*e.g.*, Sinclair *et al.*, 2005). Outward migration of the foreland basin margin (pinchout migration) is often used as a proxy for migration of orogenic load (*e.g.*, Allen and Allen, 2013; Sinclair, 2012). Modelled retroforeland basin behaviour typically shows early pinchout migration, followed by stasis as crustal thickening focuses into the prowedge (Sinclair *et al.*, 2005; Sinclair, 2012). The Aquitaine Basin shows relatively slow and constant pinchout migration at ~ 2 mm/yr throughout orogenesis with a phase of backstepping or stasis suggested during Paleocene quiescence (Fig. 7h). Late Cretaceous pinchout migration can be attributed to thermal subsidence and later migration to flexure generated by orogenic, hidden and sediment loads (Angrand *et al.*, 2018). These features illustrate the early but waning influence of thermal inheritance, with stronger and more persistent thermal inheritance in the western basin. The constant pinchout migration until the end of plate convergence also suggests that the Pyrenees never achieved a mass flux steady-state (Willett *et al.*, 1993; Willett and Brandon, 2002; Sinclair, 2012).

3.2 Pro-foreland Ebro Basin

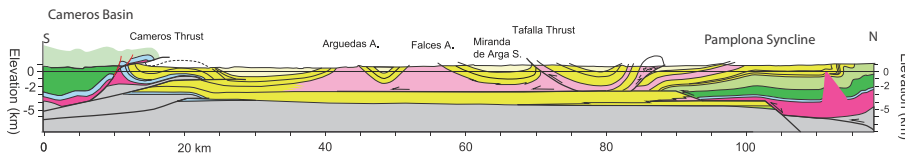
Lying on the Iberian plate, the middle Eocene-Miocene Ebro basin is 120 km at its widest, narrowing to the east and west (Figs. 3 and 5a). Older Eocene-Oligocene depocentres are preserved in thrust sheets north of the South Pyrenean Frontal Thrust. Inner thrust sheets preserve Upper Cretaceous marine turbidites (Pyrenean Trough) with thicknesses up to 6 km (Puigdefàbregas *et al.*, 1986, 1992) (Fig. 8) in the central and western sectors. The Ebro basin is bordered to the SW by the Iberian Range and to the SE by the Catalan Coastal Ranges, active during the Eocene and Eocene-Oligocene respectively (Figs. 3 and 8g; Vergés *et al.*, 1998). The basin developed principally during main collision. Due to significant deformation, erosion and migration of depocentres in the southern Pyrenees the isodepth map in Figure 5 can represent only a minimum estimate of total thickness of the syn-orogenic succession, which can reach over 8 km in western depocenters (Fig. 5a; *e.g.*, Muñoz-Jiménez and Casas-Sainz, 1997), decreasing to 1 km in the eastern depocenter due to a basin-scale westward tilt generated by rift shoulder uplift during Oligocene-Miocene opening of the Valencia Trough (Fig. 3:

Lewis *et al.*, 2000; Vergés *et al.*, 2002; Ethève *et al.*, 2018). Vitrinite reflectance studies in the eastern Ebro Basin suggest burial depths of presently outcropping sediments of between 2750 ± 250 m near the Pyrenean front and 950 ± 150 m near the Catalan Coastal Range (Clavell, 1992; Waltham *et al.*, 2000).

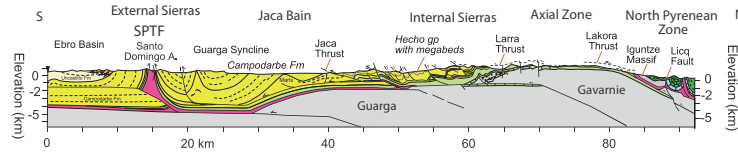
The pro-foreland system consists of distinct domains inherited from Mesozoic rift architecture (east, central, west). In the east, where Upper Triassic evaporites are thin to absent, a classic flexural basin migrated southward ahead of a relatively high friction wedge (Fig. 8g; Vergés *et al.*, 1995, 1998). In the central area, the South Central Pyrenean Unit forms a pronounced low friction salient, transported south above thick Upper Triassic salt (Figs. 8c–8f; Muñoz, 1992; Meigs and Burbank, 1997; Teixell and Muñoz, 2000). Eocene-Oligocene wedge-top depocentres on the South Central Pyrenean Unit record growth and rapid southward migration (Meigs and Burbank, 1997; Burrell and Teixell, 2021). In the Jaca basin further west Triassic evaporites and overlying Mesozoic strata are thin to absent. Less mobile tectonic units and depocentres nevertheless record consistent southward migration (Teixell, 1996; Labaume *et al.*, 2016; Labaume and Teixell, 2018). Finally, the thick (at least 5 km) and relatively narrow western depocentres of Pamplona and La Rioja (Fig. 8a) with substantial syn-orogenic evaporites are confined by the Cameros Thrust to the south and the Pamplona Thrust system to the north (Casas-Sainz and Román-Berdiel, 1999; Muñoz-Jiménez and Casas-Sainz, 1997; Larrasoña *et al.*, 2003). These depocentres link westward into the Duero depocenter, foreland basin to the Basque-Cantabrian belt (Fig. 1)

During the Eocene, the Ebro basin opened to the Atlantic and its stratigraphy records continental to marine facies belts migrating from east to west. Transverse sediment routing systems from the growing eastern Pyrenean edifice fed into longitudinal west-flowing alluvial-fluvial to deltaic to turbiditic systems controlled by actively growing structures of the South Central Pyrenean Unit (*e.g.*, Puigdefàbregas *et al.*, 1992; Nijman, 1998; Costa *et al.*, 2010; Garcés *et al.*, 2020). The late Eocene to early Oligocene corresponds to the period of maximum exhumation in the Axial Zone (*e.g.*, Sinclair *et al.*, 2005; Fillon and van der Beek, 2012; Curry *et al.*, 2021), establishing high transverse sediment supply to the central Ebro Basin. In the latest Eocene to early Oligocene (ca. 36 Ma) the basin became endorheic due to uplift of the western Pyrenees coupled with a eustatic low stand (Costa *et al.*, 2010). A thick succession of southward prograding alluvial-fluvial and lacustrine-palustrine sediments draped across the South Central Pyrenean Unit and Ebro Basin during the Oligocene and into the early Miocene (Fig. 6e; Santolaria *et al.*, 2015; Labaume *et al.*, 2016; Roigé *et al.*, 2019; Garcés *et al.*, 2020; Coll *et al.*, 2020, 2022). The Catalan Coastal Ranges and Iberian Range also provided sediment into the Oligocene basin (Garcés *et al.*, 2020). High sedimentation rates coupled with a continuous rise in base level within the endorheic Ebro Basin led to sediment aggradation that backfilled valleys and eventually buried relief by late Oligocene. along the southern margins of the Pyrenees (J4, J5, Figs. 8d and 8f; Coney *et al.*, 1996; Fillon and van der Beek, 2012) and in the Catalan Coastal Ranges (Lawton *et al.*, 1999) During the Tortonian (7.5–11 Ma) the Ebro basin was deeply incised by back-cutting drainage flowing into the Mediterranean, causing isostatic

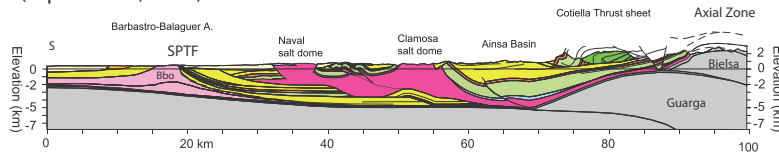
(a) J8 (Muñoz-Jiménez & Casas-Sainz 1997; Larrasoña *et al.* 2003)



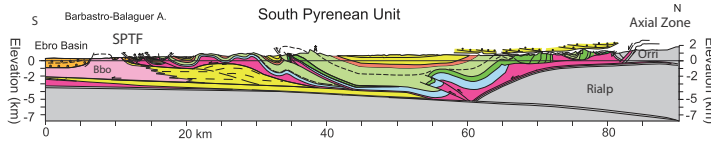
(b) J7 (Teixell, 1996)



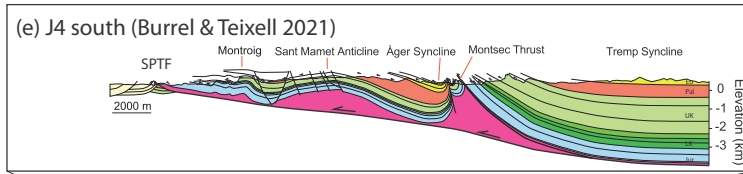
(c) J6 (Espurt *et al.*, 2019)



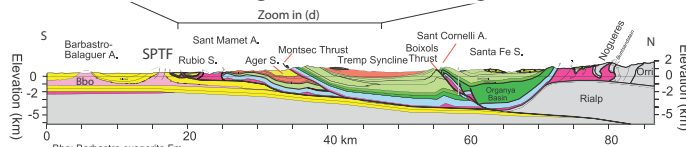
(d) J5 (Teixell & Munoz, 2000)



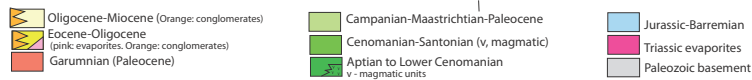
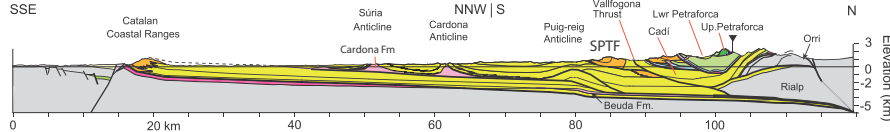
(e) J4 south (Burrell & Teixell 2021)



(f) J4 (ECORS Central, Meigs & Burbank 1997, Vergés, 1993)



(g) J3 (Vergés *et al.* 1998, Grool *et al.* 2018)



Pamplona

Jaca

South Central Pyrenean Units

Petraforca

Fig. 8. Cross-sections across the south Pyrenean proforeland system, all located in Figure 3 and organised from west to east. Shortening estimates across the whole south vergent system of cited authors, derived from cross-section restoration, are shown in brackets. (a) J8 (~ 40 km) adapted from Larrasoña *et al.* (2003) and Muñoz-Jiménez and Casas-Sainz (1997); (b) J7 (48 km), adapted from Teixell (1996). (c) J6 (85 km) adapted from Espurt *et al.* (2019a, b). (d) J5 (> 60 km) adapted from Saura *et al.* (2016). (e) Detailed section along the southern South Central Pyrenean Unit of the ECORS central line (J4 south, Fig. 3) showing strong salt influence, adapted from Burrell and Teixell (2021). (f) J4 (66–88 km) along the ECORS central deep seismic line adapted from Meigs and Burbank (1997) and Vergés (1993). (g) J3 (92 km) adapted from Vergés *et al.* (1998) and Grool *et al.* (2018).

rebound of the basin, the South Central Pyrenean Unit and south central Axial Zone (see Sect. 6.3; Garcia-Castellanos *et al.*, 2003; Fillon *et al.*, 2013b; Tucker and van der Beek, 2013; Garcia-Castellanos and Larrasoana, 2015). The opening of the Gulf of Lion in the Oligocene-Miocene also generated strong uplift and erosion of the eastern Pyrenees (*e.g.*, Gunnell *et al.*, 2008; Suc and Fauquette, 2012; Huyghe *et al.*, 2020).

Tectonic subsidence curves from the eastern Ebro Basin (Figs. 5c) record principally the main collision stage showing a “classic” acceleration in subsidence during collision (Heller *et al.*, 1988; Miall, 1995; DeCelles and Giles, 1996; Xie and Heller, 2009; Sinclair, 2012; Allen and Allen, 2013). Tectonic subsidence rates increased to 0.15 mm/yr (Vergés and Burbank, 1996; Grool *et al.*, 2018) driven by progressive subduction of the Iberian plate and topographic growth of the range (Sinclair, 2012). These tectonic subsidence rates are relatively low to moderate compared to other proforeland basins (Xie and Heller, 2009; Sinclair and Naylor, 2012) reflecting the overall low convergence of the Pyrenean orogen. Anomalously high local subsidence in the South Central Pyrenean Unit (*e.g.*, Ager Syncline, Fig. 8e) during the Paleocene quiet period was driven by halokinetic activity as shown by recent work of Burrel and Teixell (2021).

4 Pyrenean wedge dynamics and the role of salt

We here summarise the style, timing and distribution of deformation in the Pyrenean retrowedge and prowedge systems, with particular emphasis on wedge dynamics and the role of salt.

4.1 Evaporite distribution and halokinetic activity

The rapid development of new salt tectonic concepts continues to stimulate critical reassessment of, and new insights into, the dynamics of salt-rich orogenic systems (*e.g.*, Duffy *et al.*, 2018). In the Pyrenees the evaporite-rich Middle to Upper Triassic Keuper Group is the main decoupling level between Variscan basement and Mesozoic sedimentary cover (*e.g.*, McClay *et al.*, 2004; Caméra *et al.*, 2017; Muñoz, 2019) with secondary evaporite layers locally occurring in Middle Triassic Muschelkalk units and in overlying Hettangian units. Several Orogen projects, have investigated salt tectonic features on local and regional scales across the Pyrenees and adjacent regions, principally documenting the role of salt during rifting stages. In the Toulon belt of southern Provence (Fig. 1), Wicker and Ford (2021) identify halokinetic activity from Jurassic rifting to early Pyrenean compression during the Campanian along the salt-rich Toulon and Bandol Thrusts. In the Corbières-Languedoc Transfer Zone (CLTZ, Fig. 3) of the NE Pyrenees, Crémades *et al.* (2021) report three-dimensional extensional growth on faults detaching on Upper Triassic salt during the Jurassic. These complex decoupled depocentres developed above intersecting sets of extensional basement faults of the Pyrenean and alpine Tethys rift systems. In the easternmost North Pyrenean Zone, Ford and Vergés (2021) document the development of synclinal depocentres (longitudinal minibasins) between salt walls during Early Cretaceous transtension followed by Pyrenean tightening of synclines and

closure of salt walls to form near vertical welds. In the western Aquitaine foreland, Issautier *et al.* (2020) and Ducoux *et al.* (2022) describe Aptian-Cenomanian halokinetic control on syn-rift synclinal depocentres (sag basins) in the rift necking domain while, further south in the distal domain Saspiturry *et al.* (2021) and Lescoutre *et al.* (2021) evoke salt control on the development of the Mauléon and Cantabrian basins (Fig. 3). Miró *et al.* (2021) emphasise the key role of salt during extension and inversion of the Basque-Cantabrian belt. Burrel and Teixell (2021) and Burrel *et al.* (2021) document detailed tectono-stratigraphic features recording halokinetic activity in the eastern South Central Pyrenean Unit from Jurassic to Oligocene (Fig. 8f). These new results contribute to a growing body of work describing and quantifying in time and space the role of salt during different stages of the cycle (*e.g.*, Lopez-Mir *et al.*, 2014, 2015; Saura *et al.*, 2016; Caméra and Flinch, 2017; Labaume and Teixell, 2020; Hudec *et al.*, 2021). The structural and stratigraphic complexity of inverted salt-rich rift systems, the difficulties in estimating original salt volumes and its depletion or migration through time, render the construction and restoration of cross-sections and basin geometries particularly challenging in this orogen (*e.g.*, see Rowan and Ratliff, 2012).

The present-day distribution of Upper Triassic evaporites across the Pyrenees and adjacent areas is represented in Figure 9. Four onshore regions are notable for their abundant Upper Triassic evaporites (>1 km) and well-developed diapirs: two on the Iberian plate, the Basque-Cantabrian belt (up to 2700 m in southern sectors; Ramos *et al.*, 2022) and the South Central Pyrenean Unit (SCPU; up to 2700 m; Rios, 1948; Serrano and Martínez del Olmo, 1990; Lopez-Mir *et al.*, 2014; Saura *et al.*, 2016; Caméra and Flinch, 2017; Espurt *et al.*, 2019a; Burrel and Teixell, 2021), and two on the European plate, the western NPZ and western Aquitaine Basin (>1000 m; see Figs. 8a and 8c; Henry and Zolnai, 1971; Canérot, 1988; James and Canérot, 1999; Canérot *et al.*, 2005; Biteau *et al.*, 2006; Serrano *et al.*, 2006; Espurt *et al.*, 2019a; Labaume and Teixell, 2020) and the eastern North Pyrenean Zone and Corbières-Languedoc Transfer Zone (Viallard, 1987; Gorini *et al.*, 1991; Ford and Vergés, 2021; Crémades *et al.*, 2021). The remaining Pyrenean thrust belts are characterized by absent, thin and often discontinuous Upper Triassic evaporites. In the Basque-Cantabrian fold belt, Upper Triassic evaporites reach thicknesses of 6–7 km in the cores of some salt-cored anticlines and outcropping diapirs (Caméra, 2017; Miró *et al.*, 2021; Ramos *et al.*, 2022). The offshore Basque-Parentis domains also have thick Upper Triassic evaporites and abundant diapirs (Ferrer *et al.*, 2008, 2012; Roca *et al.*, 2011). The diapiric domain of the South Central Pyrenean Unit integrates the northern boundary in the Cotiella (Lopez-Mir *et al.*, 2015), Sopeira-Sant Gervàs (Saura *et al.*, 2016) and Bóixols Basins and the entire South Central Pyrenean Mesozoic Basin (allochthonous South Central Unit) with significant diapiric activity along the Montsec and Serres Marginals thrusts (Burrel and Teixell, 2021; Figs. 3 and 8). In the eastern North Pyrenean Zone and Corbières-Languedoc Transfer Zone, large diapirs are at, or just below surface in Oligocene extensional basins or are found within or below the Corbières Nappe.

In addition to Upper Triassic evaporites, four Cenozoic (Eocene to Miocene) evaporite-rich formations (Beuda,

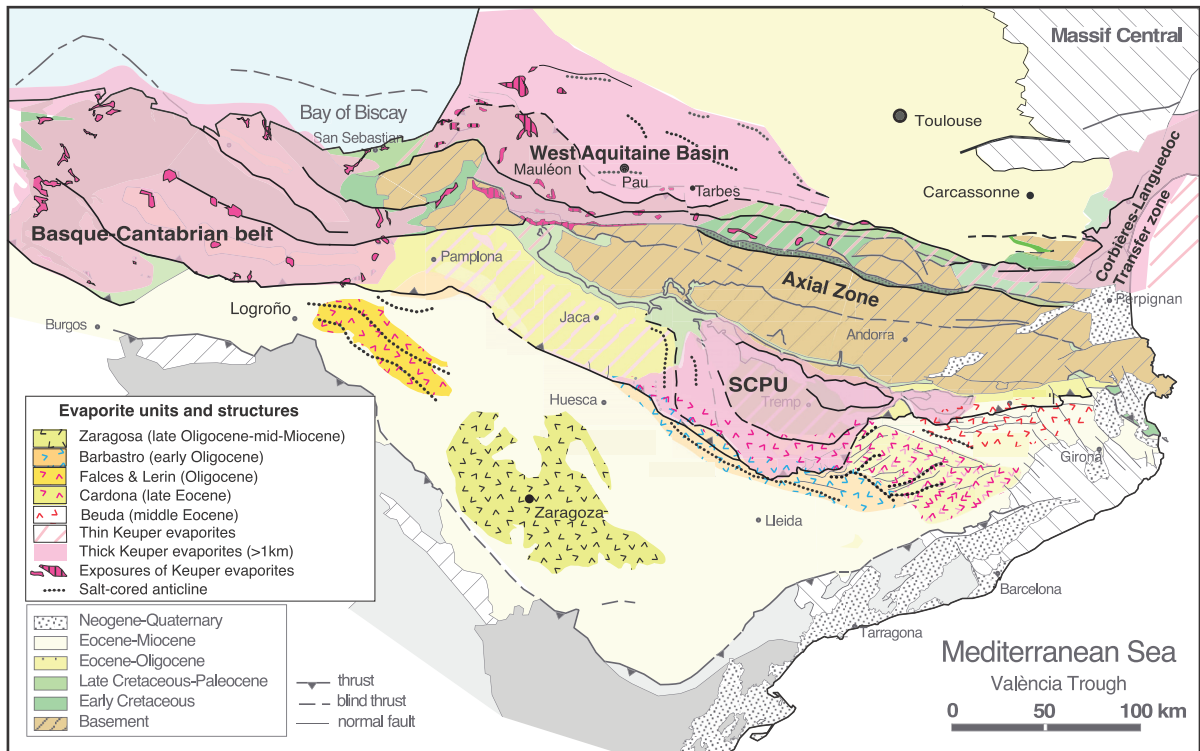


Fig. 9. Simplified tectonic map of the Pyrenees and adjacent regions (adapted from Vergés *et al.*, 2002) showing the distribution of evaporitic deposits of Upper Triassic and Cenozoic age. Based on Caméra (2017) and Caméra and Flinch (2017) for the Basque-Cantabrian belt and South Central Pyrenean Unit. In both the western Aquitaine Basin-Mauléon and the Corbières-Languedoc Transfer Zone evaporite distribution is mostly compiled from French BRGM geological maps, with data from Curnelle *et al.* (1982), Viillard (1987), Gorini *et al.* (1991) and Serrano *et al.* (2006) and Crémades *et al.* (2021). The distribution of Eocene to early Miocene marine and lacustrine evaporites in the Ebro Basin is based on Vergés (1993) in the east and Garcés *et al.* (2020) in the west.

Cardona, Barbastro, Zaragoza) were deposited in the eastern, southern and southwestern sectors of the Ebro Basin, younging progressively south and west (Figs. 9 and 8; Salvany, 1989; Vergés, 1993; Alonso-Zarza *et al.*, 2002; Garcés *et al.*, 2020). Further west, thick Oligocene evaporites (Falces and Lerin formations) were deposited in the Pamplona-Logroño region (Figs. 8a and 9; Alonso-Zarza *et al.*, 2002).

Figure 10 presents a compilation of the chronology of halokinetic activity based on recent studies across the Pyrenees, the Basque-Cantabrian belt, Provence and adjacent areas, showing a chronological relationship between the principal tectonic stages of the Pyrenean orogenic cycle and periods of diapiric activity. Upper Triassic salt was first mobilised during Jurassic gentle rifting and post-rift subsidence. This is particularly well documented in eastern Pyrenean regions that were affected by Jurassic Tethyan rifting (*e.g.*, Crémades *et al.*, 2021; Vergés *et al.*, 2020). A major phase of passive diapirism during Aptian-Cenomanian rifting affected the whole Pyrenean area. In regions of significantly thicker salt (Fig. 9), suprasalt synclinal basins and minibasins of Aptian-Cenomanian age are documented (*e.g.*, Issautier *et al.*, 2020; Ford and Vergés, 2021; Ducoux *et al.*, 2021a, b; Ramos *et al.*, 2022).

Large-scale northward verging gravity-driven extensional systems above Upper Triassic salt detachments developed

during Early to early Late Cretaceous (post-rift phase) along the northern margin of the Iberian Plate. These features are preserved along the northern edge of the South-Central Pyrenean Unit (Fig. 3) from the easternmost Upper Pedraforca thrust sheet (Vergés *et al.*, 1995), the Sopeira, Faieda and Montiberri minibasins in the Noguera Ribagorçana (Saura *et al.*, 2016; Muñoz, 2019); and the Cotiella Massif in the west (Seguret, 1972; McClay *et al.*, 2004). When Pyrenean shortening is restored, north-dipping salt-related low-angle listric normal faults, sometimes parallel to the northern flank of Upper Triassic salt walls, define a north-directed gravitational extensional system that controlled deposition of Upper Albian to Santonian halokinetic sequences (Saura *et al.*, 2016). More to the west again, the Basque-Cantabrian Basin shows widespread halokinetic activity during the Jurassic and Cretaceous (Fig. 10), most recently interpreted by Caméra (2017), Miró *et al.* (2021) and Ramos *et al.* (2022). This extensional domain is characterized by an intricate network of diachronous depocenters defined by long E-W trending salt-walls connected to shorter N-S salt walls. The north-directed gravity-driven extensional system on the Iberian margin is mirrored by south-verging gravitational systems locally documented along the eastern European margin (Ford and Vergés, 2021). Although these gravity-driven conjugate domains are beginning to be well documented (*e.g.*, Labaume

and Teixell, 2020), a complete understanding of their extensional geometries and evolution at the regional scale cannot be achieved until their original relative positions can be restored with confidence.

During the post-rift stage (early Late Cretaceous) diapiric activity also continued in the Toulon belt in Provence (Fig. 1), driven by local sediment loading (Wicker and Ford, 2021). It is now becoming clear that salt structures can have a primary influence on structural development of fold and thrust belts due to their ability to localize strain (e.g., Duffy *et al.*, 2018). As will be described below salt decoupling levels and diapiric features were variably reactivated during Pyrenean orogenesis depending on thickness of the source layer and their position in the foreland systems (e.g., Vergés *et al.*, 1992). Miró *et al.* (2021) analyse the role of Upper Triassic evaporites in the Basque-Cantabrian fold belt during both extension and compression, showing that both thin-skinned and thick-skinned styles of inversion can develop coevally depending on the thickness of pre-orogenic salt.

4.2 Dating the onset of Pyrenean shortening

Constraining the timing of onset of convergence in an orogen using different datasets can give contradictory results. However, along and across the Pyrenean domain estimates for the onset of convergence-related deformation are remarkably consistent whether derived from tectonostratigraphic field observations, foreland basin subsidence histories described here and elsewhere (Figs. 2, 5b and 5c; e.g., Teixell *et al.*, 2018; Muñoz, 2019) or low temperature thermochronology (e.g., Mouthereau *et al.*, 2014; Ternois *et al.*, 2019a, b). Bracketed between the late Santonian and early Campanian (84–83 Ma) these dates correspond well with the onset of Africa-Europe convergence (Fig. 2; Olivet, 1996a, b; Srivastava *et al.*, 2000; Vissers and Meijer, 2012a, b; Macchiavelli *et al.*, 2017; Angrand and Mouthereau, 2021).

It must be acknowledged, nevertheless, that deformation and vertical motions of Cenomanian to Santonian age across the Pyrenees and adjacent areas are documented and have been interpreted as evidence of an earlier onset of Iberia-Europe convergence, in particular in eastern sectors now destroyed by the opening of the Gulf of Lion (e.g., Guennoc *et al.*, 2000; Bache *et al.*, 2010). Two Orogen studies contribute to this debate, one on a local scale in Provence (Wicker and Ford, 2021) and the other on a more regional scale in the western and central Pyrenees (Andrieu *et al.*, 2021).

The salt-rich Toulon belt of Provence (TB, Fig. 1; Bestani *et al.*, 2016; Espurt *et al.*, 2019b) lies at the eastern-most limit of the Pyrenean orogen. Tectonostratigraphic relationships here have long been interpreted to record onset of convergence before latest Santonian (Fig. 1; Masse and Philip, 1976; Philip *et al.*, 1987; Hennuy, 2003). New structural and stratigraphic mapping by Wicker and Ford (2021) of growth structures in the eastern Toulon belt, documents strong local halokinetic activity of Keuper evaporites from Jurassic extension through to Pyrenean inversion. While these new findings provide a new explanation for Coniacian-Turonian growth strata in the area they do not negate the possibility of early onset of Pyrenean convergence in Provence. An additional observation, which may support the idea is the abrupt arrival of pure quartz sands

into Coniacian and Turonian depocentres in the Toulon area suggesting the creation of new relief, which could be related to enhanced tectonic activity (e.g., Hennuy, 2003).

Working on a more regional scale in the central Pyrenees, Andrieu *et al.* (2021) document variations in platform geometry, sedimentary facies and accommodation rates from Cenomanian to Santonian across a 400 km E-W transect of the Iberian margin. The authors attribute northward flexure of the Iberian margin during the Coniacian to early onset of Pyrenean NS compression. While this may be a possibility, differential post-rift thermal subsidence could also generate such regional basinward tilting.

4.3 Retrowedge geometry and dynamics

The North Pyrenean Zone (NPZ; width 18–30 km; Fig. 7) incorporates the inherited rift architecture and Upper Triassic evaporites, preserving a record of early convergence and main collision stages (Fig. 2; Macchiavelli *et al.*, 2017). The NPZ is here divided into western (cross-sections S6-S8; Fig. 7) and eastern sectors (cross-sections S2-S4; Fig. 7) separated by the Toulouse Fault in the foreland linking to a more diffuse transition zone in the NPZ (cross-section S5, Fig. 7). The western sector is characterised by a broad rifted area, less total shortening (described below) and a shallower erosion level. The eastern sector is more deeply eroded so that the orogenic record is more incomplete and fragmentary. Nevertheless, the distribution of orogenic deformation in time and space here is different with respect to the western sector. The eastern axis of Aptian-Albian rifting was displaced to the south with respect to the western axis. Both sectors record early convergence when domains of exhumed mantle below the Pyrenean Trough closed (e.g., Teixell *et al.*, 2016) and shortening was accommodated across the rifted margins by inversion of basement faults with formation of divergent structural fans in overlying Mesozoic successions. During main collision these early structural fans were incorporated into the NPZ to become the present day retrowedge.

While shortening in the retrowedge is difficult to constrain accurately, estimates are generally low (see Fig. 7 for published estimates) and represent some 10 to 15% of total orogen shortening, half of which was accommodated during early convergence and the rest during main collision (Grool *et al.*, 2018). The principal North Pyrenean Frontal Thrust (NPFT) is marked by an abrupt northward decrease in orogenic strain that migrated slowly north by some 50 km during orogenesis (e.g., Grool *et al.*, 2018; Espurt *et al.*, 2019a, b). On crustal scale models the NPFT roots downward onto the main tectonic boundary that accommodates underthrusting of Iberian lithosphere (Fig. 4). Its sinuous map trace follows a complex network of inverted salt-rich basement-cutting faults inherited from earlier rifting episodes (Fig. 3). These faults variably record both early inversion (Late Cretaceous) and Eocene-Oligocene thrusting (Fig. 7; Rocher *et al.*, 2000; Rougier *et al.*, 2016; Grool *et al.*, 2018; Fillon *et al.*, 2020; Labaume and Teixell, 2020; Barré *et al.*, 2021).

The western NPZ preserves distal Aptian-Cenomanian rift depocentres of the hyperthinned and exhumed mantle domains, strongly overprinted by syn-rift HT-LP metamorphism and metasomatism (Internal Metamorphic Zone, IMZ;

Figs. 7a–7c) recording geothermal gradients of 60–80 °C/km (Vacherat *et al.*, 2014; Labaume and Teixell, 2020; Saspiturry *et al.*, 2020; Izquierdo-Llavall *et al.*, 2020; Ducoux *et al.*, 2021b). Low to moderate Pyrenean shortening is recorded here (e.g., Labaume and Teixell, 2020; Lescoutre *et al.*, 2021) without significant cooling during early convergence (Vacherat *et al.*, 2014; Bosch *et al.*, 2016). NPZ Mesozoic cover was deformed by early folding and thrusting decoupled on Upper Triassic evaporites (Figs. 7a and 7b), superimposed on syn-rift folds created by halokinetic activity (minibasins) and local basinward gravity gliding above salt (e.g., Tres Crouts structure, Fig. 7b) (Corre *et al.*, 2016; Izquierdo-Llavall *et al.*, 2020; Labaume and Teixell, 2020; Saspiturry *et al.*, 2019; Teixell *et al.*, 2016). The western NPFT follows the inverted boundary between necking and distal rift domains. West of Pau the front is traced along a network of blind thrusts within Cretaceous strata, for example below the Oloron anticline on section S8 (Fig. 7a; Labaume and Teixell, 2020). There are few other significant north verging structures here. In contrast, well developed early Pyrenean south verging thrusts are traced through and around the west plunging Axial Zone (e.g., Lakora and Larra Thrusts, Figs. 7a and 7b; Teixell, 1996; Caldera *et al.*, 2021). Observations indicate that in the western NPZ, limited Pyrenean shortening during early convergence was accommodated by closure of exhumed mantle domains and development of a doubly verging deformation system involving distal rift fill and shallow basement. Paleomagnetic work of Izquierdo-Llavall *et al.* (2020) indicates that decoupled early NPZ structures were then tilted northward-by-northward emplacement of a basement wedge below Upper Triassic evaporites during main collision.

In the transition zone between western and eastern rift domains, the NPFT is an inverted normal fault sealed by Upper Cretaceous strata (S5; Fig. 7d). Cenozoic shortening propagated north to the Subpyrenean Thrust, an inverted normal fault between proximal and necking domains (S5; Fig. 7d). The thrust front thus transitions eastward to the necking-proximal domain boundary. East of the Toulouse Fault, the NPFT continues as the inverted salt-rich northern boundary of a very narrow necking domain (S2–S4, Fig. 7; Mouthereau *et al.*, 2014; Ford *et al.*, 2016; Grool *et al.*, 2018; Ford and Vergés, 2021). The degree of inversion along this fault zone decreases eastward until top basement records net extension south of the Mouthoumet Massif (Fig. 3, cross-section S2, 7g; Ford and Vergés, 2021).

The eastern NPZ is more deeply eroded than the western sector and thus structural geometries and ages are more difficult to constrain. Distinct inverted Aptian-Cenomanian grabens and half grabens (e.g., Fougax, Camarade, Bigorre, S3–S5; Fig. 7) are separated by inverted basement blocks (e.g., Arize, Trois Seigneurs, Saint Barthelemy). Thin, sparse and discontinuous Upper Triassic evaporites occur along most major tectonic boundaries and along top basement. Thin salt may be an original feature but could also be due, at least in part, to its removal through flow, extrusion, and dissolution. In the easternmost NPZ synrift salt thickness increases (Fig. 7) as recorded by salt-based synclinal basins between salt walls, rafts separated by salt rollers and turtle structures (e.g., S2, Fig. 7; Ford and Vergés, 2021). Local early post-rift (Cenomanian) basinward gravity gliding of stratal blocks is also documented here (Montagne de Tauch; de Graciansky,

1962). Pyrenean shortening created secondary welds or weld-faults, often preserved between back-to-back tightened synclines. The NPZ finally curves eastward into the N-S trending Corbières-Languedoc transfer zone (Fig. 3) where syn-orogenic successions north of the Mouthoumet massif lie in superimposed N-S and E-W folds and are overthrust from the east by the salt-rich Corbières nappe that records significant rotations (Rouvier *et al.*, 2012). The transfer zone is primarily controlled by the presence of thick Triassic salt and reactivation of both the inherited NE-trending Tethyan passive margin crustal structures and the superimposed Pyrenean E-W rift system (Crémades *et al.*, 2021).

In the eastern sector and transition zone, the Internal Metamorphic Zone (IMZ) is preserved as deeply eroded fault-bound units lying immediately north of the NPF (Figs. 7d–7g; Clerc *et al.*, 2015; Ternois *et al.*, 2019a, b; Ducoux *et al.*, 2021a). It is generally agreed that these high temperature IMZ units originated from the exhumed mantle and hyperextended domains (e.g., Clerc and Lagabrielle, 2014, 2015) and were tectonically emplaced northward (and also probably southward) onto the low grade necking domain during early orogenesis along the 3M Fault (Figs. 4d–4f and 7d–7f; Grool *et al.*, 2018; Angrand *et al.*, 2022; Ducoux *et al.*, 2021b). Similarly, the easternmost Boucheville IMZ (S2, Fig. 7g) consists of detached and shortened hot sedimentary cover that formed as an allochthonous unit bordered by divergent thrusts during closure of the distal rift domain (Fig. 5; Chelalou *et al.*, 2015; Clerc *et al.*, 2016; Ternois *et al.*, 2019a, b).

In the southern side of the easternmost Pyrenees, the oldest south-vergent thrust sheets, the Upper Pedraforca klippe (Fig. 8g) and the Bóixols thrust sheet (Organyà basin, Fig. 8f), carry non-metamorphosed syn-rift successions of the proximal Iberian margin (Muñoz, 1992; Vergés, 1993; Mouthereau *et al.*, 2014; Laumonier, 2015; Calvet *et al.*, 2020; Ternois *et al.*, 2019a, b; Figs. 4d–4f). Laumonier (2015) roots these structures into the NPZ, suggesting that along with north-vergent NPZ structures, they formed part of an early divergent structural fan, corresponding to that observed in the western NPZ (Labauume and Teixell, 2020) but largely destroyed by later uplift and erosion.

In the western Aquitaine basin, top basement remains in net extension (Figs. 7a–7d), while, above Upper Triassic salt, gentle shortening of both Late Cretaceous and Eocene-Oligocene age (total < 5 km) is focused on salt-rich fault zones and salt-cored anticlines, ridges and diapirs (e.g., Gensac and Saint Marcet anticlines, S6–S8, Fig. 7; Jourdan *et al.*, 1998; Canérot *et al.*, 2005; Serrano *et al.*, 2006; Biteau *et al.*, 2006; Rocher *et al.*, 2000). In contrast, in the eastern foreland (east of the Toulouse Fault) basement-cored north vergent anticlines (e.g., Mouthoumet, Alaric) accommodate 2–3 km of Pyrenean shortening increasing in amplitude eastward (Figs. 4 and 7e–7g; Christophoul *et al.*, 2003; Ford *et al.*, 2016; Grool *et al.*, 2018). This structural style is typical of a broken foreland, where anticlines develop due to inversion of inherited basement faults (e.g., Laramide orogen; McQueen and Beaumont, 1989; Jordan, 1995).

In the eastern sector, the Axial Zone is separated from the NPZ by the North Pyrenean Fault (NPF), a steep fault zone recording late uplift of the Axial Zone. This fault loses definition in the western sector (Figs. 3 and 7) and is lost west of Pau as the Axial Zone plunges below its Mesozoic cover,

implying that the two phenomena are related. The NPF has been variably interpreted as the Iberia-Europe plate boundary (Choukroune, 1974; Soula and Bessière, 1980; Canérot *et al.*, 2005), as a transtensional or normal fault zone inherited from Early Cretaceous rifting (Choukroune and Mattauer, 1978; Roure and Choukroune, 1998) that was later rotated and reactivated (*e.g.*, Cochelin *et al.*, 2018; Teixell *et al.*, 2018; Espurt *et al.*, 2019a; Angrand *et al.*, 2022), or some combination of these. Recent thermomechanical models simulating shortening of a salt-rich rifted lithosphere and integrating synorogenic erosion and sedimentation (*e.g.*, Grool *et al.*, 2018, 2019; Jourdon *et al.*, 2019; Ternois *et al.*, 2021b), reproduce steep faults in a similar position to the NPF that accommodate the relative uplift of the inner prowedge with respect to the more slowly evolving retrowedge. The NPF may therefore not have the plate boundary significance often attributed to it in regional models.

4.4 Prowedge geometry and dynamics

The prowedge consists of the Axial Zone and south Pyrenean thrust belt, which links westward across the Pamplona transfer zone with the Basque-Cantabrian belt (Fig. 3). The southern Pyrenees are probably one of the best-known thrust belts in the world due to extensive research facilitated by outstanding exposures, accessibility, an excellent open access geological database and deep geophysical imagery. Thrust sheets were emplaced southward onto the Iberian plate from Late Cretaceous onward but principally during early Eocene-early Miocene main collision. Eocene-Miocene growth of the prowedge and its foreland basin is principally controlled by plate kinematics, critical wedge dynamics and its interactions with surface processes and the distribution and thickness of Upper Triassic and other evaporitic levels. Inherited rift architecture also played a role but to a much lesser degree compared with the retrowedge (Jourdon *et al.*, 2019; Ternois *et al.*, 2021a). The Axial Zone consists of Iberian upper crustal allochthonous units emplaced southward to form an antiformal stack (Fig. 4; *e.g.*, Roure *et al.*, 1989; Muñoz, 1992; Beaumont *et al.*, 2000; Mouthereau *et al.*, 2014; Teixell *et al.*, 2018, *etc.*). New microstructural and petrological studies coupled with geochronological dating demonstrate that distributed shortening under sub-greenschist and greenschist conditions affected the Iberian upper crust during early Pyrenean plate convergence, followed during main collision by localization of shear onto major thrusts (Airaghi *et al.*, 2019; Bellahsen *et al.*, 2019; Waldner *et al.*, 2021). This early distributed or ductile crustal shortening represents between 1 and 2 km, and in the Eaux Chaudes massif can be higher (Caldera *et al.*, 2021).

South Pyrenean thrust sheets lie in three domains, Pedraforca (east), South Central Pyrenean Unit (centre) and Jaca (west), inherited from the Iberian Mesozoic rifted margin (Fig. 8). Upper Triassic evaporites are particularly abundant below the central area (South Central Pyrenean Unit), being thin to absent in adjacent areas (Figs. 8 and 9). The South Central Pyrenean Unit (defined by Seguret, 1972) forms a low friction salient with a well-developed Jurassic to upper Cretaceous stratigraphy arranged in three thrust sheets (Bóixols, Montsec and Serres Marginals) and bounded by

oblique ramps (Figs. 3 and 8). Triassic evaporites thin under the Montsec thrust sheet and to a lesser extent below the Serres Marginals (*e.g.*, Vergés, 1993; Saura *et al.*, 2016; Cámara and Flinch, 2017; Burrel and Teixell, 2021; Hudec *et al.*, 2021). The Aptian-Albian syn rift successions of the Bóixols and Upper Pedraforca thrust sheets originally lay along the northern rifted margin of the Iberian plate. The onset of exhumation in the basement Noguères Zone during Late Cretaceous (NT, Fig. 3; Beaumont *et al.*, 2000; Sinclair *et al.*, 2005; Fillon and van der Beek, 2012) coincided with reactivation of the Bóixols Thrust causing inversion of the Organyà Albian rift depocentre (BT, Fig. 3; Bond and McClay, 1995; Mencos *et al.*, 2015). Other examples of late Cretaceous inversion of salt-rich rift and gravity driven depocentres lie along the northern margin of the South Central Pyrenean Unit as described above (Puigdefàbregas and Souquet, 1986; Puigdefàbregas *et al.*, 1992; Vergés *et al.*, 1992; Lopez-Mir *et al.*, 2014, 2015; Burrel *et al.*, 2021).

The southern Pyrenees have become a classic case study for critical wedge dynamics (*e.g.*, Meigs and Burbank, 1997; McClay and Whitehouse, 2004). The South Central Pyrenean Unit has been modelled as a low friction depositional wedge-top system, recording alternating accretion and translation throughout Eocene and early Oligocene (*e.g.*, Meigs and Burbank, 1997). Full cross-section restoration shows that, overall, the SCPU thrust front migrated some 150 km south (Fig. 8f). Within the SCPU thrust units (and Basque-Cantabrian belt) Mesozoic cover and pre-orogenic salt structures suffered moderate to low shortening (Muñoz, 1992; Vergés, 1993; Cámara, 2017; Burrel and Teixell, 2021; Santolaria *et al.*, 2020; Ramos *et al.*, 2022; Figs. 5 and 8). In the western Jaca domain (Fig. 8b) and eastern Pedraforca domain (Fig. 8g), a thin salt décollement facilitated large displacements of thrust sheets in higher friction wedges with internal thrusting and folding (*e.g.*, Vergés *et al.*, 1998; Labaume *et al.*, 2016; Labaume and Teixell, 2018). The eastern thrust front migrated some 120 km south along with the foreland basin that accumulated a complete Eocene-Oligocene succession (Fig. 8g; Vergés *et al.*, 1995, 1998). The Ebro Basin narrows westward between converging thrust fronts of the Pyrenees and the Iberian Range (*e.g.*, Cameros thrust; Fig. 8a). At the western end of the basin, NW-SE trending salt-cored anticlines (*e.g.*, Arguedas, Falces, Fig. 8a) migrated south during the Oligocene-Miocene detached on Cenozoic evaporite levels within the basin fill (Muñoz-Jiménez and Casas-Sainz, 1997; Casas-Sainz and Román-Berdiel, 1999; Larrasoña *et al.*, 2003; Fig. 8a).

Progressive southward migration of deformation is recorded in the sequential activation of major thin-skinned thrusts that link back into thick skinned basement thrusts that built the Axial Zone (Fig. 6). Overall, an estimated 67 to 80% of total orogen shortening is accommodated in the prowedge (Grool *et al.*, 2018; Espurt *et al.*, 2019a). Balanced sections show a westward trend of decreasing prowedge shortening from 92 km to 40.6 km (Fig. 8). However, caution is necessary as the uncertainties associated with such shortening estimates in salt-rich areas can be significant. For example, pre-orogenic diapirism may locally account for a significant portion of limb rotation as demonstrated by Burrel and Teixell (2021; Fig. 8e) and Ford and Vergés (2021). The effect of this phenomenon on the pattern of regional shortening has yet to be quantified.

Although shortening may be accommodated in adjacent areas (Iberian Range, Catalan Coastal Ranges, Fig. 3) the westward decrease in shortening is consistent with an overall westward decrease both in total shortening across the whole orogen and in N-S plate convergence as reported by Macchiavelli *et al.* (2017).

East of Pedraforca (J3, Figs. 3 and 8) prowedge shortening estimates decrease abruptly to 31 km on the J2 section (Ripoll; Fig. 3, Vergés, 1993). Low shortening estimates are also reported in the easternmost northern Pyrenees and thus across the whole eastern orogen (Fig. 4; Ternois *et al.*, 2019a, b). This is problematic as, according to plate kinematic models (*e.g.*, Macchiavelli *et al.*, 2017), the eastern Pyrenees should record maximum convergence. An explanation for this discrepancy may be found in the fact that this area has also undergone strong extension, uplift and erosion due to crustal and lithospheric thinning during Oligocene-Miocene formation of the Gulf of Lion and Valencia Trough (*e.g.*, Lewis *et al.*, 2000; Vergés and Fernández, 2006; Diaz *et al.*, 2018; Jolivet *et al.*, 2020, Jolivet *et al.*, 2021a, b; Carrillo *et al.*, 2020; among others). The deep erosion of Mesozoic strata (estimated erosion > 15 km in Curry *et al.*, 2021) leading to a very incomplete surface geological record, makes it difficult to constrain shortening with the same precision achieved further west. However, the full significance of low shortening estimates in the eastern Pyrenees remains open to debate. For example, it has been suggested that the missing shortening was accommodated outside the Pyrenees such as in the Catalan Coastal Ranges (Angrand and Mouthereau, 2021).

In addition to Triassic evaporites, Cenozoic evaporite units play an important role in foreland deformation (Figs. 8 and 9; Vergés *et al.*, 1992). In the eastern Ebro Basin these units are: the > 1000 m thick Lutetian Beuda Formation, the 300 m thick latest Bartonian Cardona Formation and the > 1500 m thick late Eocene-early Oligocene Barbastro non-marine evaporites (Figs. 8 and 9). Their depocenters shifted south and SW in front of the advancing deformation front. Thrusting then progressively ramped up southward through the detachment levels in a staircase geometry (J3, Fig. 8; Vergés *et al.*, 1992). The most external eastern foreland structures are controlled by the original position and geometry of these evaporitic depocenters and by their degree of overlap (Krzywiec and Vergés, 1996; Sans *et al.*, 1996; Vergés *et al.*, 1992), as well as by their probable interaction with the Upper Triassic basal detachment (Fig. 8). The oblique arrangement of the Cardona Salt in front of the advancing South Central Pyrenean Unit was in part responsible for the oblique fold and thrust trends of the eastern Ebro Basin (Figs. 3, 5 and 8; Vergés *et al.*, 1992). The eastern and central deformation front is located along salt-cored anticlines formed above the Barbastro detachment level (Figs. 4, 9c and 9e), notably along the 40-km long WNW-ESE trending Sanaüja Anticline (SA on Figs. 3 and 8; Vergés *et al.*, 1992) and the > 100 km long WNW-ESE trending Barbastro-Balaguer Anticline in front of the South Central Pyrenean Unit, which links west with the front of the External Sierras (Senz and Zamorano, 1992; Santolaria *et al.*, 2017).

5 Thermal record of Early Convergence

In convergent settings, syn-orogenic cooling of crustal rocks, measured by low temperature thermochronology

methods, is generally assumed to record rock exhumation by surface uplift and erosion in the evolving orogenic wedge (Reiners *et al.*, 2005; Reiners and Brandon, 2006; Carrapa, 2010). Extensive Pyrenean bedrock and detrital low temperature thermochronology datasets essentially support this model recording diachronous exhumation along and across the North Pyrenean massifs and Axial Zone principally from Eocene (50 Ma) to Miocene (Yelland, 1990, 1991; Morris *et al.*, 1998; Fitzgerald *et al.*, 1999; Sinclair *et al.*, 2005; Jolivet *et al.*, 2007; Filleaudeau *et al.*, 2011; Whitchurch *et al.*, 2011; Fillon and van der Beek, 2012; Mouthereau *et al.*, 2014; Labaume *et al.*, 2016; Vacherat *et al.*, 2016; Bernard *et al.*, 2019; Curry *et al.*, 2021; Waldner *et al.*, 2021). Peak exhumation rates are identified from 37 to 30 Ma on the southern Axial Zone along the ECORS line (Fillon and van der Beek, 2012) and from 37 to 20 Ma in the western Axial Zone (Bosch *et al.*, 2016) and Jaca Basin (Labaume *et al.*, 2016).

As convergence started some 30 Myrs before onset of main collision, the question arises as to the existence and degree of orogen-related thermal cooling during the Late Cretaceous and Paleocene. Yelland (1991) was the first to produce *in situ* bedrock low-temperature thermochronology analyses recording Cretaceous cooling ages in the eastern Agly-Salvezines, massif and in the western Labourd basement massif (Figs. 3 and 4). More recent studies have investigated early orogenic and older syn-rift thermal signals using RSCM paleotemperature studies (Lescoutre *et al.*, 2019; Saspiturry *et al.*, 2021) and *in situ* bedrock low temperature thermochronology methods (Ternois *et al.*, 2019a, b; Vacherat *et al.*, 2014, 2016; Hart *et al.*, 2017) revealing variable early orogenic thermal records along the Pyrenees.

In the western North Pyrenean Zone, Vacherat *et al.* (2014) and Bosch *et al.* (2016) in the Mauléon basin and Hart *et al.* (2017) in the Labourd massif (Fig. 4) demonstrate that the thermal perturbation inherited from Aptian-Cenomanian rifting maintained temperatures during early orogenesis above the sensitivity limit of low-temperature thermochronometers (40–300 °C; *e.g.*, Carrapa, 2010; Peyton and Carrapa, 2013), thus delaying cooling until Eocene collision. Late Cretaceous inversion structures are nevertheless reported along the western North Pyrenean Thrust Front (*e.g.*, Jourdan *et al.*, 1998; Barré *et al.*, 2021). Thermal modelling of new low temperature thermochronology data from an adjacent deep borehole in the proximal foreland basin (Fillon *et al.*, 2020) shows a clear signal of early orogenic heating due to syn-orogenic burial. Sedimentary burial of the inverting rift by a thick post-rift and syn-orogenic deposits (Figs. 6 and 7) may thus have contributed to maintaining high temperatures in the western retrowedge until main collision and perhaps even later as discussed by Caldera *et al.* (2021).

Similarly, in the central Pyrenees (ECORS-central area) no *in situ* Cretaceous cooling signals are reported in basement massifs of the North Pyrenean Zone (Arize, Trois Seigneurs massifs, Fig. 7; Yelland, 1990, 1991; Morris *et al.*, 1998; Fitzgerald *et al.*, 1999; Vacherat *et al.*, 2016). Complex time-temperature histories across the massifs, derived using inversion modelling of apatite and zircon fission track and apatite U-Th/He data by Vacherat *et al.* (2016), suggest an early Cretaceous syn-rift signal (cooling) in extensional tilted basement block (crests) on the proximal rift margin. These blocks then became buried below thick flysch successions of

the Pyrenean Trough during Late Cretaceous and Paleocene until inversion during the Eocene and Oligocene main collision phase.

The Agly-Salvezines massif is the most easterly basement massif of the North Pyrenean Zone (AS, Fig. 3). It is believed to have occupied a more distal position on the European rifted margin compared with central and western basement massifs described above (*e.g.*, Arize, Trois Seigneurs, Labourd), as it is surrounded by Mesozoic strata recording some of the highest syn-rift temperatures (up to 580 °C; Boucheville and Bas Agly Synclines; Figs. 4 and 7) of the Internal Metamorphic Zone (Chelalou *et al.*, 2015; Clerc *et al.*, 2016; Ternois *et al.*, 2019a, b; Ducoux *et al.*, 2021a). A fragment of peridotite is also preserved in the IMZ Boucheville syncline, attesting to associated mantle exhumation (Fig. 7g). The basement massif itself did not, however, reach temperatures of more than 350 °C during early Cretaceous rifting, except along discrete fault zones (Ternois *et al.*, 2019a, b). The Agly-Salvezines block records extreme crustal thinning dated as early Cretaceous (Odlum *et al.*, 2019). Combining geological studies with inverse and forward modelling of single-grain AHe ages and a large ZHe dataset from this massif, Ternois *et al.* (2019a, b) build a robust model of syn-orogenic tectonic and thermal evolution, identifying two cooling episodes, one in Late Campanian-Maastrichtian and the other in Ypresian-Bartonian, as well as an earlier syn-rift cooling signal. As the area lay below the Pyrenean Trough during the Late Cretaceous (Fig. 5), early convergence cooling cannot be explained by subaerial exhumation. Ternois *et al.* (2019a, b) instead propose that, as the exhumed mantle domain closed, the Agly-Salvezines crustal block cooled between an overthrusting colder Iberian imbricate and the underthrusting colder European margin (Fig. 4f). Early orogenic crustal cooling detected in other orogens, such as Taiwan, has also been interpreted to record crustal thickening by underthrusting (*e.g.*, Mesalles *et al.*, 2014).

Dating of detrital material accumulated in adjacent foreland depocentres can also be a powerful and complementary approach to unravel the early orogenic cooling pattern of the Pyrenees. Combining detrital zircon fission track, U/He and U/Pb dating, is particularly relevant for source to sink studies because it provides information on both sedimentary provenance and denudation rates in source areas. Its increasing application to Pyrenean forelands is producing ever improving insight into the evolution of syn-orogenic sediment routing systems (*e.g.*, Beamud *et al.*, 2011; Filleaudeau *et al.*, 2011; Whitchurch *et al.*, 2011; Mouthereau *et al.*, 2014; Vacherat *et al.*, 2014; Hart *et al.*, 2017; Thomson *et al.*, 2017, 2019; Ternois *et al.*, 2019a, b). Detrital zircon dating studies in Campanian-Paleocene depocentres of the South-Central Pyrenean Units suggest late Cretaceous cooling of zircons sourced principally from eastern regions (Fig. 7a; Beamud *et al.*, 2011; Filleaudeau *et al.*, 2011; Whitchurch *et al.*, 2011; Thomson *et al.*, 2017, 2019; Odlum *et al.*, 2019). Similar data in the eastern Aquitaine Basin are so far sparse (Mouthereau *et al.*, 2014; Ternois *et al.*, 2019a, b; Léger *et al.*, 2021) but indicate similar cooling records in sediment sources. The sourcing of early orogenic (and earlier post-rift) sediments from eastern relief has long been documented by paleocurrent and sedimentology data (*e.g.*, Plaziat, 1981; Bilotte, 1985; Puigdefàbregas *et al.*, 1992; Monod and Bourroullec, 2014).

Critically, new U-Pb zircon ages can provide distinct “fingerprints” of source regions, while U-Th-Sm/He data can reveal their exhumation histories. Combined, these data have the potential to constrain evolving paleodrainage systems. For example, recent studies in the Upper Cretaceous to Paleocene sediments of the Pyrenees identify distinct Cadomian zircon populations from a major, but, as yet, unidentified eastern source. Cadomian zircons are absent from the mainly Variscan zircon populations of the Axial Zone and Ebro Massif, which also supplied some sediment into the early Pyrenean Trough (Beamud *et al.*, 2011; Filleaudeau *et al.*, 2011; Whitchurch *et al.*, 2011; Mouthereau *et al.*, 2014; Vacherat *et al.*, 2014; Hart *et al.*, 2017; Thomson *et al.*, 2017, 2019; Ternois *et al.*, 2019a, b). This eastern relief, now destroyed by the opening of the Gulf of Lion (Jolivet *et al.*, 2021b), is widely believed to have been created by early onset of Pyrenean convergence to the south of Provence. However, a critical and precise identification and quantification of such potential sources in the east require more robust statistics, and therefore a larger number of dated zircon grains. To overcome procedural limitations of conventional approaches, an integrated laser ablation micro-analytical procedure for *in situ* (U-Th-Sm)/He thermochronology on zircon has been proposed (Boyce *et al.*, 2006; Vermeesch *et al.*, 2012). It allows simultaneous *in situ* determination of parent U-Th-Sm content and measurement of U and Pb isotope concentrations (or their ratios) from which U/Pb ages are derived. Single zircon crystals or grains can thus be dated for both U/Pb and (U-Th-Sm)/He (*in situ* (U-Th)/(He-Pb) double dating (Tripathy-Lang *et al.*, 2013; Evans *et al.*, 2015; Horne *et al.*, 2016, 2019; Danišik *et al.*, 2017). Within the Orogen project, this method has been applied by Ternois *et al.* (2019b) and Léger *et al.* (2021) in the eastern retroforeland basin (SW Mouthoumet area and Corbières-Languedoc Transfer Zone). Based on robust statistical analyses, these results clearly document the evolving nature of detrital material from pre-convergence (*i.e.*, Turonian) to the main orogenic (Eocene) sediments, showing dominance of eastern sources during the transition from rifting and into early orogenesis. They particularly highlight a gradual increase of eastern denudation rates during early convergence times (Campanian-Paleocene), with exposure and erosion of basement areas that had been partially to totally reset during the previous Apto-Albian rifting episode. This confirms that during the late Cretaceous an edifice was created to the east of the present-day Pyrenees, in a region affected by Apto-Albian extension, but most probably to a lesser degree compared with the Pyrenean rift system further west. A striking lesson carried by these new data relates to the coupling of rifting and orogenic age signatures during significant early orogenic denudation episodes, which demonstrates that the orogenic edifice started to form locally by inversion of the Apto-Albian rift. Such data provides direct and robust evidence for the role of rift inheritance in early orogenic processes.

6 Orogen Dynamics

If viewed within the context of regional deformation patterns, Pyrenean evolution can help to better understand factors that control the behavior of a convergent plate boundary and how it can evolve through time. The Pyrenees

represent a low convergence or immature double wedge collisional orogen that evolved through distinct stages of early convergence, quiescence, main collision and post-convergence. Factors influencing this evolution include plate kinematics, lithospheric rheologies and thermal state, the progressive establishment of double wedge dynamics and the inherited rift template. Surface processes also strongly influenced orogen dynamics. The changing roles of these parameters at each stage of orogenesis are discussed here.

The non-cylindrical Pyrenean rift system is here separated into two sectors (described in 4.3), with the eastern sector (sections S2 to S5, Figs. 7d–7g) offset to the south with respect to the western sector (Sections S8, S7, S8, Figs. 7a and 7b) (Ducoux *et al.*, 2021b; García-Senz *et al.*, 2020). In the west, a broader Aptian-Albian rift accommodated higher extension than to the east leading to a wider rift associated with HT metamorphism and mantle exhumation (Ducoux *et al.*, 2021b). Later, Pyrenean plate convergence was lower in this western sector compared with the eastern sector according to the plate kinematic model of Macchiavelli *et al.* (2017). This is reflected in the lower shortening estimates and the dying out of the Axial Zone toward the west. In the eastern sector, although only remnants of the distal rift domain (IMZ) are preserved (Angrand and Mouthereau, 2021; Ducoux *et al.*, 2021a), the syn-rift high temperature metamorphism, metasomatism and mantle exhumation require a well-developed hyperthinned or transcurent rift system. Section restorations indicate that the eastern European rift margin was considerably narrower than in the western sector (Chelalou *et al.*, 2015; Ford and Vergés, 2021; Ducoux *et al.*, 2021b), however the distal southern margin is very poorly preserved. The Macchiavelli *et al.* (2017) model predicts highest plate convergence and thus greatest shortening in the eastern Pyrenees, however this is not supported in the easternmost sectors where sparsely preserved allochthonous units provide lower shortening than expected. As discussed above, this remains an unresolved problem. Creation of relief began earlier in eastern sectors and migrated west. Rift shoulder uplift associated with Oligocene-Miocene opening of the Gulf of Lion and Valencia Trough strongly overprinted late orogenesis in easternmost sectors (Calvet *et al.*, 2020; Jolivet *et al.*, 2021a, b). Consequently, while the western NPZ preserves most domains of a broad and well-developed Aptian-Cenomanian rift system affected by low convergence, the central and eastern NPZ record relatively more convergence that affected a well-developed, but perhaps narrower rift system.

6.1 Early convergence

During the Late Cretaceous, inversion and shortening affected many Mesozoic rift systems across a broad area from Africa to the North Sea in response to the onset of Europe-Iberia-Africa convergence (Fig. 2; Dèzes *et al.*, 2004; Nielsen *et al.*, 2005; Ziegler and Dèzes, 2006; Kley and Voigt, 2008; Lamotte *et al.*, 2011; Jolivet *et al.*, 2016; Stephenson *et al.*, 2020; Mouthereau *et al.*, 2021). Within this area, inversion of the Pyrenean rift accommodated only a small component of Africa-Europe plate convergence (see Sect. 2.2). Macchiavelli *et al.* (2017) derive estimates of Iberia-Europe N-S convergence rates of 1.1 mm/yr in the east slowing westward to 0.5 mm/yr in the Basque-Cantabrian-Bay of Biscay region. Substantial strike-slip identified in some plate reconstructions

are not well documented or quantified in the field and thus remain problematic. Within the resolution of stratigraphic and geochronological data, the onset of plate convergence around the Santonian-Campanian boundary correlates well with both onset of shortening (fault inversion; Figs. 7 and 8) and a marked acceleration in tectonic subsidence in the Pyrenean Trough (Fig. 5b).

At onset of orogenesis the lithospheric rift template was not in thermal equilibrium as only 10 Myrs had elapsed since the end of magma-poor Aptian-Cenomanian rifting. Instead of building early orogenic relief as envisaged in other orogens (*e.g.*, Babault *et al.*, 2013) early Pyrenean crustal thickening developed below the Pyrenean Trough, a subsiding marine basin driven largely by post-rift cooling and supplied by longitudinal drainage from an edifice in the east (Fig. 6a). Only the fringes of this major basin are preserved, with up to 2–3 km of Upper Cretaceous flysch preserved to the north and over 6 km preserved in the SCPU, giving an idea of its dimensions.

Slow and limited convergence during Late Cretaceous was accommodated by closure of exhumed mantle domains accompanied by distributed inversion of overlying distal rift successions to generate divergent structural fans (Mouthereau *et al.*, 2014; Ford *et al.*, 2016; Teixell *et al.*, 2016; Labaume and Teixell, 2020). These early divergent structural fans are well preserved in the western NPZ (Figs. 7a and 7b). More fragmentary data appear to indicate that the eastern rift accommodated early convergence in a very similar manner. In the east, the deformation front inverted the northern boundary of the necking domain while in the west it became localized along the boundary between proximal and distal rift domains (hyperthinned and necking domains), illustrating how inherited rift architecture controlled shortening distribution.

The thermal signature of early convergence in the Pyrenees is highly variable and ambiguous. A high residual post-rift geothermal gradient persisted throughout this period in the western north Pyrenean sector (Vacherat *et al.*, 2014; Hart *et al.*, 2017; Caldera *et al.*, 2021; Ducoux *et al.*, 2021b), where extension had been highest (Clerc and Lagabrielle, 2014; Lescoutre *et al.*, 2019; Lagabrielle *et al.*, 2020; Saspiturry *et al.*, 2020). No record of early orogenic cooling or heating is detected in basement massifs of the European proximal margin (central NPZ; Vacherat *et al.*, 2016). However, the proximal Iberian margin (Axial Zone) underwent heating to greenschist facies, accompanied by distributed deformation and weakening (Airaghi *et al.*, 2019; Waldner *et al.*, 2021). This heating may have been due to burial below the thick Pyrenean Trough as detected in the Aquitaine basin by Fillon *et al.* (2020).

Late Cretaceous early orogenic cooling is locally detected in distal rift margin units in the eastern (Agly-Salvézines massif, Ternois *et al.*, 2019a, b, 2021a, b) and western NPZ (Labourd massif; Hart *et al.*, 2017). As this cannot be explained by uplift and erosion, Ternois *et al.* (2019a, b) propose cooling of a hot thinned crustal imbricate due to emplacement between cooler crustal slices of upper and lower plates (Fig. 4f).

6.2 Transition from early convergence to main collision

The transition from distributed deformation during early convergence to the construction of a doubly vergent collisional

orogen requires the creation of a new plate boundary fault that accommodated the northward subduction of the Iberian plate. The exact tectonic processes involved in closure of exhumed mantle domains and lithospheric scale shortening during early convergence remain uncertain and difficult to constrain from field observations alone. Conceptual scenarios generally propose reactivation of a lithospheric-scale, rift-inherited low-angle detachment that later accommodated subduction of the Iberian plate (e.g., [Jammes *et al.*, 2009](#); [Masini *et al.*, 2014](#); [Teixell *et al.*, 2018](#)). More recent thermomechanical modelling of inversion of hyperthinned rift systems suggest that fault reactivation was restricted to shallow crustal levels along the rifted continental margins, while the accommodation of plate convergence on the lithospheric scale involved the development of a new convergent plate boundary fault ([Dielforder *et al.*, 2019](#); [Jourdon *et al.*, 2019](#)). In detail, these numerical simulations show that new shear zones initiate in the exhumed mantle domain during early convergence and subsequently develop into a single lithospheric-scale plate boundary fault accommodating the closure of the mantle domain and subduction of the lower plate. Further, [Jourdon *et al.* \(2019\)](#) show that the localization of the shear zone in the mantle domain is highly sensitive to the width and thermal structure of the exhumed mantle domain. In particular, in order to initiate the new plate boundary fault in the mantle, the width of exhumed mantle must be < 50 km, otherwise obduction of mantle would preferentially occur.

The creation of such a new convergent plate boundary fault in the Pyrenees may also be linked to the distribution of deformation in central and northern Europe. During the Campanian-Maastrichtian compressional stresses were transmitted across the Iberia-Europe boundary far into the European plate causing inversion of the Mesozoic Central European rift system associated with the development of substantial peripheral basins (up to 2 km of sediment fill; [Fig. 1](#); [Scheck-Wenderoth and Lamarche, 2005](#)). These peripheral basins are on a similar scale as and record similar shortening to the Upper Cretaceous Pyrenean Trough ([Kley and Voigt, 2008](#); [Deckers, 2015](#); [Deckers and van der Voet, 2018](#); [Kley, 2018](#); [Voigt *et al.*, 2021](#)). Intraplate deformation in central Europe ended in the early Paleocene, coinciding with the interruption in Africa-Iberia-Europe convergence ([Fig. 2](#); [Nielsen *et al.*, 2005](#); [Kley and Voigt, 2008](#)). In contrast to the Pyrenean realm and the Iberian plate however, shortening in central Europe did not restart when plate convergence recommenced at the end of the Paleocene. [Dielforder *et al.* \(2019\)](#) propose that this indicates that stress transmission across the plate boundary was no longer effective. They investigate the plate coupling force necessary to allow or impede stress transmission across a plate boundary fault under conditions and rheologies consistent with those experienced by the Pyrenean realm during and at the end of early convergence. The analysis demonstrates that, although the hyperthinned rift system had a low strength at the onset of convergence due to a high thermal gradient, it was initially just strong enough, due to the presence of mantle rocks close to the surface, for the transmission of sufficient stress into the European plate to drive intraplate deformation. By the end of the Cretaceous, the localization of the plate boundary fault and its related weakening decreased the mechanical coupling between the plates, thus preventing further transmission of effective stress into Europe and hence focusing deformation

into the orogen itself as the lower plate began to subduct ([Dielforder *et al.*, 2019](#)).

The coincidence in timing between the termination of intraplate deformation in Europe and the interruption of Africa-Iberia-Europe plate convergence during the Paleocene appears remarkable. While further research is required to better understand the nature of the abrupt slowdown in plate movements during the Paleocene, the decrease in plate forces across the weakening Pyrenean plate boundary fault may have simply ended stress transmission sooner and more abruptly than would have been the case if plate forces had remained constant.

6.3 Main Collision: the Pyrenean model of orogenic processes

The main collision stage of the Pyrenees is very well documented as discussed above. Once the subduction system was established, deformation and basin development became focused into the orogen and onto the weak plate boundary fault. More rapid plate convergence (4 mm/yr, [Fig. 2](#); [Macchiavelli *et al.*, 2017](#)) drove growth of the asymmetrical orogenic double wedge through imbrication of Iberian upper crust while Iberian lower crust and lithospheric mantle were subducted ([Fig. 4](#)). Creation of relief progressively propagated southward and westward (e.g., [Sinclair *et al.*, 2005](#); [Bernard *et al.*, 2019](#); [Curry *et al.*, 2021](#) and references therein). Crustal thickening drove flexural subsidence principally in the proforeland basin but also contributed to subsidence in the retroforeland basin ([Angrand *et al.*, 2018](#)). The growing edifice became the principal source of high volumes of sediment, transferred by transverse routing systems to the Ebro Basin. Considerably lower volumes of sediment reached the Aquitaine basin ([Fig. 6](#); [Sinclair *et al.*, 2005](#); [Fillon *et al.*, 2020](#)). The timing of maximum exhumation in the Axial Zone, detected in low temperature thermochronology data, youngs westward from late Eocene (~ 40 Ma) in the eastern Pyrenees to early Oligocene (~ 30 Ma) in the western Axial Zone ([Fillon and van der Beek, 2012](#); [Bosch *et al.*, 2016](#); [Labaume *et al.*, 2016](#)).

Considered as an excellent example of a collisional double wedge orogen generated by critical wedge dynamics, the central Pyrenees have been extensively simulated by 2D thermomechanical modelling to examine controlling parameters and major processes, particularly along the central ECORS deep seismic profile (e.g., [Beaumont *et al.*, 2000](#)). These 2D models demonstrate not only crustal thickening processes and evolution but also the essential role of surface processes in controlling mass flux and deformation distribution during orogen growth (e.g., [Beaumont *et al.*, 2000](#); [Fillon *et al.*, 2013a, 2013b](#); [Erdős *et al.*, 2014a, b](#); [Curry *et al.*, 2019](#); [Grool *et al.*, 2019](#)). The roles of inherited rifts and lithospheric rheological heterogeneities in the construction of the orogen have also been examined in increasingly higher resolution by numerical models (e.g., [Jammes and Huismans, 2012](#); [Erdős *et al.*, 2014a, b](#); [Jourdon *et al.*, 2019, 2020](#); [Dielforder *et al.*, 2019](#); [Grool *et al.*, 2019](#)). As demonstrated by the work of [Wolf *et al.* \(2021\)](#), this low convergence orogen lies at the lower end of a spectrum of orogen behaviors, which change with increasing convergence. Within the Orogen project, [Jourdon *et al.* \(2020\)](#) consider the role of a

thick salt layer (2 or 5 km) in a full Wilson cycle. As an extreme end member model (in terms of thickness of the salt layer, which replaces the upper crustal sedimentary cover), their results suggest the presence of very thick salt (5 km) can suppress the growth of orogenic relief, leading to a prolonged period of submarine continental accretion. Jourdon *et al.* (2019) explored the impact of the degree pre-orogenic rifting (rift maturity) on strain distribution within the subsequent orogen. Their models indicate that subduction initiation focuses on the weakest part of the central rift where mantle has been exhumed, a proposal corroborated by the work of Dieforder *et al.* (2019).

In a developing orogenic wedge, the transition from growth to steady state describes the development of orogenic relief due to crustal thickening during convergence to the point where accretionary influx equals erosional outflux (steady-state) (Willett and Brandon, 2002; Sinclair *et al.*, 2005). These terms must be used with caution, as they are applicable only to an already established crustal double prism with dynamic relief evolving above a subducting plate boundary. In the Pyrenees dynamic growth of orogen topography was not established until early Eocene with the onset of main collision and subduction of the Iberian plate. Any transition to steady state would therefore be younger. It is therefore likely that in this immature orogen steady state was never attained.

7 Transition from syn- to post-convergence

7.1 Signals of end of plate convergence

Uplift and erosion of an actively converging mountain belt will normally coincide with ongoing loading and hence subsidence in the proximal foreland basin (e.g., Flemings and Jordan, 1990). Transverse sediment routing systems are thus trapped adjacent to the thrust front and can be diverted into longitudinal systems by active structures in a wedge-top basin (Allen *et al.*, 2013). In contrast, the end of active plate convergence in a collisional orogen is expected to generate simultaneous isostatic rebound of both the mountain belt and the proximal flexural foreland basin (Heller *et al.*, 1988; Flemings and Jordan, 1990; Burbank, 1992; Cederbom *et al.*, 2004; Allen and Heller, 2012; Allen *et al.*, 2013; Tucker and van der Beek, 2013). The consequent diminishing accommodation in the foreland basin relative to ongoing high sediment supply from the orogen will generate outwardly extending gravel systems across the foreland with an extensive transverse flow piedmont (low depositional slopes and long depositional lengths; Allen *et al.*, 2013). However, other factors can substantially increase sediment supply with respect to accommodation in foreland basins such as climate change, mantle dynamics or drainage reorganization, thus triggering transverse flow piedmont sedimentary systems (Allen *et al.*, 2013). It is important to be able to distinguish between these different mechanisms. In order to clearly identify isostatic rebound related to end of convergence a foreland stratigraphic signal should coincide with a cooling signal in the mountain range (uplift and erosion) detectable, for example, in low temperature thermochronology data. Integrating Orogen results and other published studies, we here discuss the significance of transverse flow piedmont systems deposited on both sides of the Pyrenean orogen during late to post-convergence. We also consider all signatures of post-convergence isostatic rebound

and discuss the role of other possible drivers of orogen exhumation during this critical period. Both the work of Bernard *et al.* (2020) in the Orogen project and that of Ortiz *et al.* (2020) within Orogen's sister project *Source to Sink*, document the syn to post-convergence period in the Aquitaine Basin. Other relevant Orogen studies investigate the same period in the Axial Zone using low temperature thermochronology, thermal and tectonic studies (e.g., Bellahsen *et al.*, 2019; Bernard *et al.*, 2019; Fillon *et al.*, 2020). The prowedge system has been extensively investigated and debated over two decades (see below) and we integrate a summary of key work into our discussion.

Plate reconstructions consistently indicate that N-S convergence between Europe and Iberia ended in the Aquitanian (Fig. 3; 23–20 Ma; e.g., Roest and Srivastava, 1991; Macchiavelli *et al.*, 2017). From then on, Africa-Iberia-Europe convergence was principally accommodated along the southern border of the Iberian plate in the Betic-Rif system (Soler y Jose *et al.*, 1983; Guimerá and Alvaro, 1990; Mas *et al.*, 1993; Geel and Roep, 1998; Gaspar-Escribano *et al.*, 2004; Sàbat *et al.*, 2011; Vergés and Fernández, 2012; Daudet *et al.*, 2020; Mouthereau *et al.*, 2021). To the east of Iberia, subduction dynamics had already changed around 35 to 30 Ma (Priabonian-Rupelian) with the onset of rapid slab retreat in the Apennine-Ionian subduction system, leading to the opening of, first, the Liguro-Provençal backarc basin (Fig. 1; including Gulf of Lion and Valencia Trough) and then the Tyrrhenian Sea (Fig. 1; see Jolivet *et al.*, 2021a for synthesis). While the onset of west Mediterranean backarc extension took place within the framework of ongoing Africa-Europe convergence, it clearly predates the end of Iberia-Europe convergence by some 10 Myrs. It is therefore not described here as post-convergence extension with respect to the Pyrenean orogeny. It can, however, be described as post-convergence for the Provençal segment of the belt. Possible triggering mechanisms for this major change in subduction dynamics are widely debated as discussed in Jolivet *et al.* (2021a, b) and in Séranne *et al.* (2021). For example, Ethève *et al.* (2018) and Mouthereau *et al.* (2021) argue that the southward propagation of the West European continental rift system into the Gulf of Lion area in the Oligocene may have played a key role. Based on new dating constraints, Séranne *et al.* (2021), however, argue that the West European continental rift system propagated southward into the area between the Alpine and Pyrenean orogens during the Priabonian (Fig. 6e), some 5 Myrs before the onset of Apennine slab rollback. The evolving Alpine orogeny to the east also undoubtedly played a major role (e.g., Dèzes *et al.*, 2004).

Oligocene-Miocene extension overprinted late orogenesis in both the pro and retro-wedges in the easternmost Pyrenees, and the Pyrenean-Provençal fold belt in southern France (Guieu and Roussel, 1990; Gorini *et al.*, 1991; Maerten and Séranne, 1995; Vergés and Fernández, 2006; Maurel *et al.*, 2008; Calvet *et al.*, 2020; Milesi *et al.*, 2020; Séranne *et al.*, 2021; Wicker and Ford, 2021). Debated causes of uplift of this age in the easternmost Pyrenees include rift shoulder uplift (Maurel *et al.*, 2008; Milesi *et al.*, 2020; Calvet *et al.*, 2020; Jolivet *et al.*, 2020) and mantle related processes such as delamination and magmatism (Gunnell *et al.*, 2008; Huyghe *et al.*, 2020). A component of later post-convergence rebound cannot be excluded (e.g., Desegaulx and Brunet, 1990). Because of the dominance of Oligocene-Miocene extension-related

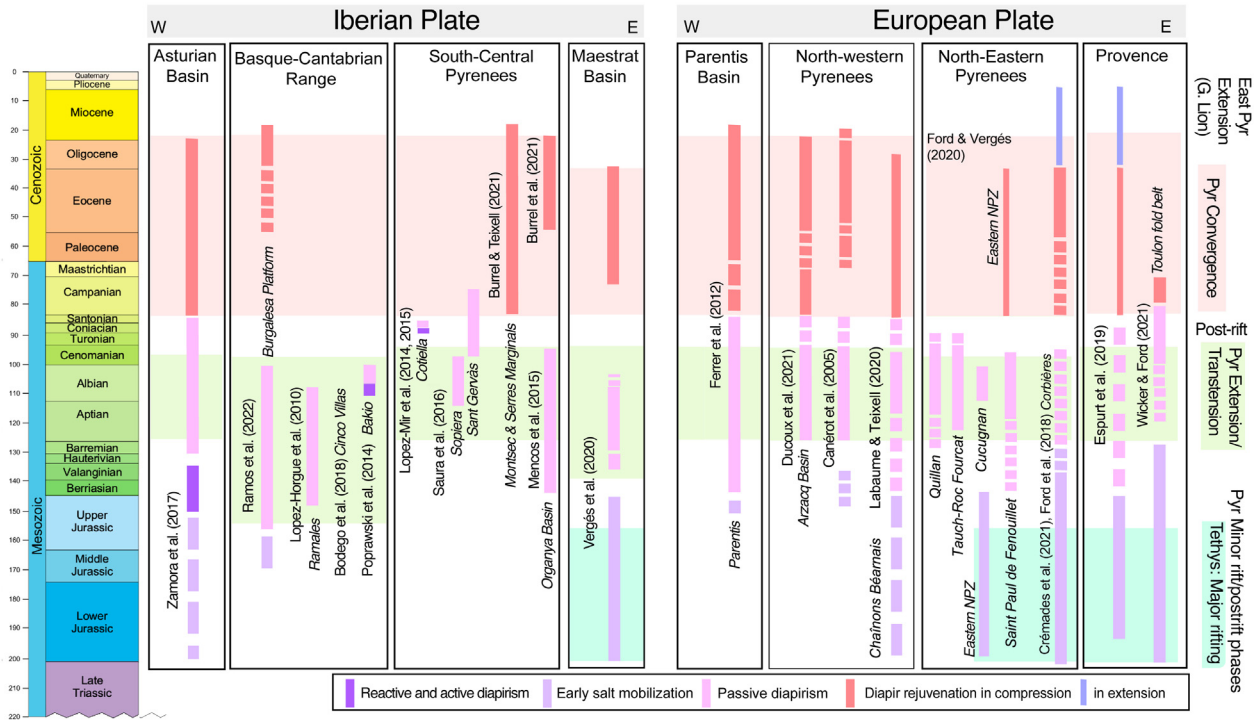


Fig. 10. Compilation and correlation of periods of diapiric activity with major tectonic events across inverted Pyrenean, Basque-Cantabrian and adjacent fold belts of the Iberian and European plates. Adapted and completed from Vergés *et al.* (2020) and Ford and Vergés (2021) integrating data from Canérot *et al.* (2005), López-Horgue *et al.* (2010), Ferrer *et al.* (2012), Lopez-Mir *et al.* (2014, 2015), Poprawski *et al.* (2014), Mencos *et al.* (2015), Saura *et al.* (2016), Zamora *et al.* (2017), Bodego *et al.* (2018), Ford *et al.* (2016), Espurt *et al.* (2019a, b), Ford and Vergés (2021), Labaume and Teixell (2020), Vergés *et al.* (2020), Burrel and Teixell (2021), Burrel *et al.* (2021), Crémades *et al.* (2021), Wicker and Ford (2021), Ducoux *et al.* (2022) and Ramos *et al.* (2022).

processes, this area is unsuitable for the detection and analysis of any isostatic response to the end of convergence. This signature is most appropriately sought in central sectors of the orogen. As seen above, the pro and retro Pyrenean foreland systems had very different configurations and sediment routing systems during collision (Sinclair *et al.*, 2005; Ortiz *et al.*, 2020; Garcés *et al.*, 2020). Both developed transverse flow piedmont systems but at different times. We here explore the distinct structural and stratigraphic record in each basin from late to post-convergence. We discuss the significance of transverse flow piedmont systems in each basin and identify the dominant controlling processes.

We have chosen not to include here a review of the debate on the significance of perched erosion surfaces preserved across the Pyrenean orogen. The reader will find a rich and complete presentation and discussion of these and other geomorphological features in Calvet *et al.* (2020) and references therein.

7.2 Pyrenean retrowedge: Aquitaine Basin

Since its inception the Aquitaine Basin has always opened to the west into the Bay of Biscay (Fig. 6). During main collision (Eocene-Oligocene) the basin was principally supplied from growing orogen relief, and from mid-Miocene onward the Massif Central also became a significant sediment

source (Ortiz *et al.*, 2020). The transition from syn to post-convergence predicted by theoretical models described above has been recognized in the central and western Aquitaine Basin where sedimentation continued into the Pliocene and Quaternary (Bernard *et al.*, 2020; Ortiz *et al.*, 2020). Using seismic reflection profiles and borehole data, Ortiz *et al.* (2020) document two post-convergence periods in the retroforeland basin. From end Chattian to early Tortonian (Fig. 6e; over some 15 Myrs) a progressive basin-wide uplift reduced accommodation in the basin. Orogen-derived alluvial sedimentation changed from being largely confined in proximal foreland depocentres to extensive transverse flow piedmont systems that built thin, broad fans across the foreland platform. The best known of these fans, the Lannemezan fan, has a radius of 40–75 km with a maximum thickness of only 40–60 m (Patin, 1967; Mouchéné *et al.*, 2017). During the second post-convergence period (Tortonian to Pliocene) the Aquitaine platform was characterized by full bypass and lateral transfer of sediments to the Bay of Biscay deep offshore basin. Ortiz *et al.* (2020) relate this uplift of the Aquitaine platform to west European-scale mantle dynamics. Other authors alternatively relate the event to late alpine collision (Ziegler and Dèzes, 2006) or to extensional tectonic activity in the western Pyrenees (Jolivet *et al.*, 2007; Fillon *et al.*, 2020).

Bernard *et al.* (2020) investigate the sedimentary signature of the end of convergence at a higher resolution across the

retrowedge source to sink boundary in the central Aquitaine Basin. Here, a Miocene sediment drape lies across folded, faulted and eroded frontal ranges. Miocene conglomerates dated as young as 12 Ma are preserved up to 600 m altitude, which is over 300 m above the present-day thrust front. These key observations indicate that sedimentation continued for some 8 Myrs after the end of plate convergence, backfilling over eroded late structures along the thrust front. [Bernard *et al.* \(2020\)](#) use a numerical box model based on [Tucker and van der Beek \(2013\)](#) to simulate the syn to post-convergence transition with parameter values approximating those of the northern Pyrenees and the Aquitaine Basin, that was open to an external sink representing the Bay of Biscay basin ([Fig. 11](#)). By tracking four key parameters (range elevation, basin elevation, sediment flux from the range into the basin and sediment flux exiting the basin) through a series of evolutionary steps from syn to post-convergence, [Bernard *et al.* \(2020\)](#) show that a post-convergence sediment drape is generated by initial sustained high sediment influx from the uplifting range relative to the outflux from the basin to the external sink ([Fig. 11b](#)). The gradual decay of influx over some millions of years after the end of convergence until bypass dominates ([Fig. 11d](#)), is linked to the dying out of subsidence in the proximal basin as the orogenic load diminishes and isostatic rebound eventually becomes dominant causing uplift and incision of the sediment drape and proximal foreland basin. This model suggests that a post-convergence sediment drape deposited across the frontal mountain range during the early transitional stage, may be responsible for at least some of the elevated low-gradient surfaces (see [Calvet *et al.*, 2020](#) and references therein) and preserved remnants of continental sedimentation draping the outer margins of the northern Pyrenean thrust wedge. These relatively thin sediment drapes (some tens of metres thick) have a low preservation potential. They may have been preserved in the northern Pyrenees because of the gentle nature of post-convergence rebound linked to low overall shortening in the retrowedge and/or to low sedimentation rates in the retro foreland system. In older orogens or in those with higher convergence, such as the Western Alps, such sediment drapes would have a relatively low preservation potential due to more significant post-convergence uplift and erosion.

7.3 Pyrenean prowedge: Ebro Basin

In the southern Pyrenees youngest Pyrenean compressional structures are well dated as Aquitanian, for example, along the Serres Marginals (20–25 Ma, [Meigs *et al.*, 1996](#); U-Pb dating of calcite in veins and faults, [Cruset *et al.*, 2020](#), [Hoareau *et al.*, 2021](#); magnetostratigraphy in frontal conglomerates with growth, 22.5–21.4 Ma, [Oliva-Urcia *et al.*, 2019](#)), in the Jaca Basin (low temperature thermochronology, 20 Ma, [Labaume *et al.*, 2016](#); U-Pb and (U-Th)/He double dating of volcanic zircon in detrital growth strata as Aquitanian, [Coney *et al.*, 1996](#); [Roigé *et al.*, 2019](#)) and along the eastern thrust front (dating of illite crystals in fault gouge, 24 Ma, [Rahl *et al.*, 2011](#)). Principal deformation in the Iberian Range is also dated from 35 to 20 Ma ([Rat *et al.*, 2019](#)). We would therefore expect to see an isostatic response

to the end of plate convergence in deposits aged Aquitanian and younger.

As described earlier ([Sect. 3.2](#)), during the late Eocene to early Oligocene a significant transverse gravel drape built a piedmont across the southern Axial Zone, which involved the backfilling of palaeovalleys with up to 2.6 km of conglomerates, and across the South Central Pyrenean Unit and the Ebro Basin ([Fillon *et al.*, 2013a](#)). Although some authors have proposed that this gravel drape records the syn to post-convergence transition ([Coney *et al.*, 1996](#); [Nichols and Hirst, 1998](#); [Babault and Van Den Driessche, 2005](#)), it has become clear that it predates the end of plate convergence. [Allen *et al.* \(2013\)](#) demonstrate that such a transverse and strongly prograding gravel system can also be generated by high sediment supply from a rapidly exhuming mountain belt coupled with a reduction in accommodation in the flanking basin. They propose that the Ebro system records the gradual decay of late Pyrenean orogenesis with the endorheic condition of the basin being a critical condition for its overfilling. Low temperature thermochronology data and inverse thermal history modelling of both the southern Axial Zone ([Fillon and van der Beek, 2012](#)) and the South Central Pyrenean Unit along the ECORS Central profile ([Fillon *et al.*, 2013a](#)) confirm coeval deposition of piedmont gravel systems and rapid exhumation of the southern Axial Zone (2.5 km Myr⁻¹) from 37 to 30 Ma followed by a period of very slow exhumation (0.2 km Myr⁻¹) until around 9 Ma. Plate kinematic models such as that of [Macchiavelli *et al.* \(2017\)](#), indicate that Iberia-Europe convergence rates remained steady and high in the central and eastern Pyrenees throughout the Eocene and Oligocene only to decrease abruptly in the Aquitanian ([Fig. 3a](#)).

During the Oligocene-Miocene the southward prograding alluvial systems passed into lacustrine-palustrine facies to the southwest where sedimentation continued into the post-convergence period and up to latest Middle Miocene ([Fig. 6e](#); ~12 Ma; [Pérez-Rivarés *et al.*, 2004](#); [García-Castellanos and Larrasoña, 2015](#)). No significant change in the distribution of facies belts or in sedimentation rates is detected at the transition from syn to post-convergence around 20–23 Ma (*e.g.*, [Oliva-Urcia *et al.*, 2019](#); [Garcés *et al.*, 2020](#)). Instead, some 10 Myrs later, during the Tortonian (12–7.5 Ma) a river system incised upstream from the east to capture the Ebro's elevated base level, establishing sediment efflux into the Mediterranean. This dramatic fall in base level caused the rapid erosion of at least 22% of basin fill ([Riba *et al.*, 1983](#); [García-Castellanos *et al.*, 2003](#); [Costa *et al.*, 2010](#); [Tucker and van der Beek, 2013](#)). [García-Castellanos and Larrasoña \(2015\)](#) reconstruct the distribution and thickness of maximum sedimentary infill of the Ebro basin before late drainage capture. Comparison between the end of the endorheic period and present-day allows the calculation of the isostatic rebound of the Ebro Basin and the outermost Pyrenean fold belt where the Oligo-Miocene conglomerates were stripped off. This Late Miocene incision of the conglomerate drape across the southern Pyrenees has been detected in thermal history of Garumnian sediments along the ECORS Central profile ([Fillon *et al.*, 2013b](#)).

In the eastern Ebro Basin and eastern Pyrenees Oligocene-Miocene exhumation was driven by a combination of significant erosion of sedimentary successions and consequent isostatic rebound of the whole basin, as well as flexural rebound in the footwall of the Neogene extensional fault

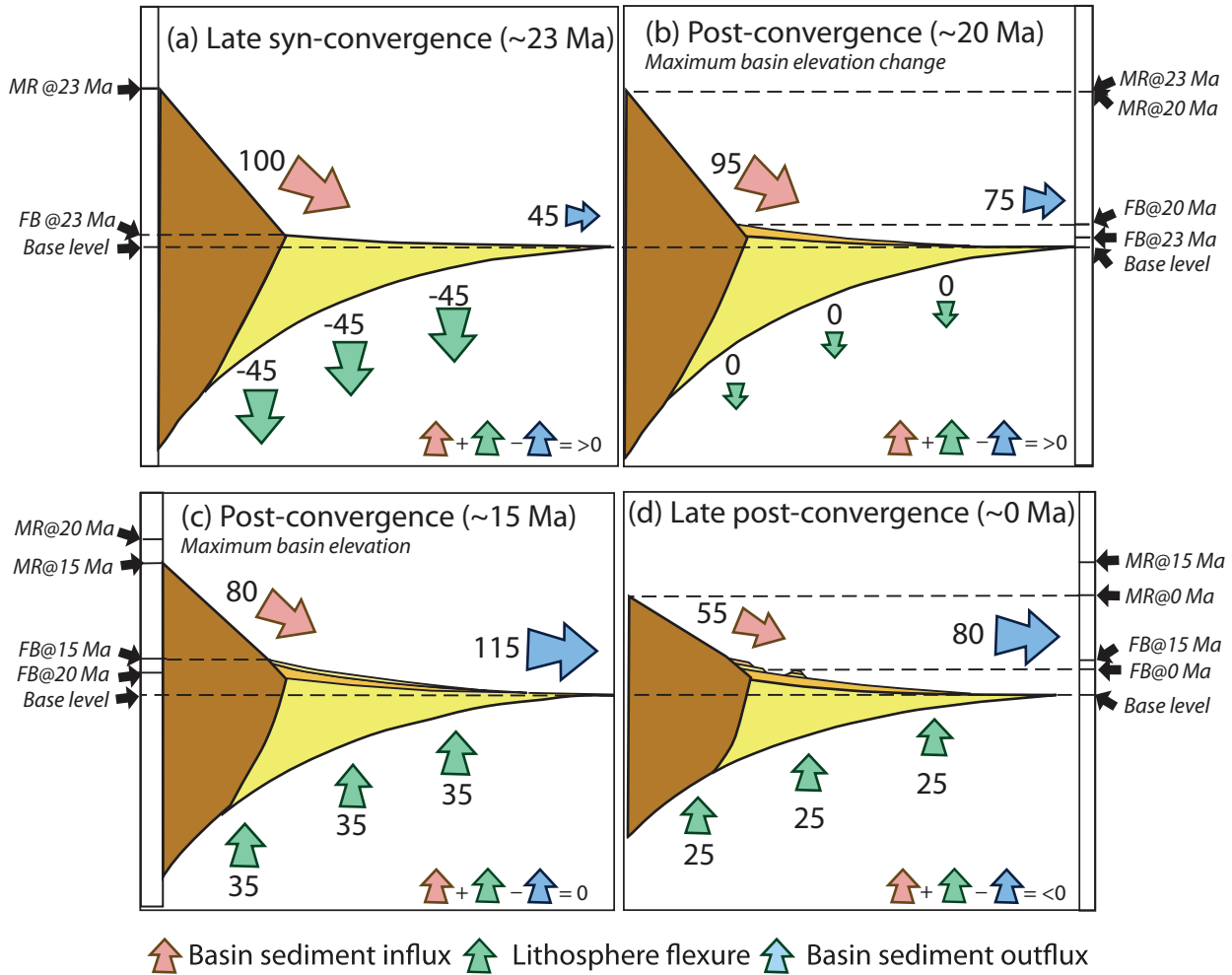


Fig. 11. Schematic representation of results of numerical modelling of Bernard *et al.* (2020) simulating the transition from syn-convergence to post-convergence in four time frames, designed to represent the sedimentation and erosion record along the North Pyrenean thrust front from early Miocene to present day. Red, green and blue arrows correspond respectively to three controlling parameters, the basin influx from the orogen, lithospheric flexure (positive is uplift, negative is subsidence) and basin outflux. Numbers next to arrows indicate a percentage contribution to the basin elevation based on model results detailed in Bernard *et al.* (2020). The sum of these values (see inset on each cartoon) results in an increase in elevation of the foreland basin in (a) and (b), stasis in (c), and erosion leading to a decrease in elevation in (d). (a) Latest syn-orogenesis at ~ 23 Ma (end of plate convergence). (b) Early post-orogenesis at ~ 20 Ma when positive elevation change of the foreland basin is maximum. (c) Post-orogenesis at ~ 15 Ma when elevation of the foreland basin is maximum. (d) Post-orogenesis at ~ 0 Ma when elevation of both the range and foreland basin are decreasing. Black arrows indicate elevation of the mountain range (MR) and foreland basin (FB) for the specific time frame and for the previous step for comparison. Adapted from Bernard *et al.* (2020).

system (NE-SW trending faults along the Catalan Coastal Ranges and NNW-SSE trending faults along the Transverse Ranges, Fig. 3, Lewis *et al.*, 2000), and lithospheric thinning due to West Mediterranean rifting (*e.g.*, Vergés and Fernández, 2006; Jolivet *et al.*, 2021a, b). In the footwall area at the intersection of the NE-SW and NNW-SSE fault systems, total exhumation is greater than 1.3 km whereas it is 0.6 km in the footwall of the Transverse Ranges limiting the Empordà Basin (Fig. 3).

Unlike the Aquitaine Basin, the transition from syn to post-convergence in the early Miocene has no clear signal in the Ebro basin. The alluvial sedimentary system appears to have been relatively insensitive to post-convergence isostatic rebound as the internal, isolated base level and overfilled

nature of the basin kept topography stable. The isostatic blanketing effect of a thick sediment drape over the southern flank of the mountain belt could also have had a dampening effect on any post-convergence rebound as recently simulated by thermomechanical modelling of the Alpine foreland basin (Erdős *et al.*, 2019). Substantial erosion of Miocene sediments also limits the resolution of late stratigraphic signals across southern deformation fronts. Finally, the drastic change in base level that occurred around 10 Ma generated its own strong erosional isostatic rebound. Datasets tracking vertical motions (*e.g.*, low temperature thermochronology data) that have detected this strong post-convergence motion lack, as yet, sufficient resolution to distinguish any preceding weaker signal, for example, that of a post-orogenic rebound that would

have started some 10 Myrs before. If we exclude the easternmost Pyrenees where Gulf of Lion extension dominated late to post-convergence dynamics, there is now general agreement that, the change from an endorheic to an exorheic base-level in the Ebro Basin exerted the principal control on late to post-convergence vertical motions and topographic development across the southern Pyrenean foreland system rather than the end of plate convergence or other factors such as climate (Fillon and van der Beek, 2012; Fillon *et al.*, 2013a).

8 Conclusions and future challenges

As a small low convergence collisional orogen the Pyrenees preserves an excellent record of the progressive establishment of continental subduction without being preceded by oceanic subduction. The orogen provides a record of early rift inversion often destroyed or overprinted in more mature orogens. The record also demonstrates that orogen behavior changed markedly, during two critical transitions, early convergence to main collision and main collision to post-convergence, reflecting changes in lithospheric processes and in the role of different tectonic drivers. Studies in the Orogen, RGF Pyrenees and ANR-PYRAMID projects have focused principally on the northern Pyrenees, where the inverted rift system is preserved. These projects have produced considerable new knowledge and data on a wide range of issues including the two critical transitions and the early convergence period. Outstanding new datasets have been provided by passive seismic tomography campaigns (ANR-PYROPE and Orogen projects; Chevrot *et al.*, 2022 and references therein) and new low temperature thermochronology analytical techniques and isotopic dating techniques (*e.g.*, Airaghi *et al.*, 2019; Ternois *et al.*, 2019a, b, 2021a, b; Fillon *et al.*, 2020; Léger *et al.*, 2021). Principal findings are summarized below:

- A preexisting rift is essential for the development of a doubly vergent orogen. Thermal, rheological and structural rift inheritance impacts all aspects of orogen evolution, particularly during early orogenesis.
- During early convergence, plate forces were distributed across the near and far field causing inversion of rift structures and depocentres across Europe as stress was transmitted across a sufficiently strong plate boundary. Rift inheritance dictates where deformation became focused while plate kinematics directly controlled timing and amount of deformation. No significant lithospheric body forces were at work. Early crustal thickening and cooling has been detected in new Zircon He data. In other orogens, typically those evolved from rifts or passive margins, similar early inversion stages are recognized (*e.g.*, Babault *et al.*, 2013; Cooper and Warren, 2020), but are often poorly preserved.
- Early deformation occurred below a broad marine flexural basin where subsidence was generated by post-rift thermal cooling with a secondary and variable contribution from crustal thickening. Sediment was principally supplied by longitudinal sediment routing systems from poorly constrained relief to the east, probably created by early plate convergence.

- The transition from early convergence to main collision requires the creation of a weak plate boundary fault and the initiation of subduction of the Iberian plate leading to establishment of double-wedge orogenic growth.
- Isostatic rebound at the transition from syn to post-convergence is recorded and preserved in the sedimentary record of the retro-foreland basin that has continuously been open to an external sink. High syn-orogenic sedimentation and draping across the deformation front in a closed foreland system, as seen in the Ebro basin, appears to mask any post-convergence isostatic rebound signal in the prowedge.
- Once continental subduction was established, the Cenozoic collision stage in the Pyrenees can be compared to the critical wedge model. The prowedge consists of two linked dynamic wedges, a high friction wedge building the Axial Zone and a low friction wedge forming the external fold and thrust belt detached on Triassic evaporites. The presence of evaporites between these two wedges is critical to their interaction. Growth and steady state steps in the development of orogen relief can relate only to the main collision stage and cannot be clearly identified in the Pyrenees.
- Creation of orogen relief migrated westward and southward during main collision establishing high sediment supply by transverse drainage systems into the foreland basins.
- Through widespread studies of salt related features at various scales across the orogen, we continue to build a better understanding of halokinetic activity during the full Wilson cycle. Early salt mobilization is recorded in the Jurassic particularly in the vicinity of Tethyan margins, with passive diapirism during Aptian-Cenomanian rifting on both rift margins, and diapir rejuvenation during Pyrenean compression. Domains of particularly thick Keuper evaporites correlate with areas of strongly decoupled deformation between basement and cover. Thermomechanical modelling shows that the presence of thick (kms), weak evaporites strongly impacts crustal scale deformation (Grool *et al.*, 2019; Jourdon *et al.*, 2020).

These results allow us to better understand, challenge and improve the relevance of generic models for the growth of collisional orogens, in particular by tracking and quantifying key processes at varying resolutions in space and time. Many outstanding questions remain on the Pyrenean orogen and its basins. For example, what was the true amount and distribution of strike-slip deformation during both extension and compressional phases? What controls the perseverance of thermal anomalies in western Pyrenean basins? Ongoing improvements and developments in analytical techniques and data processing in the domain of low temperature thermochronology and isotopic dating (*e.g.*, calcite dating of faults, Hoareau *et al.*, 2021; Parizot *et al.*, 2021) also have the potential to provide high resolution tracking of rock trajectories and thermal evolution of the orogen. As shown by recent studies the application of new concepts and ideas developed in the domain of salt tectonics are providing significant new data and challenging established models on basin and orogen dynamics

in the Pyrenees. Future challenges to improve investigations into orogen structure, rheology and processes include the need to better integrate large geophysical datasets (*e.g.*, passive seismic tomography) and uncertainty analysis of structural interpretations, and to improve statistical analysis of large and complex analytical datasets (*e.g.*, low temperature thermochronology).

Acknowledgements. This paper is a contribution to the Orogen project funded by Total, the BRGM and the CNRS. It is also a contribution to the ANR PYRAMID and RGF Pyrénées projects. While all authors have contributed to this work, the opinions are biased toward those of the first author. The authors salute and thank the whole Orogen Community and the innumerable colleagues and experts of the Pyrenean geoscience community. This work has grown from and greatly benefited from discussions with them all. We thank reviewers P. Labaume and A. Casas-Sainz and editor A. Teixell for their constructive reviews that greatly improved the manuscript.

References

- Airaghi L, Bellahsen N, Dubacq B, Rosenberg C, Janots E, Waldner M, *et al.* 2019. Pre-orogenic upper crustal softening by lower greenschist facies metamorphic reactions in granites of the central Pyrenees. *Journal of Metamorphic Geology* 38(2): 1–22. <https://doi.org/10.1111/jmg.12520>.
- Al Reda S, Jocelyn B, Gautheron C, Eric L, Loget N, Pinna-Jamme R, *et al.* 2021. Thermal record of the building of an orogen in the retroforeland basin: insight from basement and detrital thermochronology in the eastern Pyrenees and the north Pyrenean basin (France). *Basin Res.* 33: 2763–2791. <https://doi.org/10.1111/bre.12583>.
- Allen PA, Allen JR. 2013. Basin analysis: Principles and application to petroleum play assessment. John Wiley & Sons, 451 pp.
- Allen PA, Heller PL. 2012. Dispersal and preservation of tectonically generated alluvial gravels in sedimentary basins. In: Busby CJ, Azor A, (Eds.). *Tectonics of sedimentary basins*. Wiley-Blackwell, pp. 111–130. <https://doi.org/10.1002/9781444347166.ch6>.
- Allen PA, Armitage JJ, Carter A, Duller RA, Michael NA, Sinclair HD, *et al.* 2013. The Qs problem: Sediment volumetric balance of proximal foreland basin systems. *Sedimentology* 60: 102–130. <https://doi.org/10.1111/sed.12015>.
- Alonso-Zarza AM, Sánchez-Moya Y, Bustillo MA, Sopena A, Delgado A. 2002. Silicification and dolomitization of anhydrite nodules in argillaceous terrestrial deposits: An example of meteoric-dominated diagenesis from the Triassic of central Spain. *Sedimentology* 49: 303–317.
- Andrieu S, Saspiturry N, Lartigau M, Issautier B, Angrand P, Lasseur E. 2021. Large-scale vertical movements in Cenomanian to Santonian carbonate platform in Iberia: indicators of a Coniacian pre-orogenic compressive stress. <https://doi.org/10.1051/bsgf/2021011/5278319/bsgf>.
- Angrand P, Mouthereau F. 2021. Evolution of the Alpine orogenic belts in the Western Mediterranean region as resolved by the kinematics of the Europe-Africa diffuse plate boundary. *BSGF* 192: 1–44. <https://doi.org/10.1051/bsgf/2021031>.
- Angrand P, Ford M, Watts AB. 2018. Lateral variations in foreland flexure of a rifted continental margin: The Aquitaine Basin (SW France). *Tectonics* 37. <https://doi.org/10.1002/2017TC004670>.
- Angrand P, Mouthereau F, Masini E, Asti R. 2020. A reconstruction of Iberia accounting for W-Tethys/N-Atlantic kinematics since the late Permian-Triassic. *Solid Earth Discuss.*: 1–24. <https://doi.org/10.5194/se-2020-24>.
- Angrand P, Ford M, Ducoux M, de Saint Blanquat M. 2022. Extension and early orogenic inversion along the basal detachment of a hyper-extended rifted margin: an example from the Central Pyrenees (France). *Journal of the Geological Society* 179. <https://doi.org/10.1144/jgs2020-003>.
- Asti R, Saspiturry N, Angrand P. 2022. The Mesozoic Iberia-Eurasia diffuse plate boundary: A wide domain of distributed transtensional deformation progressively focusing along the North Pyrenean Zone. *Earth-Science Rev.* 230: 104040. <https://doi.org/10.1016/j.earscirev.2022.104040>.
- Babault J, Van Den Driessche J. 2005. L'érosion des chaînes de montagnes: influence de la sédimentation de piedmont. *Comptes Rendus Geosci.* 337: 1431–1438. <https://doi.org/10.1016/j.crte.2005.09.010>.
- Babault J, Teixell A, Struth A, Driessche J van den, Arboleya ML, Teson E. 2013. Shortening, structural relief and drainage evolution in inverted rifts: insights from the Atlas Mountains, the Eastern Cordillera of Colombia and the Pyrenees. In: Nemock M, Mora A, Cosgrove JW, (Eds.). *Thick-skin-dominated orogens from initial inversion to full accretion*. Geological Society London Special Publication 377, pp. 141–158.
- Bache F, Olivet JL, Gorini C, Aslanian D, Labails C, Rabineau M. 2010. Evolution of rifted continental margins: the case of the Gulf of Lions (Western Mediterranean Basin). *Earth and Planetary Science Letters* 292: 345–356.
- Barbarand J, Lucazeau F, Pagel M, Séranne M. 2001. Burial and exhumation history of the south-eastern Massif Central (France) constrained by apatite fission-track thermochronology. *Tectonophysics* 335: 275–290. [https://doi.org/10.1016/S0040-1951\(01\)00069-5](https://doi.org/10.1016/S0040-1951(01)00069-5).
- Barnett-Moore N, Hosseinpour M, Maus S. 2016. Assessing discrepancies between previous plate kinematic models of Mesozoic Iberia and their constraints. *Tectonics* 35: 1843–1862. <https://doi.org/10.1002/2015TC004019>.
- Barnolas A, Courbouleix S. 2001. Synthèse géologique et géophysique des Pyrénées – Volume 3: Cycle alpin: Phénomènes alpins. Édition BRGM – ITGE.
- Barré G, Fillon C, Ducoux M, Mouthereau F, Gaucher EC, Calassou S. 2021. The North Pyrenean Frontal Thrust: structure, timing and late fluid circulation inferred from seismic and thermal-geochemical analyses of well data. *BSGF – Earth Sci. Bull.* 192: 1–95. <https://doi.org/10.1051/bsgf/2021046/5451728/bsgf>.
- Beamud E, Muñoz JA, Fitzgerald PG, Baldwin SL, Garcés M, Cabrera L, *et al.* 2011. Magnetostratigraphy and detrital apatite fission track thermochronology in syntectonic conglomerates: constraints on the exhumation of the South-Central Pyrenees. *Basin Res.* 23: 309–331. <https://doi.org/10.1111/j.1365-2117.2010.00492.x>.
- Beaumont C, Muñoz JA, Hamilton J, Fullsack P. 2000. Factors controlling the Alpine evolution of the central Pyrenees inferred from a comparison of observations and geodynamical models. *J. Geophys. Res.* 105: 8121–8145. <https://doi.org/10.1029/1999JB900390>.
- Bellahsen N, Jolivet L, Lacombe O, Bellanger M, Boutoux A, Garcia S, *et al.* 2012. Mechanisms of margin inversion in the external Western Alps: Implications for crustal rheology. *Tectonophysics* 560-561: 62–83. <https://doi.org/10.1016/j.tecto.2012.06.022>.
- Bellahsen N, Mouthereau F, Boutoux A, Bellanger M, Lacombe O, Jolivet L, *et al.* 2014. Collision kinematics in the western external Alps. *Tectonics* 33: 1055–1088. <https://doi.org/10.1002/2013TC003453>.

- Bellahsen N, Bayet L, Denèle Y, Waldner M, Airaghi L, Rosenberg C, *et al.* 2019. Shortening of the Axial Zone, Pyrenees: Shortening sequence, upper crustal mylonites and crustal strength. *Tectonophysics* 766: 433–452.
- Beltrando M, Frasca G, Compagnoni R, Vitale-Brovarone A. 2012. The Valaisan controversy revisited: Multi-stage folding of a Mesozoic hyper-extended margin in the Petit St. Bernard pass area (Western Alps). *Tectonophysics* 579: 17–36. <https://doi.org/10.1016/j.tecto.2012.02.010>.
- Bernard T, Sinclair HD, Gailleton B, Mudd SM, Ford M. 2019. Lithological control on the post-orogenic topography and erosion history of the Pyrenees. *Earth Planet. Sci. Lett.* 518: 53–66. <https://doi.org/10.1016/j.epsl.2019.04.034>.
- Bernard T, Sinclair HD, Naylor M, Christophoul F, Ford M. 2020. Post-orogenic sediment drape in the Northern Pyrenees explained using a box model. *Basin Res.* <https://doi.org/10.1111/bre.12457>.
- Berné S, Gorini C. 2005. The Gulf of Lion: An overview of recent studies within the French “Margins” programme. *Mar. Pet. Geol.* 22: 691–693. <https://doi.org/10.1016/j.marpetgeo.2005.04.004>.
- Bestani L, Espurt N, Lamarche J, Bellier O, Hollender F. 2016. Reconstruction of the Provence Chain evolution, southeastern France. *Tectonics* 35: 1506–1525. <https://doi.org/10.1002/2016TC004115>.
- Bilotte M. 1985. Le Crétacé supérieur des plates-formes est-pyrénéennes. PhD thesis, Paul Sabatier University, Toulouse, Strata, 5, 438 pp.
- Biteau J-J, Le Marrec A, Le Vot M, Masset J-M. 2006. The Aquitaine Basin. *Pet. Geosci.* 12: 247–273. <https://doi.org/10.1144/1354-079305-674>.
- Bodego A, Iriarte E, López-Horgue MA, Álvarez I. 2018. Rift-margin extensional forced folds and salt tectonics in the eastern Basque-Cantabrian rift basin (western Pyrenees). *Mar. Pet. Geol.* 91: 667–682.
- Bond CE. 2015. Uncertainty in structural interpretation: Lessons to be learnt. *Journal of Structural Geology.* <https://doi.org/10.1016/j.jsg.2015.03.003>.
- Bond RMG, McClay KR. 1995. Inversion of a Lower Cretaceous extensional basin, south central Pyrenees, Spain. *Geol. Soc. London, Spec. Publ.* 88: 415 LP-431. <https://doi.org/10.1144/GSL.SP1995.088.01.22>.
- Bosch G, Teixell A, Jolivet M, Labaume P, Stockli D, Domènech M, *et al.* 2016. Timing of Eocene-Miocene thrust activity in the Western Axial Zone and Chaînons Béarnais (west-central Pyrenees) revealed by multi-method thermochronology. *Comptes Rendus Geosci.* 348: 246–256. <https://doi.org/10.1016/j.crte.2016.01.001>.
- Bourgeois O, Ford M, Diraison M, Le Carlier de Veslud C, Gerbault M, Pik R, *et al.* 2007. Separation of rifting and lithospheric folding signatures in the NW-Alpine foreland. *Int. J. Earth Sci.* 96: 1003–1031. <https://doi.org/10.1007/s00531-007-0202-2>.
- Boyce JW, Hodges KV, Olszewski WJ, Jercinovic MJ, Carpenter BD, Reiners PW. 2006. Laser microprobe (U-Th)/He geochronology. *Geochim. Cosmochim. Acta* 70: 3031–3039. <https://doi.org/10.1016/j.gca.2006.03.019>.
- Burbank DW. 1992. Magnetostratigraphic chronology, mammalian faunas, and stratigraphic evolution of the Lower Freshwater Molasse, Haute-Savoie, France. *Eclogae Geol. Helv.* 85: 399–431.
- Burrell L, Teixell A. 2021. Contractional salt tectonics and role of pre-existing diapiric structures in the Southern Pyrenean foreland fold thrust belt (Montsec and Serres Marginal). *J. Geol. Soc. London* 178: jgs2020-085.
- Burrell L, Teixell A, Gómez-gras D, Coll X. 2021. Basement-involved thrusting, salt migration and intramontane conglomerates: a case from the Southern Pyrenees. *BSGF–Earth Sci. Bull.* 192: 24. <https://doi.org/10.1051/bsgf/2021013/5292189/bsgf>.
- Cadenas P, Fernandez-Viejo G, Pulgar JA, Tugand J, Manatschal G, Minshull TA. 2018. Constraints Imposed by Rift Inheritance on the Compressional Reactivation of a Hyperextended Margin: Mapping Rift Domains in the North Iberian Margin and in the Cantabrian Mountains. *Tectonics* 37: 758–785. <https://doi.org/10.1002/2016TC004454>.
- Cadenas P, Lescoutre R, Manatschal G. 2021. The role of extensional detachment systems in thinning the crust and exhuming granulites: analogies between the offshore Le Danois High and the onshore Labourd Massif in the Biscay/Pyrenean rifts. *BSGF–Earth Sci. Bull.* 192. <https://doi.org/10.1051/bsgf/2021045/5463953/bsgf>.
- Caldera N, Teixell A, Grier A, Labaume P, Lahfid A. 2021. Recumbent folding in the Upper Cretaceous Eaux-Chaudes Massif: A Helvetic-type nappe in the Pyrenees? *Terra Nova* 33: 320–331.
- Calvet M, Gunnell Y, Laumonier B. 2020. Denudation history and palaeogeography of the Pyrenees and their peripheral basins: an 84-million-year geomorphological perspective. *Earth-Science Rev.* 103436. <https://doi.org/10.1016/j.earscirev.2020.103436>.
- Caméra P. 2017. Salt and strike-slip tectonics as main drivers in the structural evolution of the Basque-Cantabrian Basin, Spain. In: *Permo-Triassic Salt Provinces of Europe, North Africa and the Atlantic Margins*, pp. 371–393.
- Caméra JI, Flinch JF. 2017. The Southern Pyrenees: A salt-based fold-and -thrust belt. In: Caméra JI, Flinch JF, Tari G, (Eds.). *Permo-Triassic Salt Provinces of Europe, North Africa and the Atlantic Margins*, pp. 395–415.
- Caméra JI, Flinch JI, Tari G (Eds.), 2017. Permo-Triassic salt provinces of Europe, North Africa and the Atlantic Margins. Elsevier.
- Canérot J. 1988. Manifestations de l’halocinèse dans les chaînons béarnais (Zone Nord-Pyrénéenne) au Crétacé inférieur. *Comptes Rendus de l’Académie des Sciences, Paris* 306 (2): 1099–1102.
- Canérot J. 2017. The pull-apart-type Tardets-Mauléon Basin, a key to understand the formation of the Pyrenees. *BSGF–Earth Sciences Bulletin* 188: 35. <https://doi.org/10.1051/bsgf/2017198>.
- Canérot J, Hudec MR, Rockenbauch K. 2005. Mesozoic diapirism in the Pyrenean orogen: Salt tectonics on a transform plate boundary. *Am. Assoc. Pet. Geol. Bull.* 89: 211–229. <https://doi.org/10.1306/09170404007>.
- Carrapa B. 2010. Resolving tectonic problems by dating detrital minerals. *Geology* 38: 191–192. <https://doi.org/10.1130/focus022010.1>.
- Carrillo E, Guinea A, Casas A, Rivero L, Cox N, Vázquez-Taset YM. 2020. Tectono-sedimentary evolution of transverse extensional faults in a foreland basin: Response to changes in tectonic plate processes. *Basin Research* 32: 1388–1412.
- Casas-Sainz AM, Román-Berdiel T. 1999. Geologia De Los Alrededores De Calahorra Rioja Baja. *Zubia* 17: 165–194.
- Casas A, Kearey P, River L, Adam CR. 1997. Gravity anomaly map of the Pyrenean region and a comparison of the deep geological structure of the western and eastern Pyrenees. *Earth Planet. Science Lett.* 150: 65–78.
- Cederbom CE, Sinclair HD, Schlunegger F, Rahn MK. 2004. Climate-induced rebound and exhumation of the European Alps. *Geology* 32: 709. <https://doi.org/10.1130/G20491.1>.
- Chelalou R, Nalpas T, Bousquet R, Prevost M, Lahfid A, Poujol M, *et al.* 2015. Tectonics, tectonophysics: New sedimentological, structural and paleo-thermicity data in the Boucheville Basin (eastern North Pyrenean Zone, France). *Comptes Rendus–Géoscience.* <https://doi.org/10.1016/j.crte.2015.11.008>.

- Chevrot S, Villaseñor A, Sylvander M, Benahmed S, Beucler E, Cougoulat G, *et al.* 2014. High-resolution imaging of the Pyrenees and Massif Central from the data of the PYROPE and IBERARRAY portable array deployments. *J. Geophys. Res. Solid Earth* 119: 6399–6420.
- Chevrot S, Sylvander M, Diaz J, Martin R, Mouthereau F, Manatschal G, *et al.* 2018. The non-cylindrical crustal architecture of the Pyrenees. *Sci. Rep.* 8: 9591. <https://doi.org/10.1038/s41598-018-27889-x>.
- Chevrot S, Sylvander M, Villaseñor A, Diaz J, Stehly L, Boué P, *et al.* 2022. Passive imaging of collisional orogens: a review of a decade of geophysical studies in the Pyrénées. *BSGF–Earth Sci. Bull.* 193: 1–18. <https://doi.org/10.1051/bsgf/2021049/5514862/bsgf>.
- Choukroune P. 1974. Structure et évolution tectonique de la zone nord-pyrénéenne: analyse de la déformation dans une portion de chaîne à schistosité sub-verticale. PhD thesis, Université des sciences et techniques de Montpellier 2, France.
- Choukroune P. 1976. A discussion on natural strain and geological structure – Strain patterns in the Pyrenean Chain. *Philos. Trans. R. Soc. London. Ser. A, Math. Phys. Sci.* 283(1312): 271–280.
- Choukroune P. 1989. The ECORS Pyrenean deep seismic profile reflection data and the overall structure of an orogenic belt. *Tectonics* 8: 23–39. <https://doi.org/10.1029/TC008i001p00023>.
- Choukroune P, Mattauer M. 1978. Tectonique des plaques et Pyrénées; sur le fonctionnement de la faille transformante nord-pyrénéenne; comparaisons avec des modèles actuels. *Bull. la Société géologique Fr.* 7: 689–700.
- Choukroune P, Roure F, Pinet B, TEAM EP. 1990. Main results of the ECORS Pyrenees profile. *Tectonophysics* 173: 411–423.
- Christophoul F, Soula J-C, Brusset S, Elibana B, Roddaz M, Bessiere G, *et al.* 2003. Time, place and mode of propagation of foreland basin systems as recorded by the sedimentary fill: examples of the Late Cretaceous and Eocene retro-foreland basins of the north-eastern Pyrenees. *Geol. Soc. London, Spec. Publ.* 208: 229–252. <https://doi.org/10.1144/GSL.SP2003.208.01.11>.
- Clavell E. 1992. Geologia del petroli de les conques terciàries de Catalunya. Univ. de Barcelona.
- Clerc C, Lagabrielle Y. 2014. Thermal control on the modes of crustal thinning leading to mantle exhumation: Insights from the Cretaceous Pyrenean hot paleomargins. *Tectonics* 33: 1340–1359. <https://doi.org/10.1002/2013TC003471>.
- Clerc C, Lahfid A, Monié P, Lagabrielle Y, Chopin C, Poujol M, *et al.* 2015. High-temperature metamorphism during extreme thinning of the continental crust: a reappraisal of the north Pyrenean paleo-passive margin. *Solid Earth Discuss.* 7: 797–857. <https://doi.org/10.5194/sed-7-797-2015>.
- Clerc C, Lagabrielle Y, Labaume P, Ringenbach J-C, Vauchez A, Nalpas T, *et al.* 2016. Basement–Cover decoupling and progressive exhumation of metamorphic sediments at hot rifted margin. Insights from the Northeastern Pyrenean analog. *Tectonophysics* 686: 82–97. <https://doi.org/10.1016/j.tecto.2016.07.022>.
- Cochelin B, Lemirre B, Denèle Y, de Saint Blanquat M, Lahfid A, Duchêne S. 2018. Structural inheritance in the central pyrenees: The variscan to Alpine tectonometamorphic evolution of the Axial Zone. *J. Geol. Soc. London.* 175: 336–351. <https://doi.org/10.1144/jgs2017-066>.
- Coll X, Gómez-Gras D, Roigé M, Teixell A, Boya S, Mestres N. 2020. Heavy-mineral provenance signatures during the infill and uplift of a foreland basin: An example from the Jaca basin (Southern Pyrenees, Spain). *Journal of Sedimentary Research* 90: 1747–1769. <https://doi.org/10.2110/jsr.2020.084>.
- Coll X, Roigé M, Gómez-Gras D, Teixell A, Boya S, Mestres N. 2022. Interplay of multiple sediment routing systems revealed by combined sandstone petrography and Heavy Mineral Analysis (HMA) in the South Pyrenean Foreland Basin. *Minerals* 12: 262.
- Coney PJ, Muñoz JA, McClay KR, Evenchick CA. 1996. Syntectonic burial and post-tectonic exhumation of the southern Pyrenees foreland fold-thrust belt. *J. Geol. Soc. London* 153: 9–16.
- Conti P, Cornamusini G, Carmignani L. 2020. An outline of the geology of the Northern Apennines (Italy), with geological map at 1: 250 000 scale. *Int. J. Geosci.* 139: 149–194.
- Cooper M, Warren MJ. 2020. Inverted fault systems and inversion tectonic settings. In: Scarselli N, Adam J, Chiarella D, Roberts DG, Bally AW, (Eds.). *Regional geology and tectonics: Principles of geologic analysis*. Elsevier pp. 169–204. <https://doi.org/10.1016/b978-0-444-64134-2.00009-2>.
- Corre B, Lagabrielle Y, Labaume P, Fourcade S, Clerc C, Ballèvre M. 2016. Deformation associated with mantle exhumation in a distal, hot passive margin environment: New constraints from the Sarailié Massif (Chaînons Béarnais, North-Pyrenean Zone). *Comptes Rendus Geosci.* 348: 279–289. <https://doi.org/10.1016/j.cre.2015.11.007>.
- Costa E, Garcés M, López-Blanco M, Beamud E, Gómez-Paccard M, Larrasoana JC. 2010. Closing and continentalization of the South Pyrenean foreland basin (NE Spain): magnetochronological constraints. *Basin Res.* 22: 904–917.
- Crémades A, Ford M, Charreau J. 2021. Evidence of decoupled deformation during Jurassic rifting and Cenozoic inversion phases in the salt-rich Corbières-Languedoc Transfer Zone (Pyreneo-Provençal orogen, France). *BSGF–Earth Sci. Bull.* 192.
- Critelli S, Mongelli G, Perri F, Martín-algarra A, Martín-martín M, Perrone V, *et al.* 2008. Compositional and Geochemical Signatures for the Sedimentary Evolution of the Middle Triassic–Lower Jurassic Continental Redbeds from Western-Central Mediterranean Alpine Chains. *J. Geol.* 116: 375–386. <https://doi.org/10.1086/588833>.
- Cruset D, Vergés J, Albert R, Gerdes A, Benedicto A, Cantarero I, *et al.* 2020. Quantifying deformation processes in the SE Pyrenees using U-Pb dating of fracture-filling calcites. *J. Geol. Soc. London* 177: 1186–1196. <https://doi.org/10.1144/jgs2020-014>.
- Curnelle R, Dubois P, Seguin JC. 1982. The Mesozoic-Tertiary Evolution of the Aquitaine Basin. *Philos. Trans. R. Soc. London, Ser. A* 305: 63–84.
- Curry ME, van der Beek P, Huisman RS, Wolf SG, Muñoz J-A. 2019. Evolving paleotopography and lithospheric flexure of the Pyrenean Orogen from 3D flexural modeling and basin analysis. *Earth Planet. Sci. Lett.* 515: 26–37. <https://doi.org/10.1016/j.epsl.2019.03.009>.
- Curry ME, van der Beek P, Huisman RS, Wolf SG, Fillon C, Muñoz JA. 2021. Spatio-temporal patterns of Pyrenean exhumation revealed by inverse thermo-kinematic modeling of a large thermochronologic data set. *Geology* 49: 738–742. <https://doi.org/10.1130/G48687.1>.
- Danišik M, McInnes BIA, Kirkland CL, McDonald BJ, Evans NJ, Becker T. 2017. Seeing is believing: Visualization of He distribution in zircon and implications for thermal history reconstruction on single crystals. *Sci. Adv.* 3: e1601121. <https://doi.org/10.1126/sciadv.1601121>.
- Daudet M, Mouthereau F, Brichau S, Crespo-Blanc A, Gautheron C, Angrand P. 2020. Tectono-stratigraphic and thermal evolution of the western Betic flysch: implications for the geodynamics of South Iberian margin and Alboran Domain. *Tectonics* 39: e2020TC006093.
- de Graciansky PC. 1962. Données stratigraphiques et tectoniques nouvelles sur la Montagne de Tauch. *Bull. la Soc. Géologique Fr.* 7 IV: 509–527.

- de Saint Blanquat M, Bajolet F, Grand'Homme A, Proietti A, Zanti M, Boutin A, *et al.* 2016. Cretaceous mantle exhumation in the central Pyrenees: New constraints from the peridotites in eastern Ariège (North Pyrenean zone, France). *Comptes Rendus–Geosci.* 348. <https://doi.org/10.1016/j.crte.2015.12.003>.
- Debrand-Passard S, Courbouleix S, Lienhardt MJ. 1984. Synthèse géologique du sud-est de la France. *Mémoire de la Bureau de Recherche géologique et Minières. BRGM.*
- DeCelles PG. 2012. Foreland basin systems revisited: Variations in response to tectonic settings. In: Busby C, Azor A, (Eds.). *Tectonics of Sedimentary Basins*. Wiley-Blackwell, pp. 405–426. <https://doi.org/10.1002/9781444347166.ch20>.
- DeCelles PG, Giles K 1996. Foreland basin systems. *Basin Res.* 8: 105–123. <https://doi.org/10.1046/j.1365-2117.1996.01491.x>.
- Deckers J. 2015. The Paleocene stratigraphic records in the Central Netherlands and close surrounding basins: highlighting the different responses to a late Danian change in stress regime within the Central European Basin System. *Tectonophysics* 659: 102–108.
- Deckers J, van der Voet E. 2018. A review on the structural styles of deformation during Late Cretaceous and Paleocene tectonic phases in the southern North Sea area. *J. Geodyn.* 115: 1–9.
- Desegaulx P, Brunet M-F. 1990. Tectonic subsidence of the Aquitaine basin since Cretaceous times. *Bull. la Société géologique Fr.* 8: 295–306.
- Desegaulx P, Roure F, Villein A. 1990. Structural evolution of the Pyrenees: tectonic inheritance and flexural behaviour in the continental crust. *Tectonophysics* 182: 211–225.
- Dewey JF, Helman ML, Turco E, Hutton DWH, Knott SD. 1989. Kinematics of the western Mediterranean. In: Coward MP, Dietrich D, Park RG, (Eds.). *Alpine Tectonics*. Geological Society, London, Special Publication, pp. 265–284.
- Dèzes P, Schmid SM, Ziegler PA. 2004. Evolution of the European Cenozoic Rift System: interaction of the Alpine and Pyrenean orogens with their foreland lithosphere. *Tectonophysics* 389: 1–33. <https://doi.org/10.1016/j.tecto.2004.06.011>.
- Diaz J, Vergès J, Chevrot S, Antonio-Vigil A, Ruiz M, Sylvander M, *et al.* 2018. Mapping the crustal structure beneath the eastern Pyrenees. *Tectonophysics* 744: 296–309. <https://doi.org/10.1016/j.tecto.2018.07.011>.
- Dielforder A, Frasca G, Brune S, Ford M. 2019. Formation of the Iberian-European Convergent Plate Boundary Fault and Its Effect on Intraplate Deformation in Central Europe. *Geochemistry, Geophys. Geosystems* 20. <https://doi.org/10.1029/2018GC007840>.
- Dubois P, Seguin J-C. 1978. Les flyschs crétacé et éocène de la zone commingeoise et leur environnement. *Bull. la Société Géologique Fr.* 7(XX): 657–671. <https://doi.org/10.2113/gssgfbull.S7-XX.5.657>.
- Ducoux M, Jolivet L, Callot JP, Aubourg C, Masini E, Lahfid A, *et al.* 2019. The Nappe des Marbres Unit of the Basque-Cantabrian Basin: The Tectono-thermal Evolution of a Fossil Hyperextended Rift Basin. *Tectonics* 38: 3881–3915. <https://doi.org/10.1029/2018TC005348>.
- Ducoux M, Jolivet L, Cagnard F, Baudin T. 2021a. Basement-cover decoupling during the inversion of a hyperextended basin: insights from the Eastern Pyrenees. *Tectonics* 40: 1–23. <https://doi.org/10.1029/2020TC006512>.
- Ducoux M, Jolivet L, Masini E, Augier R, Lah A, Bernet M, *et al.* 2021b. Distribution and intensity of High-Temperature Low-Pressure metamorphism across the Pyrenean-Cantabrian belt: constraints on the thermal record of the pre-orogenic hyperextension rifting. *BSGF–Earth Sci. Bull.* 192: 43. <https://doi.org/10.1051/bsgf/2021029/5432657/bsgf>.
- Ducoux M, Masini E, Tugend J, Gómez-Romeu J, Calassou S. 2022. Basement-decoupled hyperextension rifting: The tectono-stratigraphic record of the salt-rich Pyrenean necking zone (Arzacq Basin, SW France). *GSA Bull.* 134: 941–964. <https://doi.org/10.1130/B35974.1>.
- Duffy OB, Dooley TP, Hudec MR, Jackson MPA, Fernandez N, Jackson CAL, *et al.* 2018. Structural evolution of salt-influenced fold-and-thrust belts: A synthesis and new insights from basins containing isolated salt diapirs. *J. Struct. Geol.* 114: 206–221. <https://doi.org/10.1016/j.jsg.2018.06.024>.
- Erdős Z, Huismans RS, van der Beek P, Thieulot C. 2014a. Extensional inheritance and surface processes as controlling factors of mountain belt structure. *J. Geophys. Res. Solid Earth* 119: 9042–9061.
- Erdős Z, van der Beek P, Huismans RS. 2014b. Evaluating balanced section restoration with thermochronology data: A case study from the Central Pyrenees. *Tectonics* 33: 617–634. <https://doi.org/10.1002/2013TC003481>.
- Erdős Z, Huismans RS, van der Beek P. 2019. Control of increased sedimentation on orogenic fold-and-thrust belt structure—insights into the evolution of the Western Alps. *Solid Earth* 10(2): 391–404.
- Espurt N, Angrand P, Teixell A, Labaume P, Ford M, de Saint Blanquat M, *et al.* 2019a. Crustal-scale balanced cross-section and restorations of the Central Pyrenean belt (Nestes-Cinca transect): Highlighting the structural control of Variscan belt and Permian-Mesozoic rift systems on mountain building. *Tectonophysics* 764: 25–45. <https://doi.org/10.1016/j.tecto.2019.04.026>.
- Espurt N, Wattellier F, Philip J, Hippolyte JC, Bellier O, Bestani L. 2019b. Mesozoic halokinesis and basement inheritance in the eastern Provence fold-thrust belt, SE France. *Tectonophysics* 766: 60–80. <https://doi.org/10.1016/j.tecto.2019.04.027>.
- Ethève N, Mohn G, Lamotte DF de, Roca E, Tugend J, Gómez-romeu J. 2018. Extreme Mesozoic Crustal Thinning in the Eastern Iberia Margin: The Example of the Columbrets Basin (Valencia Trough). *Tectonics* 37: 1–27. <https://doi.org/10.1002/2017TC004613>.
- Evans NJ, McInnes BIA, McDonald B, Danišik M, Becker T, Vermeesch P, *et al.* 2015. An *in situ* technique for (U-Th-Sm)/He and U-Pb double dating. *J. Anal. At. Spectrom.* 30: 1636–1645. <https://doi.org/10.1039/C5JA00085H>.
- Ferrer O, Roca E, Benjumea B, Muñoz JA, Ellouz N, MARCONI Team. 2008. The deep seismic reflection MARCONI-3 profile: Role of extensional Mesozoic structure during the Pyrenean contractional deformation at the eastern part of the Bay of Biscay. *Mar. Pet. Geol.* 25: 714–730. <https://doi.org/10.1016/j.marpetgeo.2008.06.002>.
- Ferrer O, Jackson MPA, Roca E, Rubinat M. 2012. Evolution of salt structures during extension and inversion of the Offshore Parentis Basin (Eastern Bay of Biscay). *Geol. Soc. Spec. Publ.* 363: 361–380. <https://doi.org/10.1144/SP363.16>.
- Filleaudeau PY, Mouthereau F, Pik R. 2011. Thermo-tectonic evolution of the south-central Pyrenees from rifting to orogeny: Insights from detrital zircon U/Pb and (U-Th)/He thermochronometry. *Basin Res.* 24: 401–417. <https://doi.org/10.1111/j.1365-2117.2011.00535.x>.
- Fillon C, van der Beek P. 2012. Post-orogenic evolution of the southern Pyrenees: constraints from inverse thermo-kinematic modelling of low-temperature thermochronology data. *Basin Res.* 24: 418–436. <https://doi.org/10.1111/j.1365-2117.2011.00533.x>.
- Fillon C, Gautheron C, van der Beek P. 2013a. Oligocene-Miocene burial and exhumation of the Southern Pyrenean foreland quantified by low-temperature thermochronology. *J. Geol. Soc. London* 170: 67–77.

- Fillon C, Huismans RS, van der Beek P, Muñoz JA. 2013b. Syntectonic sedimentation controls on the evolution of the southern Pyrenean fold-and-thrust belt: Inferences from coupled tectonic-surface processes models. *J. Geophys. Res.* 118: 1–16. <https://doi.org/10.1002/jgrb.50368>.
- Fillon C, Huismans RS, van der Beek P. 2013c. Syntectonic sedimentation effects on the growth of fold-and-thrust belts. *Geology* 41: 83–86. <https://doi.org/10.1130/G33531.1>.
- Fillon C, Mouthereau F, Calassou S, Pik R, Bellahsen N, Gautheron C, *et al.* 2020. Post-orogenic exhumation in the western Pyrenees: evidence for extension driven by pre-orogenic inheritance. *J. Geol. Soc. London* jgs2020-079. <https://doi.org/10.1144/jgs2020-079>.
- Fitzgerald PG, Muñoz JA, Coney PJ, Baldwin SL. 1999. Asymmetric exhumation across the Pyrenean orogen: implications for the tectonic evolution of a collisional orogen. *Earth Planet. Sci. Lett.* 173: 157–170. [https://doi.org/10.1016/S0012-821X\(99\)00225-3](https://doi.org/10.1016/S0012-821X(99)00225-3).
- Flemings PB, Jordan TE. 1990. Stratigraphic modeling of foreland basins: interpreting thrust deformation and lithosphere rheology. *Geology* 18: 430–434.
- Ford M. 2004. Depositional wedge tops: Interaction between low basal friction external orogenic wedges and flexural foreland basins. *Basin Res.* 16: 361–375.
- Ford M, Vergés J. 2021. Evolution of a salt-rich transtensional rifted margin, eastern North Pyrenees, France. *J. Geol. Soc. London* 178: jgs2019-157. <https://doi.org/10.1144/jgs2019-157>.
- Ford M, Hemmer L, Vacherat A, Gallagher K, Christophoul F. 2016. Retro-wedge foreland basin evolution along the ECORS line, eastern Pyrenees, France. *J. Geol. Soc. London* 173: 419–437. <https://doi.org/10.1144/jgs2015-129>.
- Frasca G, Manatschal G, Cadenas P, Miró J, Lescoutre R. 2021. A kinematic reconstruction of Iberia using intracontinental slip corridors. *Terra Nov.* 1–9. <https://doi.org/10.1111/ter.12549>.
- Garcés M, López-blanco M, Valero L, Beamud E, Muñoz J-A, Olivaria B, *et al.* 2020. Paleogeographic and sedimentary evolution of the South Pyrenean foreland basin. *Mar. Pet. Geol.* 113.
- García-Castellanos D, Larrasoña JC. 2015. Quantifying the post-tectonic topographic evolution of closed basins: The Ebro basin (northeast Iberia). *Geology* 43: 2–5. <https://doi.org/10.1130/G36673.1>.
- García-Castellanos D, Vergés J, Gaspar-Escribano J, Cloetingh S. 2003. Interplay between tectonics, climate and fluvial transport during the Cenozoic evolution of the Ebro Basin (NE Iberia). *J. Geophys. Res.* 208: 2347. <https://doi.org/10.1029/2002JB002073>.
- García-Senz J, Pedrera A, Ayala C, Ruiz-constán ANA, Robador A, Rodríguez-fernández R. 2020. Inversion of the north Iberian hyperextended margin: the role of exhumed mantle indentation during continental collision. In: Hammerstein JA, Cuia R Di, Cottam MA, Zamora G, Butler RW, (Eds.). *Fold and thrust belts: Structural style, evolution and exploration*. Geological Society London Special Publication 490, pp. 177–198.
- Gaspar-Escribano JM, García-Castellanos D, Roca E, Cloetingh S. 2004. Cenozoic vertical motions of the Catalan Coastal Ranges (NE Spain): The role of tectonics, isostasy and surface transport. *Tectonics* 23.
- Geel T, Roep TB. 1998. Oligocene to middle Miocene basin development in the Eastern Betic Cordilleras, SE Spain (Velez Rubio Corridor-Espuna): reflections of west Mediterranean plate-tectonic reorganizations. *Basin Res.* 10: 325–344.
- Gómez-Romeu J, Masini E, Tugend J, Ducoux M, Kusznir N. 2019. Role of rift structural inheritance in orogeny highlighted by the Western Pyrenees case-study. *Tectonophysics* 766: 131–150. <https://doi.org/10.1016/j.tecto.2019.05.022>.
- Gorini C, Viallard P, Déramond J. 1991. Inversion négative bassin de Narbone. *Comptes Rendu Académie Sci. Paris* 312 Série: 1013–1019.
- Grool AR, Ford M, Vergés J, Huismans RS, Christophoul F, Dielforder A. 2018. Insights into the crustal-scale dynamics of a doubly vergent orogen from a quantitative analysis of its forelands: A case study of the Eastern Pyrenees. *Tectonics* 37: 450–476. <https://doi.org/10.1002/2017TC004731>.
- Grool AR, Huismans RS, Ford M. 2019. Salt décollement and rift inheritance controls on crustal deformation in orogens. *Terra Nov.* 31. <https://doi.org/10.1111/ter.12428>.
- Guennoc P, Gorini C, Mauffret A. 2000. Histoire géologique du Golfe du Lion et cartographie du rift oligo-aquitain et de la surface messinienne. *Géologie de la France*: 67–97.
- Guieu G, Roussel J. 1990. Arguments for the pre-rift uplift and rift propagation in the Ligurian-Provençal Basin (northwestern Mediterranean) In the light of Pyrenean Provençal Orogeny. *Tectonics* 9: 1113–1142.
- Guimera J, Alvaro M. 1990. Structure et évolution de la compression alpine dans la Chaîne Ibérique et la Chaîne côtière catalane (Espagne). *Bull. la Société géologique Fr.* 6: 339–348.
- Gunnell Y, Zeyen H, Calvet M. 2008. Geophysical evidence of a missing lithospheric root beneath the Eastern Pyrenees: Consequences for post-orogenic uplift and associated geomorphic signatures. *Earth Planet. Sci. Lett.* 276: 302–313. <https://doi.org/10.1016/j.epsl.2008.09.031>.
- Handy MR, Schmid S, Bousquet R, Kissling E, Bernoulli D. 2010. Reconciling plate-tectonic reconstructions of Alpine Tethys with the geological-geophysical record of spreading and subduction in the Alps. *Earth-Science Rev.* 102: 121–158. <https://doi.org/10.1016/j.earscirev.2010.06.002>.
- Hart NR, Stockli DF, Lavier LL, Hayman NW. 2017. Thermal evolution of a hyperextended rift basin, Mauléon Basin western Pyrenees. *Tectonics* 36: 2016TC004365. <https://doi.org/10.1002/2016TC004365>.
- Heller PL, Angevine CL, Winslow NS, Paola C. 1988. Two-phase stratigraphic model of foreland-basin sequences. *Geology* 16: 501–504.
- Hennuy J. 2003. Sédimentation carbonatée et silicoclastique sous contrôle tectonique, le bassin sud-provençal et sa plate-forme carbonatée du turonien moyen au coniacien moyen. Évolutions séquentielle, diagénétique, paléogéographique. PhD thesis, Université Aix Marseille 1: 194.
- Henry J, Zolnai G. 1971. Sur le Trias résédimenté dans le sud-ouest du bassin aquitain. *Cent. Rech. Pau, Bull.* 5: 389–398.
- Hinsbergen DJJ Van, Torsvik TH, Schmid SM, Matenco LC, Maffione M, Vissers RLM, *et al.* 2020. Orogenic architecture of the Mediterranean region and kinematic reconstruction of its tectonic evolution since the Triassic. *Gondwana Res.* 81: 79–229. <https://doi.org/10.1016/j.gr.2019.07.009>.
- Hoareau G, Crognier N, Lacroix B, Aubourg C, Roberts NM, Niemi N, *et al.* 2021. Combination of $\Delta 47$ and U-Pb dating in tectonic calcite veins unravel the last pulses related to the Pyrenean Shortening (Spain). *Earth and Planetary Science Letters* 553: 116636.
- Horne AM, van Soest MC, Hodges KV, Tripathy-Lang A, Hourigan JK. 2016. Integrated single crystal laser ablation U/Pb and (U-Th)/He dating of detrital accessory minerals – Proof-of-concept studies of titanites and zircons from the Fish Canyon tuff. *Geochim. Cosmochim. Acta* 178: 106–123. <https://doi.org/10.1016/j.gca.2015.11.044>.
- Horne AM, van Soest MC, Hodges KV. 2019. U/Pb and (U-Th-Sm)/He “double” dating of detrital apatite by laser ablation: A critical

- evaluation. *Chem. Geol.* 506: 40–50. <https://doi.org/10.1016/j.chemgeo.2018.12.004>.
- Horton BK, Plate M. 2018. Sedimentary record of Andean mountain building. *Earth-Science Rev.* 178: 279–309. <https://doi.org/10.1016/j.earscirev.2017.11.025>.
- Hudec MR, Dooley TP, Burrell L, Teixell A, Fernandez N. 2021. An alternative model for the role of salt depositional configuration and preexisting salt structures in the evolution of the Southern Pyrenees, Spain. *J. Struct. Geol.* 146: 104325. <https://doi.org/10.1016/j.jsg.2021.104325>.
- Huyghe D, Mouthereau F, Ségalen L, Furió M. 2020. Long-term dynamic topographic support during post-orogenic crustal thinning revealed by stable isotope ($\delta^{18}\text{O}$) paleo-altimetry in eastern Pyrenees. *Sci. Rep.* 10: 1–8. <https://doi.org/10.1038/s41598-020-58903-w>.
- Issautier B, Nicolas S, Serrano O. 2020. Role of structural inheritance and salt tectonics in the formation of pseudosymmetric continental rifts on the European margin of the hyperextended Mauléon basin (Early Cretaceous Arzacq and Tartas Basins). *Mar. Pet. Geol.* 118: 104395. <https://doi.org/10.1016/j.marpetgeo.2020.104395>.
- Izquierdo-Llavall E, Menant A, Aubourg C, Callot JP, Hoareau G, Camps P, *et al.* 2020. Preorogenic Folds and Syn-Orogenic Basement Tilts in an Inverted Hyperextended Margin: The Northern Pyrenees Case Study. *Tectonics* 39: 1–32. <https://doi.org/10.1029/2019TC005719>.
- James V, Canérot J. 1999. Diapirisme et structuration post-triasique des Pyrénées occidentales et de l'Aquitaine méridionale (France). *Eclogae Geologicae Helveticae* 92: 63–72.
- Jammes S, Huismans RS. 2012. Structural styles of mountain building: Controls of lithospheric rheologic stratification and extensional inheritance. *Journal of Geophysical Research* 117: B10403. <https://doi.org/10.1029/2012B009376>.
- Jammes S, Manatschal G, Lavier L, Masini E. 2009. Tectonosedimentary evolution related to extreme crustal thinning ahead of a propagating ocean: Example of the western Pyrenees. *Tectonics* 28: n/a–n/a. <https://doi.org/10.1029/2008TC002406>.
- Jammes S, Tiberi C, Manatschal G. 2010. 3D architecture of a complex transcurrent rift system: The example of the Bay of Biscay-Western Pyrenees. *Tectonophysics* 489: 210–226. <https://doi.org/10.1016/j.tecto.2010.04.023>.
- Jolivet M, Labaume P, Monié P, Brunel M, Arnaud N, Campani M. 2007. Thermochronology constraints for the propagation sequence of the south Pyrenean basement thrust system (France–Spain). *Tectonics* 26: TC5007. <https://doi.org/10.2006TC002080>.
- Jolivet L, Faccena C, Agard P, Frizon de la Motte D, Menant A, Sternai P, *et al.* 2016. Neo-Tethys geodynamics and mantle convection: from extension to compression in Africa and a conceptual model for obduction. *Can. J. Earth Sci.* 53: 1–15. <https://doi.org/10.1139/cjes-2015-0118>.
- Jolivet L, Romagny A, Gorini C, Maillard A, Thion I, Couëffé R, *et al.* 2020. Fast dismantling of a mountain belt by mantle flow: Late-orogenic evolution of Pyrenees and Liguro-Provençal rifting. *Tectonophysics* 776. <https://doi.org/10.1016/j.tecto.2019.228312>.
- Jolivet L, Baudin T, Calassou S, Chevrot S, Ford M, Issautier B, *et al.* 2021a. Geodynamic evolution of a wide plate boundary in the Western Mediterranean, near-field versus far-field interactions. *BSGF–Earth Sci. Bull.* 192: 48. <https://doi.org/10.1051/bsgf/2021043>.
- Jolivet L, Menant A, Roche V, Pourhiet L, Le Maillard A, Augier R, *et al.* 2021b. Transfer zones in Mediterranean back-arc regions and tear faults. <https://doi.org/10.1051/bsgf/2021006/5260048/bsgf>.
- Jordan TE. 1995. Retroarc foreland and related basins. In: Busby CJ, Ingersoll RV, (Eds.). *Tectonics of sedimentary basins*. Blackwell Science, pp. 331–361.
- Jourdan JM, Philippe Y, Moen-Maurel L, Tégou C, Bailly G, Bringuier F, *et al.* 1998. Bilan du permis La Noue après retraitement 2D (bassins de Tarbes et du Comminges). *Internal Report Elf Aquitaine Exploration Production France*.
- Jourdon A, Le Pourhiet L, Mouthereau F, Masini E. 2019. Role of rift maturity on the architecture and shortening distribution in mountain belts. *Earth Planet. Sci. Lett.* 512: 89–99. <https://doi.org/10.1016/j.epsl.2019.01.057>.
- Jourdon A, Mouthereau F, Le Pourhiet L, Callot J. 2020. Topographic and tectonic evolution of mountain belts controlled by salt thickness and rift architecture. *Tectonics* 39: e2019TC005903. <https://doi.org/10.1029/2019TC005903>.
- Kley J. 2018. Timing and spatial patterns of Cretaceous and Cenozoic inversion in the Southern Permian Basin. In: Kilhams B, Kukla PA, Mazur S, McKie T, Munlieff H, Van Ojik K, (Eds.). *Mesozoic resource potential in the Southern Permian Basin*. Geological Society, London, Special Publications 469, pp. 19–31.
- Kley J, Voigt T. 2008. Late Cretaceous intraplate thrusting in central Europe: Effect of Africa-Iberia-Europe convergence, not Alpine collision. *Geology* 36: 839–842. <https://doi.org/10.1130/G24930A.1>.
- Krzywiec P, Vergés Jaume. 1996. Role of the foredeep evaporites in wedge tectonics and formation of triangle zones: Comparison of the Carpathian and Pyrenean thrust fronts. In: Lacombe O, Lavé J, Roure F, Vergés J, (Eds.). *Thrust belts and foreland basins*. Springer, pp. 385–396.
- Labaume P, Teixell A. 2018. 3D structure of subsurface thrusts in the eastern Jaca Basin, southern Pyrenees. *Geodyn. Acta* 16: 477–498. <https://doi.org/10.1344/GeologicaActa2018.16.4.9>.
- Labaume P, Teixell A. 2020. Evolution of salt structures of the Pyrenean rift (Châinons Béarnais, France): From hyper-extension to tectonic inversion. *Tectonophysics* 228451. <https://doi.org/10.1016/j.tecto.2020.228451>.
- Labaume P, Meresse F, Jolivet M, Teixell A, Lahfid A. 2016. Tectonothermal history of an exhumed thrust-sheet-top basin: An example from the south Pyrenean thrust belt. *Tectonics* 35: 1280–1313. <https://doi.org/10.1002/2016TC004192>.
- Lagabrielle Y, Bodinier JL. 2008. Submarine reworking of exhumed subcontinental mantle rocks: Field evidence from the Lherz peridotites, French Pyrenees. *Terra Nov.* 20: 11–21. <https://doi.org/10.1111/j.1365-3121.2007.00781.x>.
- Lagabrielle Y, Labaume P, de Saint Blanquat M. 2010. Mantle exhumation, crustal denudation, and gravity tectonics during Cretaceous rifting in the Pyrenean realm (SW Europe): insights from the geological setting of the lherzolite bodies. *Tectonics* 29: TC4012.
- Lagabrielle Y, Asti R, Duretz T, Clerc C, Fourcade S, Teixell A, *et al.* 2020. A review of Cretaceous smooth-slopes extensional basins along the Iberia-Eurasia plate boundary: How pre-rift salt controls the models of continental rifting and mantle exhumation. *Earth-Science Rev.* 201: 103071. <https://doi.org/10.1016/j.earscirev.2019.103071>.
- Lamotte DF, De Raulin C, Mouchot N, Christophe J, Daveau W, Blanpied C, *et al.* 2011. The southernmost margin of the Tethys realm during the Mesozoic and Cenozoic: Initial geometry and timing of the inversion processes. *Tectonics* 30: 1–22. <https://doi.org/10.1029/2010TC002691>.
- Larrasoana JC, Parés JM, Millán H, del Valle J, Pueyo EL. 2003. Paleomagnetic, structural, and stratigraphic constraints on transverse fault kinematics during basin inversion: The Pamplona Fault (Pyrenees, north Spain). *Tectonics* 22. <https://doi.org/10.1029/2002TC001446>.

- Laumonier B. 2015. Les Pyrénées alpines sud-orientales (France, Espagne) – essai de synthèse. *Rev. Géologie pyrénéenne* 2.
- Lawton TF, Roca E, Guimerà J. 1999. Kinematic-stratigraphic evolution of a growth syncline and its implications for tectonic development of the proximal foreland basin, southeastern Ebro basin, Catalunya, Spain. *Geol. Soc. Am. Bull.* 111: 412–431.
- Le Breton E, Brune S, Ustaszewski K, Zahirovic S, Seton M, Müller RD. 2020. Kinematics and extent of the Piemont-Liguria Basin – implications for subduction processes in the Alps. *Solid Earth Discuss.* 2020: 1–42. <https://doi.org/10.5194/se-2020-161>.
- Le Maire P, Thion I, Tugend J, Issautier B, Martelet G, Paquet F, *et al.* 2021. New Magnetic compilation and interpretation of the Bay of Biscay and surrounding continental shelves. *BSGF-Earth Sci. Bull.* 192: 58.
- Léger J, Pik R, Ford M, Tibari B, Ternois S, Frasca G, *et al.* 2021. Detrital (U-Th-Sm)/He and U/Pb geo-thermochronometry as a tool to reveal past orogen dynamics and source to sink evolution. A case study from the Corbières, eastern Pyrenees, France. Abstract, ThermoNet. Barcelonnette.
- Lehuteur M, Chevrot S, Villaseñor A, Masini E, Saspiturry N, Lescoutre R, *et al.* 2021. Three-dimensional shear velocity structure of the Mauléon and Arzacq Basins (Western Pyrenees). *BSGF-Earth Sci. Bull.* 192. <https://doi.org/10.1051/bsgf/2021039/5432932/bsgf>.
- Leleu S, Hartley AJ, van Oosterhout C, Kennan L, Ruckwied K, Gerdes K. 2016. Structural, stratigraphic and sedimentological characterisation of a wide rift system: The Triassic rift system of the Central Atlantic Domain. *Earth-Science Rev.* 158: 89–124. <https://doi.org/10.1016/j.earscirev.2016.03.008>.
- Lescoutre R, Manatschal G. 2020. Role of rift-inheritance and segmentation for orogenic evolution: example from the Pyrenean-Cantabrian system. *BSGF-Earth Sci. Bull.* 191.
- Lescoutre R, Tugend J, Brune S, Masini E, Manatschal G. 2019. Thermal evolution of asymmetric hyperextended magma-poor rift systems: results from numerical modelling of Pyrenean field observations. *Geochemistry, Geophysics, Geosystems* 20: 4567–4587. <https://doi.org/10.1029/2019GC008600>.
- Lescoutre R, Manatschal G, Muñoz JA. 2021. Nature, Origin, and Evolution of the Pyrenean-Cantabrian Junction. *Tectonics* 40: 1–40. <https://doi.org/10.1029/2020TC006134>.
- Lewis CJ, Vergés J, Marzo M. 2000. High mountains in a zone of extended crust – Insights into the Neogene-Quaternary topographic development of northeastern Iberia. *Tectonics* 19: 86–102.
- López-Horgue MA, Iriarte E, Schröder S, Fernández-Mendiola PA, Caline B, Corneylie H, *et al.* 2010. Structurally controlled hydrothermal dolomites in Albian carbonates of the Asón valley, Basque Cantabrian Basin, Northern Spain. *Mar. Pet. Geol.* 27: 1069–1092.
- Lopez-Mir B, Muñoz JA, García-Senz J. 2014. Restoration of basins driven by extension and salt tectonics: Example from the Cotiella Basin in the central Pyrenees. *J. Struct. Geol.* 69: 147–162. <https://doi.org/10.1016/j.jsg.2014.09.022>.
- Lopez-Mir B, Muñoz JA, García-Senz J. 2015. Extensional salt tectonics in the partially inverted Cotiella post-rift basin (south-central Pyrenees): structure and evolution. *Int. J. Earth Sci.* 104: 419–434.
- Luis F. 2001. La cinématique de l’Atlantique Nord: la question de la déformation intraplaque. Ifremer, PhD thesis, Université de Brest.
- Macchiavelli C, Vergés J, Schettino A, Fernández M, Turco E, Casciello E, *et al.* 2017. A New Southern North Atlantic Isochron Map: Insights Into the Drift of the Iberian Plate Since the Late Cretaceous. *J. Geophys. Res. Solid Earth* 122: 9603–9626. <https://doi.org/10.1002/2017JB014769>.
- Maerten L, Séranne M. 1995. Extensional tectonics of the Oligo-Miocene Hérault Basin (S France), Gulf of Lion margin. *Bull. Soc. Geol. Fr.* 166: 739–749.
- Manatschal G, Chenin P, Lescoutre R, Miró J, Cadenas P, Saspiturry N, *et al.* 2021. The role of inheritance in forming rifts and rifted margins and building collisional orogens: a Biscay-Pyrenean perspective. *BSGF-Earth Sci. Bull.* <https://doi.org/10.1051/bsgf/2021042>.
- Marroni M, Monechi S, Perilli N, Principi G, Treves B. 1992. Late Cretaceous flysch deposits of the Northern Apennines, Italy: age of inception of orogenesis-controlled sedimentation. *Cretac. Res.* 13: 487–504. [https://doi.org/10.1016/0195-6671\(92\)90013-G](https://doi.org/10.1016/0195-6671(92)90013-G).
- Martin-Rojas I, Somma R, Delgado F, Estévez A, Iannace A, Perrone V, *et al.* 2009. Triassic continental rifting of Pangaea: Direct evidence from the Alpujarride carbonates, Betic Cordillera, SE Spain. *J. Geol. Soc. London.* 166: 447–458. <https://doi.org/10.1144/0016-76492008-091>.
- Mas JR, Alonso A, Guimera J. 1993. Evolución tectonosedimentaria de una cuenca extensional intraplaque: la cuenca finijurásica-eocretácica de Los Cameros (La Rioja-Soria). *Rev. la Soc. Geológica España* 6: 129–144.
- Masini E, Manatschal G, Tugend J, Mohn G, Flament J-M. 2014. The tectono-sedimentary evolution of a hyper-extended rift basin: the example of the Arzacq-Mauléon rift system (Western Pyrenees, SW France). *Int. J. Earth Sci.* 103: 1569–1596.
- Masse J-P, Philip J. 1976. Paléogéographie et tectonique du crétacé moyen en Provence: révision du concept d’isthme durencien. *Rev. Géographie Phys. Géologie Dyn.* XVIII: 49–66.
- Maufrangeas A, Leleu S, Loisy C, Roperch P, Jolley D, Vinciguerra C, *et al.* 2020. Stratigraphy of the Paleocene continental sedimentary succession of the northern Pyrenean basin (Corbières, southern France) using $\delta^{13}\text{C}_{\text{org}}$ isotopes. *J. Geol. Soc. London* 177: 752–765.
- Maurel O, Monié P, Pik R, Arnaud N, Brunel M, Jolivet M. 2008. The Meso-Cenozoic thermo-tectonic evolution of the Eastern Pyrenees: an $^{40}\text{Ar}/^{39}\text{Ar}$ fission track and (U-Th)/He thermochronological study of the Canigou and Mont-Louis massifs. *Int. J. Earth Sci.* 97: 565–584. <https://doi.org/10.1007/s00531-007-0179-x>.
- McClay K, Whitehouse PS. 2004. Analog modeling of doubly vergent thrust wedges. *AAPG Mem.* 82: 184–206.
- McClay K, Muñoz JA, García-Senz J. 2004. Extensional salt tectonics in a contractional orogen: A newly identified tectonic event in the Spanish Pyrenees. *Geology* 32: 737–740. <https://doi.org/10.1130/G20565.1>.
- McQueen HWS, Beaumont C. 1989. Mechanical models of tilted block basins. In: *Origin and evolution of sedimentary basins and their energy and mineral resources*. Geophysical Monograph Series. pp. 65–71. <https://doi.org/10.1029/GM048p0065>.
- Meigs AJ, Burbank DW. 1997. Growth of the South Pyrenean orogenic wedge. *Tectonics* 16: 239–258.
- Meigs AJ, Vergés J, Burbank DW. 1996. Ten-million-year history of a thrust sheet. *Geol. Soc. Am. Bull.* 108: 1608–1625.
- Mencos J, Carrera N, Muñoz JA. 2015. Influence of rift basin geometry on the subsequent post-rift sedimentation and basin inversion: The Organyà Basin and the Bóixols thrust sheet (south central Pyrenees). *Tectonics* 34. <https://doi.org/10.1002/2014TC003692>.
- Mesalles L, Mouthereau F, Bernet M, Chang C-P, Lin AT-S, Fillon C, *et al.* 2014. From submarine continental accretion to arc-continent orogenic evolution: The thermal record in southern Taiwan. *Geology* 42: 907–910. <https://doi.org/10.1130/G35854.1>.
- Miall AD. 1995. Collision-related foreland basins. In: Busby CJ, Ingersoll RV, (Eds.). *Tectonics of sedimentary basins*. Blackwell Science, Oxford, pp. 393–424.

- Milesi G, Monié P, Münch P, Soliva R, Taillefer A, Bruguier O, *et al.* 2020. Tracking geothermal anomalies along a crustal fault using (U-Th)/He apatite thermochronology and rare-earth element (REE) analyses: The example of the Têt fault (Pyrenees, France). *Solid Earth* 11: 1747–1771. <https://doi.org/10.5194/se-11-1747-2020>.
- Miró J, Manatschal G, Cadenas P, Muñoz JA. 2021. Reactivation of a hyperextended rift system: The Basque-Cantabrian Pyrenees case. *Basin Res.*: 1–25. <https://doi.org/10.1111/bre.12595>.
- Molli G. 2008. Northern Apennine–Corsica orogenic system: an updated overview. In: Siegesmund S, Fügenschuh B, Froitzheim N, (Eds.). *Tectonic Aspects of the Alpine-Dinaride-Carpathian System*. Geological Society of London Special Publication 298, pp. 413–442.
- Monod B, Bourroullec I. 2014. Digital geological map at 1/250 000 the the Midi-Pyrénées region. In: Notice Technique, Bureau Des Recherches Géologiques et Minières, Orléans, France.
- Morris RG, Sinclair HD, Yelland AJ. 1998. Exhumation of the Pyrenean orogen: implications for sediment discharge. *Basin Res.* 10: 69–85.
- Mouchéné M, van der Beek P, Carretier S, Mouthereau F. 2017. Autogenic versus allogenic controls on the evolution of a coupled fluvial megafan–mountainous catchment system: numerical modelling and comparison with the Lannemezan megafan system (northern Pyrenees, France). *Earth Surf. Dyn.* 5: 125–143. <https://doi.org/10.5194/esurf-5-125-2017>.
- Mouthereau F, Filleaudeau P, Vacherat A, Pik R, Lacombe O, Fellin MG, *et al.* 2014. Placing limits to shortening evolution in the Pyrenees: Role of margin architecture and implications for the Iberia/Europe convergence. *Tectonics* 33: 1–32. <https://doi.org/10.1002/2014TC003663>.
- Mouthereau F, Angrand P, Jourdon A, Calassou S, Ford M, Jolivet L, *et al.* 2021. Cenozoic mountain building and topographic evolution in Western Europe: impact of billion years lithosphere evolution and plate tectonics. *BSGF–Earth Sci. Bull.*: 1–132.
- Müller RD, Cannon J, Qin X, Watson RJ, Gurnis M, Williams S, *et al.* 2018. GPlates: building a virtual Earth through deep time. *Geochemistry, Geophys. Geosyst.* 19: 2243–2261.
- Muñoz JA. 1992. Evolution of a continental collision belt: ECORS-Pyrenees crustal balanced cross-section. In: McClay K, (Ed.). *Thrust Tectonics*. Chapman and Hall, London, pp. 235–246.
- Muñoz JA. 2002. The Pyrenees. In: Gibbons W, Moreno T, (Eds.). *The Geology of Spain*. Geological Society of London, pp. 370–385.
- Muñoz JA. 2019. Alpine orogeny: Deformation and structure in the Northern Iberian Margin (Pyrenees s.l.). In: Quesada C, Oliveira JT, (Eds.). *The geology of Iberia: A geodynamic approach*. Springer International Publishing, pp. 433–451.
- Muñoz-Jiménez A, Casas-Sainz AM. 1997. The Rioja Trough (N Spain): tectosedimentary evolution of a symmetric foreland basin. *Basin Res.* 9: 65–85.
- Naylor M, Sinclair HD. 2008. Pro- vs. retro-foreland basins. *Basin Res.* 20: 285–303. <https://doi.org/10.1111/j.1365-2117.2008.00366.x>.
- Nichols GJ, Hirst JP. 1998. Alluvial fans and fluvial distributary systems, Oligo-Miocene, northern Spain: contrasting processes and products. *J. Sediment. Res.* 68: 879–889.
- Nielsen SB, Thomsen E, Hansen DL, Clausen OR. 2005. Plate-wide stress relaxation explains European Palaeocene basin inversions, pp. 195–198.
- Nijman W. 1998. Cyclicity and basin axis shift in a piggyback basin: towards modelling of the Eocene Tresp-AGE Basin, South Pyrenees, Spain. *Geol. Soc. London, Spec. Publ.* 134: 135–162.
- Nirrengarten M, Manatschal G, Tugend J, Kuszniir NJ, Sauter D. 2017. Nature and origin of the J-magnetic anomaly offshore Iberia-Newfoundland: implications for plate reconstructions. *Terra Nov.* 29: 20–28. <https://doi.org/10.1111/ter.12240>.
- Nirrengarten M, Manatschal G, Tugend J, Kuszniir N, Sauter D. 2018. Kinematic Evolution of the Southern North Atlantic: Implications for the Formation of Hyperextended Rift Systems. *Tectonics* 37: 89–118. <https://doi.org/10.1002/2017TC004495>.
- Odlum ML, Stockli DF, Capaldi TN, Thomson KD, Clark J, Puigdefàbregas C, *et al.* 2019. Tectonic and sediment provenance evolution of the South Eastern Pyrenean foreland basins during rift margin inversion and orogenic uplift. *Tectonophysics* 765: 226–248. <https://doi.org/10.1016/j.tecto.2019.05.008>.
- Oliva-Urcia B, Beamud E, Arenas C, Pueyo EL, Garcés M, Soto R, *et al.* 2019. Dating the northern deposits of the Ebro foreland basin; implications for the kinematics of the SW Pyrenean front. *Tectonophysics* 765: 11–34. <https://doi.org/10.1016/j.tecto.2019.05.007>.
- Olivet JL. 1996a. La cinématique de la plaque Ibérique. *Bull. Cent. Rech. Explor. Prod. Elf Aquitaine* 20: 131–195.
- Olivet JL. 1996b. Kinematics of the Iberian Plate. *Bull. des Centres Rech. Explor. Elf Aquitaine* 20: 131–195.
- Ortiz A, Guillocheau F, Lasseur E, Briais J, Robin C, Serrano O, *et al.* 2020. Sediment routing system and sink preservation during the post-orogenic evolution of a retro-foreland basin: The case example of the North Pyrenean (Aquitaine, Bay of Biscay) Basins. *Mar. Pet. Geol.* 112: 104085. <https://doi.org/10.1016/j.marpetgeo.2019.104085>.
- Ortiz A, Guillocheau F, Robin C, Lasseur E, Briais J, Fillon C. 2022. Siliciclastic sediment volumes and rates of the North Pyrenean retro-foreland basin. *Basin Res.* n/a. <https://doi.org/10.1111/bre.12665>.
- Parizot O, Missenard Y, Haurine F, Blaise T, Barbarand J, Benedicto A, *et al.* 2021. When did the Pyrenean shortening end? Insight from U-Pb geochronology of syn-faulting calcite (Corbières area, France). *Terra Nov.*: 1–9. <https://doi.org/10.1111/ter.12547>.
- Patin J. 1967. L'évolution morphologique du plateau de Lannemezan. *Rev. géographique des Pyrénées du Sud-Ouest. Sud-Ouest Eur.* 38: 325–337.
- Pérez-Rivarés FJ, Tirapu GMP, Abad MCA, Crespo MG. 2004. Magnetostratigraphy of the Miocene continental deposits of the Montes de Castejón (central Ebro basin, Spain): geochronological and paleoenvironmental implications. *Geol. Acta* 2: 221–234.
- Peyaud JB, Barbarand J, Carter A, Pagel M. 2005. Mid-Cretaceous uplift and erosion on the northern margin of the Ligurian Tethys deduced from thermal history reconstruction. *Int. J. Earth Sci.* 94: 462–474. <https://doi.org/10.1007/s00531-005-0486-z>.
- Peyton SL, Carrapa B. 2013. An introduction to low-temperature thermochronologic techniques, methodology and applications. In: Knight C, Cuzella J, (Eds.). *Application of structural methods to rocky mountain hydrocarbon exploration and development*, pp. 15–36. <https://doi.org/10.1306/13381688St653578>.
- Philip J, Masse J-P, Machhour L. 1987. L'évolution paléogéographique et structurale du front de chevauchement nord-toulonnais (Basse-Provence occidentale, France). *Bull. al Soc. géologique Fr.* (III): 541–550.
- Platt JP, Behrmann JH, Cunningham PC, Dewey JF, Helman M, Parish M, *et al.* 1989. Kinematics of the Alpine arc and the motion history of Adria. *Nature* 337: 158–161.
- Plaziat J-C. 1981. Late Cretaceous to late Eocene palaeogeographic evolution of southwest Europe. *Palaeogeogr. Palaeoclimatol. Palaeoecol. Paleogene paleogeography and the geological events at the Eocene/Oligocene boundary* 36: 263–320. [https://doi.org/10.1016/0031-0182\(81\)90110-3](https://doi.org/10.1016/0031-0182(81)90110-3).

- Poprawski Y, Basile C, Agirrezabala LM, Jaillard E, Gaudin M, Jacquin T. 2014. Sedimentary and structural record of the Albian growth of the Bakio salt diapir (the Basque Country, northern Spain). *Basin Res.* 26: 746–766. <https://doi.org/10.1111/bre.12062>.
- Puigdefàbregas C, Souquet P. 1986. Tecto-sedimentary cycles and depositional sequences of the Mesozoic and Tertiary from the Pyrenees. *Tectonophysics* 29: 173–203.
- Puigdefàbregas C, Muñoz JA, Marzo M. 1986. Thrust belt development in the eastern {Pyrenees} and related depositional sequences in the southern foreland basin. *Forel. Basins*: 229–246.
- Puigdefàbregas C, Muñoz JA, Vergés J. 1992. Thrusting and foreland basin evolution in the Southern Pyrenees. In: McClay KR, (Ed.). *Thrust Tectonics*. Chapman & Hall, London, pp. 247–254.
- Rahl JM, Haines SH, van der Pluijm BA. 2011. Links between orogenic wedge deformation and erosional exhumation: Evidence from illite age analysis of fault rock and detrital thermochronology of syntectonic conglomerates in the Spanish Pyrenees. *Earth Planet. Sci. Lett.* 307: 180–190. <https://doi.org/10.1016/j.epsl.2011.04.036>.
- Ramos A, García-Senz J, Pedrera A, Ayala C, Rubio F, Peropadre C, *et al.* 2022. Salt control on the kinematic evolution of the Southern Basque-Cantabrian Basin and its underground storage systems (Northern Spain). *Tectonophysics* 822: 229178. <https://doi.org/10.1016/j.tecto.2021.229178>.
- Randle CH, Bond CS, Lark RM, Monaghan AA. 2018. Can uncertainty in geological cross-section interpretations be quantified and predicted? *Geosphere* 154(3): 1087–1100. <https://doi.org/10.1130/GES01510.1>.
- Rat J, Mouthereau F, Brichau S, Crémades A, Bernet M, Balvay M, *et al.* 2019. Tectonothermal evolution of the Cameros Basin: Implications for tectonics of North Iberia. *Tectonics* 38: 440–469. <https://doi.org/10.1029/2018TC005294>.
- Reiners PW, Brandon MT. 2006. Using thermochronology to understand orogenic erosion. *Annual Review of Earth and Planetary Sciences* 34: 419–466. <https://doi.org/10.1146/annurev.earth.34.031405.125202>.
- Reiners PW, Ehlers TA, Zeitler PK. 2005. Past, present, and future of thermochronology. *Rev. Mineral. Geochemistry* 58: 1–18. <https://doi.org/10.2138/rmg.2005.58.1>.
- Riba O, Reguant S, Villena J. 1983. Ensayo de síntesis estratigráfica y evolutiva de la cuenca terciaria del Ebro. *Geol. España* 2: 131–159.
- Ríos J. 1948. Diapirismo. *Boletín Inst. Geológico y Min. España* 60: 155–390.
- Roca E, Muñoz JA, Ferrer O, Ellouz N. 2011. The role of the Bay of Biscay Mesozoic extensional structure in the configuration of the Pyrenean orogen: constraints from the MARCONI deep seismic reflection survey. *Tectonics* 10: 405–408. <https://doi.org/10.1029/2010TC002735>.
- Rocher M, Lacombe O, Angelier J, Deffontaines B, Verdier F. 2000. Cenozoic folding and faulting in the south Aquitaine Basin (France): insights from combined structural and paleostress analyses. *J. Struct. Geol.* 22: 627–645. [https://doi.org/10.1016/S0191-8141\(99\)00181-9](https://doi.org/10.1016/S0191-8141(99)00181-9).
- Roest WR, Srivastava PS. 1991. Kinematics of the plate boundaries between Eurasia, Iberia, and Africa in the North Atlantic from the Late Cretaceous to the present. *Geology* 19: 613–616.
- Roigé M, Gómez-Gras D, Remacha E, Daza R, Boya S. 2016. Tectonic control on sediment sources in the Jaca basin (Middle and Upper Eocene of the South-Central Pyrenees). *Comptes Rendus – Geosci.* 348: 236–245. <https://doi.org/10.1016/j.crte.2015.10.005>.
- Roigé M, Gomez-Gras D, Stockli DF, Teixell A, Boya S, Remacha E. 2019. Detrital zircon U-Pb insights into the timing and provenance of the South Pyrenean Jaca basin. *J. Geol. Soc. London* 176: 1182–1190.
- Rosenbaum G, Lister GS, Duboz C. 2002a. Relative motions of Africa, Iberia and Europe during Alpine orogeny. *Tectonophysics* 359: 117–129.
- Rosenbaum G, Lister GS, Duboz C. 2002b. Reconstruction of the tectonic evolution of the western Mediterranean since the Oligocene. *J. Virtual Explor.* 8: 107–126.
- Rougier G, Ford M, Christophoul F, Bader A-G. 2016. Stratigraphic and tectonic studies in the central Aquitaine Basin, northern Pyrenees: Constraints on the subsidence and deformation history of a retro-foreland basin. *Comptes Rendus – Geosci.* 348: 224–235. <https://doi.org/10.1016/j.crte.2015.12.005>.
- Roure F. 2008. Foreland and Hinterland basins: what controls their evolution? *Swiss J. Geosci.* 101: S5–S29. <https://doi.org/10.1007/s00015-008-1285-x>.
- Roure F, Choukroune P. 1998. Contribution of the ECORS seismic data to the Pyrenean Geology: crustal architecture and geodynamic evolution of the Pyrenees. *Mémoire Hors-Série de La Société Géologique de France*, pp. 37–52.
- Roure F, Choukroune P, Berastegui X, Muñoz JA, Villien A, Matheron P, *et al.* 1989. ECORS deep seismic data and balanced cross-sections: geometric constraints on the evolution of the Pyrenees. *Tectonics* 8: 41–50.
- Rouvier H, Henry B, Le Goff M. 2012. Mise en évidence par le paléomagnétisme de rotations régionales dans la virgation des Corbières (France). *Bull. la Société géologique Fr.* 183: 409–424.
- Rowan MG, Ratliff RA. 2012. Cross-section restoration of salt-related deformation: Best practices and potential pitfalls. *J. Struct. Geol.* 41: 24–37. <https://doi.org/10.1016/j.jsg.2011.12.012>.
- Sàbat F, Gelabert B, Rodríguez-Perea A, Giménez J. 2011. Geological structure and evolution of Majorca: Implications for the origin of the Western Mediterranean. *Tectonophysics* 510: 217–238.
- Salas R, Guimerà J, Mas R, Martin-Closas C, Meléndez A, Alonso A. 2001. Evolution of the Mesozoic Central Iberian Rift System and its inversion (Iberian chain). In: Ziegler PA, Cavazza W, Robertson AHF, Crasquin-Soleau S, (Eds.). *Peri-Tethys Memoir 6: Peri-Tethyan Rift/Wrench Basins and Passive Margins*. Mémoires du Muséum national d'histoire naturelle volume 186, pp. 145–185.
- Salvany JM. 1989. Los sistemas lacustres evaporíticos del sector navarro-riojano de la Cuenca del Ebro durante el Oligoceno y Mioceno inferior. *Acta Geol. Hisp.* 24: 231–241.
- Sans M, Muñoz JA, Vergés J. 1996. Thrust wedge geometries related to evaporitic horizons (Southern Pyrenees). *Bull. Can. Pet. Geol.* 44: 375–384.
- Santolaria P, Vendeville BC, Graveleau F, Soto R, Casas-Sainz A. 2015. Double evaporitic décollements: Influence of pinch-out overlapping in experimental thrust wedges. *J. Struct. Geol.* 76: 35–51. <https://doi.org/10.1016/j.jsg.2015.04.002>.
- Santolaria P, Casas-Sainz AM, Soto R, Casas A. 2017. Gravity modelling to assess salt tectonics in the western end of the South Pyrenean Central Unit. *J. Geol. Soc. London.* 174: 269–288.
- Santolaria P, Ayala C, Pueyo EL, Rubio FM, Soto R, Calvín P, *et al.* 2020. Structural and geophysical characterization of the western termination of the South Pyrenean triangle zone. *Tectonics* 39: e2019TC005891.
- Saspiturry N, Razin P, Baudin T, Serrano O, Issautier B, Lasseur E, *et al.* 2019. Symmetry vs. asymmetry of a hyper-thinned rift: Example of the Mauléon Basin (Western Pyrenees, France). *Mar. Pet. Geol.* 104: 86–105. <https://doi.org/10.1016/j.marpetgeo.2019.03.031>.
- Saspiturry N, Allanic C, Razin P, Issautier B, Baudin T, Lasseur E, *et al.* 2020. Closure of a hyperextended system in an orogenic lithospheric pop-up, Western Pyrenees: The role of mantle buttressing and rift structural inheritance. *Terra Nov.* 32: 253–260. <https://doi.org/10.1111/ter.12457>.

- Saspiturry N, Issautier B, Razin P, Baudin T, Asti R, Lagabrielle Y, *et al.* 2021. Review of Iberia-Eurasia plate-boundary basins: Role of sedimentary burial and salt tectonics during rifting and continental breakup. *Basin Res.* 33: 0–2. <https://doi.org/10.1111/bre.12529>.
- Saspiturry N, Allanic C, Serrano O, Courrioux G, Baudin T, Le Bayon B, *et al.* 2022. Upper lithospheric transfer zones driving the non-cylindricity of the West-Pyrenean orogenic prism (Mauléon hyperextended basin). *J. Struct. Geol.* 156: 104535. <https://doi.org/10.1016/j.jsg.2022.104535>.
- Saura E, Ardèvol L, Teixell A, Vergés J. 2016. Rising and falling diapirs, shifting depocenters and flap overturning in the Cretaceous Sopeira and Sant Gervàs subbasins (Ribagorça basin, Southern Pyrenees). *Tectonics* 35: 638–662. <https://doi.org/10.1002/2015TC004001>.
- Scheck-Wenderoth M, Lamarche J. 2005. Crustal memory and basin evolution in the Central European Basin System—New insights from a 3D structural model. *Tectonophysics* 397: 143–165.
- Schettino A, Turco E. 2011. Tectonic history of the western Tethys since the Late Triassic. *Geol. Soc. Am. Bull.* 123: 89–105.
- Schettino A, Turco E. 2009. Breakup of Pangaea and plate kinematics of the central Atlantic and Atlas regions. *Geophys. J. Int.* 178: 1078–1097. <https://doi.org/10.1111/j.1365-246X.2009.04186.x>.
- Seguret M. 1972. Étude tectonique des nappes et séries décollées de la partie centrale du versant sud des Pyrénées: caractère synsédimentaire, rôle de la compression et de la gravité. Université des sciences et techniques du Languedoc.
- Senz JG, Zamorano M. 1992. Evolución tectónica y sedimentaria durante el Priabonense superior-Mioceno inferior, en el frente de cabalgamiento de las Sierras Marginales occidentales.
- Séranne M. 1999. The Gulf of Lion continental margin (NW Mediterranean) revisited by IBS: an overview. In: Durand B, Jolivet L, Horváth F, Séranne M, eds. *The Mediterranean basins: Tertiary extension within the Alpine Orogen*. Volume Special Publication 156. London: The Geological Society, pp. 15–36.
- Séranne M, Couëffé R, Husson E, Baral C, Villard J. 2021. The transition from Pyrenean shortening to Gulf of Lion rifting in Languedoc (South France)—A tectonic-sedimentation analysis. *BSGF—Earth Sci. Bull.* 192: 1–29. <https://doi.org/10.1051/bsgf/2021017/5302093/bsgf>.
- Serrano A, Martínez del Olmo W. 1990. Tectónica salina en el Dominio Cántabro-Navarro: Evolución, edad y origen de las estructuras salinas. In: Ortí F, Salvany JM, (Eds.). *Formaciones Evaporíticas de La Cuenca Del Ebro y Cadenas Periféricas, y de La Zona de Levante*. Enresa, Madrid, pp. 39–53.
- Serrano O, Delmas J, Hanot F, Vially R, Herbin J-P, Houel P, *et al.* 2006. Le bassin d'Aquitaine: valorisation des données sismiques, cartographique structurale et potentiel pétrolier.
- Sibuet J-C, Srivastava SP, Spakman W. 2004. Pyrenean orogeny and plate kinematics. *J. Geophys. Res. Solid Earth* 109: B08104. <https://doi.org/10.1029/2003JB002514>.
- Sinclair H. 2012. Thrust Wedge/Foreland Basin Systems. In: Busby C, Azor A, (Eds.). *Tectonics of Sedimentary Basins*. Wiley-Blackwell, pp. 522–537. <https://doi.org/10.1002/9781444347166.ch26>.
- Sinclair HD, Naylor M. 2012. Foreland basin subsidence driven by topographic growth versus plate subduction. *Geol. Soc. Am. Bull.* 124: 368–379. <https://doi.org/10.1130/B30383.1>.
- Sinclair HD, Gibson M, Naylor M, Morris RG. 2005. Asymmetric growth of the Pyrenees revealed through measurement and modeling of orogenic fluxes. *Am. J. Sci.* 305: 369–406. <https://doi.org/10.2475/ajs.305.5.369>.
- Soler y Jose R, Martínez del Olmo W, Megias AG, Abeger Monteagudo JA. 1983. Rasgos básicos del neógeno del Mediterráneo español. *Mediterránea Serv. Geológicos* 1: 71–83.
- Soula J-C, Bessièrre G. 1980. Sinistral horizontal shearing as a dominant process of deformation in the Alpine Pyrenees. *J. Struct. Geol.* 2: 69–74.
- Srivastava SP, Roest WR, Kovacs LC, Oakey G, Levesque S, Verhoef J, *et al.* 1990a. Motion of Iberia since the Late Jurassic: results from detailed aeromagnetic measurements in the Newfoundland Basin. *Tectonophysics* 184: 229–260.
- Srivastava SP, Schouteni H, Roest WR, Klitgordi KD, Kovacs LC, Verhoef J, *et al.* 1990b. Iberian plate kinematics: a jumping plate boundary between Eurasia and Africa. *Nature* 344: 756–759.
- Srivastava SP, Sibuet J-C, Cande S, Roest WR, Reid ID. 2000. Magnetic evidence for slow seafloor spreading during the formation of the Newfoundland and Iberian margins. *Earth Planet. Sci. Lett.* 182: 61–76.
- Stephenson R, Schiffer C, Peace A, Nielsen B, Jess S. 2020. Late Cretaceous-Cenozoic basin inversion and palaeostress fields in the North Atlantic-western Alpine-Tethys realm: implications for intraplate tectonics. *Earth Sci. Rev.* 210: 103252.
- Suc J-P, Fauquette S. 2012. The use of pollen floras as a tool to estimate palaeoaltitude of mountains: The eastern Pyrenees in the Late Neogene, a case study. *Palaeogeogr. Palaeoclim. Palaeoecol.* 321–322: 41–54.
- Sutra E, Manatschal G, Mohn G, Unternehr P. 2013. Quantification and restoration of extensional deformation along the Western Iberia and Newfoundland rifted margins. *Geochemistry, Geophys. Geo-systems* 14: 2575–2597. <https://doi.org/10.1002/ggge.20135>.
- Teixell A. 1996. The Ansó transect of the southern Pyrenees: basement and cover thrust geometries. *J. Geol. Soc. London* 153: 301–310.
- Teixell A, Muñoz JA. 2000. Evolución tectosedimentaria del Pirineo meridional durante el Terciario: una síntesis basada en la transversal del río Noguera Ribagorçana. *Rev. la Soc. Geológica España* 13: 251–264.
- Teixell A, Labaume P, Lagabrielle Y. 2016. The crustal evolution of the west-central Pyrenees revisited: Inferences from a new kinematic scenario. *Comptes Rendus Geosci.* 348: 257–267. <https://doi.org/10.1016/j.crte.2015.10.010>.
- Teixell A, Labaume P, Ayarza P, Espurt N, de Saint Blanquat M, Lagabrielle Y. 2018. Crustal structure and evolution of the Pyrenean-Cantabrian belt: A review and new interpretations from recent concepts and data. *Tectonophysics* 724–725: 146–170. <https://doi.org/10.1016/j.tecto.2018.01.009>.
- Ternois S, Odlum M, Ford M, Pik R, Stockli D, Tibari B, *et al.* 2019a. Thermochronological evidence of early Orogenesis, Eastern Pyrenees, France. *Tectonics* 38: 1308–1336. <https://doi.org/10.1029/2018TC005254>.
- Ternois S, Pik R, Ford M, Tibari B, Mercadier J, Lebel F, *et al.* 2019b. Unravelling early growth of a collisional orogen using *in situ* laser ablation double dating on detrital zircon, eastern North Pyrenees, France. In: *EGU General Assembly 2019 Conference Abstracts, Vienna, Austria*, p. 12965.
- Ternois S, Mouthereau F, Jourdon A. 2021a. Decoding low-temperature thermochronology signals in mountain belts: modelling the role of rift thermal imprint into continental collision. *BSGF—Earth Sci. Bull.* 192: 38. <https://doi.org/10.1051/bsgf/2021028>.
- Ternois S, Mouthereau F, Jourdon A. 2021b. Erratum to: Decoding low-temperature thermochronology signals in mountain belts: modelling the role of rift thermal imprint into continental collision. *BSGF—Earth Sci. Bull.* 192: 0–2. <https://doi.org/10.1051/bsgf/2021028>.

- Thomson KD, Stockli DF, Clark JD, Puigdefàbregas C, Fildani A. 2017. Detrital zircon (U-Th)/(He-Pb) double-dating constraints on provenance and foreland basin evolution of the Ainsa Basin, south-central Pyrenees, Spain. *Tectonics* 36: 2017TC004504. <https://doi.org/10.1002/2017TC004504>.
- Thomson KD, Stockli DF, Odlum ML, Tolentino P, Puigdefàbregas C, Clark J, *et al.* 2019. Sediment provenance and routing evolution in the Late Cretaceous–Eocene Ager Basin, south-central Pyrenees, Spain. *Basin Res.* 0. <https://doi.org/10.1111/bre.12376>.
- Torsvik TH, Müller RD, van der Voo R, Steinberger B, Gaina C. 2008. Global plate motion frames: Toward a unified model. *Rev. Geophys.* 46: RG3004. <https://doi.org/10.1029/2007RG000227>.
- Tripathy-Lang A, Hodges KV, Monteleone BD, van Soest MC. 2013. Laser (U-Th)/He thermochronology of detrital zircons as a tool for studying surface processes in modern catchments: Detrital zircon thermochronology. *J. Geophys. Res. Earth Surf.* 118: 1333–1341. <https://doi.org/10.1002/jgrf.20091>.
- Trümpy R. 1980. An outline of the geology of Switzerland. Wepf & Co, Basel, Switzerland.
- Tucker GE, van der Beek P. 2013. A model for post-orogenic development of a mountain range and its foreland. *Basin Res.* 24: 241–259. <https://doi.org/10.1111/j.1365-2117.2012.00559.x>.
- Tugend J, Manatschal G, Kuszniir NJ, Masini E. 2014a. Characterizing and identifying structural domains at rifted continental margins: application to the Bay of Biscay margins and its Western Pyrenean fossil remnants. *Geol. Soc. London, Spec. Publ.* 413: 171–203. <https://doi.org/10.1144/SP413.3>.
- Tugend J, Manatschal G, Kuszniir NJ, Masini E, Mohn G, Thinin I. 2014b. Formation and deformation of hyperextended rift systems: Insights from rift domain mapping in the Bay of Biscay-Pyrenees. *Tectonics* 33: 1239–1276. <https://doi.org/10.1002/2014TC003529>.
- Tugend J, Manatschal G, Kuszniir NJ. 2015. Spatial and temporal evolution of hyperextended rift systems: Implication for the nature, kinematics, and timing of the Iberian-European plate boundary. *Geology* 43: 15–18. <https://doi.org/10.1130/G36072.1>.
- Vacherat A, Mouthereau F, Al E. 2014. Thermal imprint of rift-related processes in orogens as recorded in the Pyrenees. *Earth Planet. Sci. Lett.* 408: 296–306. <https://doi.org/10.1016/j.epsl.2014.10.014>.
- Vacherat A, Mouthereau F, Pik R, Bellahsen N, Gautheron C, Bernet M, *et al.* 2016. Rift-to-collision transition recorded by tectono-thermal evolution of the northern Pyrenees. *Tectonics* 35: 907–933. <https://doi.org/10.1002/2015TC004016>.
- Vacherat A, Mouthereau F, Pik R, Huyghe D, Paquette JL, Christophoul F, *et al.* 2017. Rift-to-collision sediment routing in the Pyrenees: A synthesis from sedimentological, geochronological and kinematic constraints. *Earth-Science Rev.* 172. <https://doi.org/10.1016/j.earscirev.2017.07.004>.
- Van Hoorn B. 1970. Sedimentology and paleogeography of an Upper Cretaceous turbidite basin in the south-central Pyrenees, Spain. *Leidse Geologische Mededelingen* 45: 73–154.
- Vergés J. 1993. Estudi geològic del vessant sud del Pirineu oriental i central Evolució cinemàtica en 3D. Barcelona University.
- Vergés J, Burbank DW. 1996. Eocene-Oligocene thrusting and basin configuration in the eastern and central Pyrenees (Spain). In: *Tertiary basins of Spain: The stratigraphic record of crustal kinematics*. Cambridge University Press, pp. 120–133.
- Vergés J, Fernandez M. 2006. Ranges and basins in the Iberian Peninsula: their contribution to the present topography. In: Gee DG, Stephenson RA, (Eds.). *European lithosphere dynamics*. Geological Society London Memoirs, pp. 223–234.
- Vergés J, Fernández M. 2012. Tethys-Atlantic interaction along the Iberia-Africa plate boundary: The Betic-Rif orogenic system. *Tectonophysics* 579: 144–172. <https://doi.org/10.1016/j.tecto.2012.08.032>.
- Vergés J, Muñoz JA, Martínez A. 1992. South Pyrenean fold and thrust belt: The role of foreland evaporitic levels in thrust geometry. In: McClay K, (Ed.). *Thrust Tectonics*. Chapman & Hall, London, pp. 255–264.
- Vergés J, Millán H, Roca E, Muñoz JA, Marzo M, Cirés J, *et al.* 1995. Eastern Pyrenees and related foreland basins: pre-, syn- and post-collisional crustal-scale cross-sections. *Mar. Pet. Geol.* 12: 903–915. [https://doi.org/10.1016/0264-8172\(95\)98854-X](https://doi.org/10.1016/0264-8172(95)98854-X).
- Vergés J, Marzo M, Santaclàudia T, Serra-Kiel J, Burbank DW, Muñoz JA, *et al.* 1998. Quantified vertical motions and tectonic evolution of the SE Pyrenean foreland basin. *Geol. Soc. London, Spec. Publ.* 134: 107–134. <https://doi.org/10.1144/GSL.SP1998.134.01.06>.
- Vergés J, Fernández M, Martínez A. 2002. The Pyrenean orogen: pre-, syn-, and post-collisional evolution. *J. Virtual Explor.* 8: 55–74.
- Vergés J, Kullberg JC, Casas-Sainz A, de Vicente G, Duarte LV, Fernández M, *et al.* 2019. An introduction to the Alpine Cycle in Iberia. In: Quesada C, Oliveira JT (Eds.). *The geology of Iberia: A geodynamic approach*. Springer Nature, Switzerland, pp. 1–14. https://doi.org/10.1007/978-3-030-11295-0_1.
- Vergés J, Poprawski Y, Almar Y, Drzawiecki PA, Moragas M, Bover-Arnal T, *et al.* 2020. Tectono-sedimentary evolution of Jurassic-Cretaceous diapiric structures: Miravete anticline, Maestrat Basin, Spain. *Basin Res.*: 0–21. <https://doi.org/10.1016/j.optmat.2011.11.002>.
- Vermeech P, Sherlock SC, Roberts NMW, Carter A. 2012. A simple method for in-situ U-Th-He dating. *Geochim. Cosmochim. Acta* 79: 140–147. <https://doi.org/10.1016/j.gca.2011.11.042>.
- Viallard P. 1987. Un modèle de charriage égyptique: la nappe des Corbières orientales (Aude, France). *Bull. La Soc. Geol. Fr.* 8: 551–559.
- Vinciguerra C. 2020. Reconstruction des paléo-drainages des bassins précoces péri-orogéniques (Crétacé terminal-Paléocène) à partir des dépôts fluviaux dans le système pyrénéen oriental. PhD thesis, Université Michel de Montaigne-Bordeaux III, France.
- Vinciguerra C, Leleu S, Desmares D, Emmanuel L, Martinez L, Loisy C. 2022. Global carbon isotopic events in a Campanian-Maastrichtian deltaic succession (Tresp-Graus Basin, Spain) and multiproxy stratigraphy for high sedimentation rate environments. *Cretac. Res.* 137: 105222. <https://doi.org/10.1016/j.cretres.2022.105222>.
- Vissers RLM, Meijer PT. 2012a. Mesozoic rotation of Iberia: Subduction in the Pyrenees? *Earth-Science Rev.* 110: 93–110. <https://doi.org/10.1016/j.earscirev.2011.11.001>.
- Vissers RLM, Meijer PT. 2012b. Iberian plate kinematics and Alpine collision in the Pyrenees. *Earth-Science Rev.* 114: 61–83. <https://doi.org/10.1016/j.earscirev.2012.05.001>.
- Voigt T, Kley J, Voigt S. 2021. Dawn and dusk of Late Cretaceous basin inversion in central Europe. *Solid Earth* 12: 1443–1471.
- Waldner M, Bellahsen N, Mouthereau F, Bernet M, Pik R, Rosenberg CL, *et al.* 2021. Central Pyrenees Mountain Building: Constraints From New LT Thermochronological Data From the Axial Zone. *Tectonics* 40: e2020TC006614. <https://doi.org/10.1029/2020TC006614>.
- Waltham D, Taberner C, Docherty C. 2000. Error estimation in decompacted subsidence curves. *Am. Assoc. Pet. Geol. Bull.* 84: 1087–1094.
- Wang Y, Chevrot S, Monteiller V, Komatitsch D, Mouthereau F, Manatschal G, *et al.* 2016. The deep roots of the western Pyrenees revealed by full waveform inversion of teleseismic P waves. *Geology* 44. <https://doi.org/10.1130/G37812.1>.

- Wehr H, Chevrot S, Courrioux G, Guillen A. 2018. A three-dimensional model of the Pyrenees and their foreland basins from geological and gravimetric data. *Tectonophysics* 734-735: 16–32. <https://doi.org/10.1016/j.tecto.2018.03.017>.
- Whitchurch AL, Carter A, Sinclair HD, Duller RA, Whittaker AC, Allen PA. 2011. Sediment routing system evolution within a diachronously uplifting orogen: Insights from detrital zircon thermochronological analyses from the South-Central Pyrenees. *Am. J. Sci.* 311: 442–482.
- Wicker V, Ford M. 2021. Assessment of the tectonic role of the Triassic evaporites in the North Toulon fold-thrust belt. *BSGF – Earth Sci. Bull.* 192: 51. <https://doi.org/10.1051/bsgf/2021033/5451740/bsgf>.
- Willett SD, Brandon MT. 2002. On steady states in mountain belts. *Geology* 30: 175–178. [https://doi.org/10.1130/0091-7613\(2002\)030<0175:OSSIMB>2.0.CO;2](https://doi.org/10.1130/0091-7613(2002)030<0175:OSSIMB>2.0.CO;2).
- Willett S, Beaumont C, Fullsack P. 1993. Mechanical model for the tectonics of doubly vergent compressional orogens. *Geology* 21: 371–374.
- Wolf SG, Huismans RS, Muñoz JA, Curry ME, van der Beek P. 2021. Growth of collisional orogens from small and cold to large and hot – Inferences from geodynamic models. *Journal of Geophysical Research: Solid Earth* 126: e2020JB021168.
- Xie X, Heller PL. 2009. Plate tectonics and basin subsidence history. *Geol. Soc. f Am. Bull.* 121: 55–64. <https://doi.org/10.1130/B26398.1>.
- Yelland AJ. 1990. Fission track thermotectonics in the Pyrenean orogen. *Int. J. Radiat. Appl. Instrum. Part D. Nucl. Tracks Radiat. Meas.* 17: 293–299. [https://doi.org/10.1016/1359-0189\(90\)90049-4](https://doi.org/10.1016/1359-0189(90)90049-4).
- Yelland AJ. 1991. Fission track thermotectonics of the Iberian-Eurasian plate orogen. PhD thesis, Birkbeck University of London, London.
- Zamora G, Fleming M, Gallastegui J. 2017. Salt tectonics within the offshore Asturian Basin: North Iberian margin. In: *Permo-Triassic Salt Provinces of Europe, North Africa and the Atlantic Margins*. Elsevier, pp. 353–368.
- Ziegler PA, Dèzes P. 2006. Crustal evolution of Western and Central Europe. In: Gee DG, Stephenson RA, (Eds.). *European lithosphere dynamics*. Memoir of the Geological Society, London 32, pp. 43–56.

Cite this article as: Ford M, Masini E, Vergés J, Pik R, Ternois S, Léger J, Dielforder A, Frasca G, Grool A, Vinciguerra C, Bernard T, Angrand P, Crémades A, Manatschal G, Chevrot S, Jolivet L, Mouthereau F, Thinon I, Calassou S. 2022. Evolution of a low convergence collisional orogen: a review of Pyrenean orogenesis, *BSGF - Earth Sciences Bulletin* 193: 19.